Distribution Agreement

In presenting this thesis or dissertation as a partial fulfillment of the requirements for an advanced degree from Emory University, I hereby grant to Emory University and its agents the non-exclusive license to archive, make accessible, and display my thesis or dissertation in whole or in part in all forms of media, now or hereafter known, including display on the world wide web. I understand that I may select some access restrictions as part of the online submission of this thesis or dissertation. I retain all ownership rights to the copyright of the thesis or dissertation. I also retain the right to use in future works (such as articles or books) all or part of this thesis or dissertation.

Signature:

_____ _____

Amanda N. Ruggieri Date

MEK inhibition mediates immunomodulatory factors and cell populations in advanced biliary tract cancer

By

Amanda N. Ruggieri
Doctor of Philosophy

Graduate Division of Biological and Biomedical Science
Cancer Biology

Gregory B. Lesinski, Ph.D, MPH
Advisor

Mandy L. Ford, Ph.D
Committee Member

Haydn T. Kissick, Ph.D
Committee Member

Cheng-Kui Qu, M.D, Ph.D
Committee Member

Periasamy Selvaraj, Ph.D
Committee Member

Accepted:

Kimberly Jacob Arriola, Ph.D, MPH
Dean of the James T. Laney School of Graduate Studies

Date

MEK inhibition mediates immunomodulatory factors and cell populations in advanced biliary tract cancer

By

Amanda N. Ruggieri
B.S., Quinnipiac University, 2016
M.S., Quinnipiac University, 2017

Advisor: Gregory B. Lesinski, Ph.D., MPH

An abstract of
A dissertation submitted to the Faculty of the
James T. Laney School of Graduate Studies of Emory University
in partial fulfillment of the requirements for the degree of
Doctor of Philosophy
in the Graduate Division of Biological and Biomedical Science
in Cancer Biology
2022

Abstract

MEK inhibition mediates immunomodulatory factors and cell populations in advanced biliary tract cancer

By Amanda N. Ruggieri

Biliary tract cancer (BTC) is a rare group of aggressive gastrointestinal malignancies with a five-year survival rate of less than 10%. Patients are often diagnosed at late stages when tumors are refractory to treatment and resection is not possible. The Ras/Raf/MEK/ERK signaling pathway has an important role in the development and progression of this disease, but inhibitors of MEK have had limited success in patients with BTC. Immunotherapy has also produced modest efficacy in advanced BTC and is largely limited by a lack of tumor-infiltrating lymphocytes characteristic of these tumors. However, MEK inhibitors have been shown to increase infiltration of $CD8^+$ T cells in various other tumor models and combine with immune checkpoint blockade to improve anti-tumor activity. A recent clinical trial demonstrated that combining the MEK inhibitor cobimetinib with the PD-L1 blocking antibody atezolizumab leads to improved progression-free survival in patients with advanced, metastatic BTC. In this dissertation, we investigate the effects of systemic MEK inhibition (MEKi) combined with PD-L1 blockade in these patients and seek to understand the mechanism by which MEK inhibition leads to increased T cell infiltration and improved anti-tumor activity. We show that dual MEK/PD-L1 blockade alters the concentrations of growth factors and populations of immune cells in peripheral blood, correlating with improved clinical outcomes. We also demonstrate that MEK inhibition does not limit cell viability in BTC cell lines *in vitro*, but does alter the production of immunomodulatory cytokines and chemokines, suggesting that MEKi elicits anti-tumor activity on the tumor microenvironment rather that on tumor cells directly. Finally, we highlight that MEKi limits $CD8^+$ T cell activation in patients with advanced BTC and discuss the role of T cell costimulatory agonists in enhancing the efficacy of dual MEK/PD-L1 blockade. Overall, the data presented here provides a foundation for future investigation to identify potential therapeutic strategies to enhance the efficacy of MEK inhibitors with immune checkpoint blockade in this aggressive disease.

MEK inhibition mediates immunomodulatory factors and cell populations in advanced biliary tract cancer

By

Amanda N. Ruggieri
B.S., Quinnipiac University, 2016
M.S., Quinnipiac University, 2017

Advisor: Gregory B. Lesinski, Ph.D., MPH

A dissertation submitted to the Faculty of the
James T. Laney School of Graduate Studies of Emory University
in partial fulfillment of the requirements for the degree of
Doctor of Philosophy
in the Graduate Division of Biological and Biomedical Science
in Cancer Biology
2022

Table of Contents

List of Figures

List of Tables

Chapter 1: Introduction

1.1. Introduction

In 2020, it is estimated that over 19 million new cancer cases were diagnosed globally and nearly 10 million deaths were attributed to cancer[1]. These figures are increasing rapidly around the world due to several factors including extended life expectancy, declines in mortality due to stroke and coronary heart disease, and exposure to cancer-associated risk factors[2]. Significant advances have been made over the last 50 years in screening and diagnostic methods, as well as in the development of treatments for various cancers. However, cancer is highly heterogeneous, differing from patient to patient even within the same cancer type, complicating the progress toward establishing therapeutic strategies beneficial for large populations of patients. As we advance our understanding of the mechanisms of cancer progression and development, especially in less commonly diagnosed cancers, we aim to expand the availability of treatments for all cancer patients to reduce cancer burden and decrease mortality worldwide.

Biliary tract cancer (BTC) is a rare cancer in many Western countries, though incidence has been steadily rising over the last several years. Patients are often diagnosed after progressing to advanced disease, with an abysmal five-year survival rate of less than 10%. Despite the low incidence in countries like the United States and United Kingdom, BTCs are found at rates nearly 40 times higher in Southeast Asia, highlighting the need for improved clinical management. The advent of immunotherapy has brought significant promise for patients across many malignancies, including BTC, where we are able to harness the power of the human immune system to elicit tumor-killing effects. However, immunotherapy has remained largely unsuccessful, due to a number of factors including natural and acquired resistance to therapy and a lack of consistent

biomarkers or features across patients that these therapies can target[3]. Many gaps still exist in our understanding of the immune response in several cancer types, especially biliary tract cancers, that we aim to overcome to improve treatment strategies for patients with advanced disease. This dissertation investigates the use of MEK inhibitors in combination with immunotherapy for the treatment of advanced BTC, which is deserving of significant research to improve clinical outcomes for this disease.

1.2. Fundamentals of the human immunological response

The human immune system is comprised of complex mechanisms necessary to protect the body from infections from foreign pathogens. Bacteria, viruses, and other pathogenic microorganisms enter the human body and infect host cells to replicate and cause disease. Our immune system has evolved intricate means for identifying infected cells, especially in terms of distinguishing infected cells from healthy cells. There are two main components of the immune response: innate immunity and adaptive immunity. The elements of innate immunity are encoded in the germline and are initiated immediately at the onset of infection. Pathogens are recognized broadly by pattern recognition receptors (PRRs), which recognize pathogen-associated molecular patterns (PAMPs)[4]. These PAMPs are common among classes of pathogens that PRRs can react to quickly to initiate a swift immune response[5]. Innate immune effector cells include macrophages, NK cells, neutrophils, and dendritic cells, all of which have roles in controlling the initial immune response and preparing the next phase – the adaptive immune response[4]. This stage of the immune response takes longer to initiate, but the recognition of pathogens is based on specific antigen recognition rather than broader PAMPs. Antigen recognition receptors, which consist of T-cell receptors (TCRs) on T cells and immunoglobulins on B cells, are not expressed exactly as they are encoded

in the germline like PRRs[6]. Rather, these receptors are assembled via somatic recombination of germline genes to generate millions of different antigen receptors, up to 1018 different possible combinations, versus only a few hundred PRRs[6-8].

An important facet of the human immune system is the ability to recognize infectious non-self from non-infectious self[9]. PRRs in the innate immune response have evolved to recognize PAMPs that are not produced by healthy human cells and are shared by large classes of microbes. As examples, the primary categories of PAMPs include lipopolysaccharides present on all gram-negative bacteria; unmethylated CpG motifs characteristic of bacterial DNA but not mammalian; double-stranded RNA characteristic of RNA viruses but never found in mammalian cells; and mannans present only in the cell walls of yeast[5]. Distinguishing self from non-self by the adaptive immune system is more complex, where the recognition of specific antigens is required to mount a targeted immune response[9]. T cell development occurs in the thymus, where pre-T cells begin the process of TCR assembly[10]. The TCR is comprised of a combination of one V, one D, and one J segment that are randomly spliced together to form a structure that recognizes one of a vast number of amino acid sequences for binding an antigen[11]. This process is regulated by the recombination activating genes RAG-1 and RAG-2[12]. Double positive T cells, which express both CD4 and CD8 at this point, will move through processes to test the specificity and affinity of the newly generated TCRs[13]. First, the TCR must bind with low avidity to self-major histocompatibility complex (MHC) to demonstrate that it is functional. However, if the TCR binds too highly to self-MHC, it is eliminated[14]. Additionally, this selection process utilizes the AIRE gene, which generates peptides that represent normal human tissues that T cells must be tolerant toward[15, 16]. Finally, double positive T cells that interact with MHC class I mature into $CD8^+$ T cells, and those that interact with MHC class II become $CD4^+$ T cells. These newly single-positive

cells will mature in the thymus when they interact with their cognate antigen on a thymic antigen-presenting cell (APC). Mature T cells can then enter the periphery to encounter other APCs expressing its cognate antigen and elicit effector functions. B cells mature in a similar manner to TCRs, except that it occurs in the bone marrow and does not have to interact with its antigen in order to mature[13]. There are 5 distinct classes of these receptors, also known as immunoglobulins (IgM, IgD, IgG, IgA, and IgE), and switching among these classes can occur to produce different effector functions but maintain antigen specificity[17].

The two main classes of T cells express either the CD4 or CD8 glycoproteins. CD4 T cells, known as T helper (Th) cells, can differentiate into several subsets: Th1, Th2, Th9, Th17, Th22, T regulatory cells (Tregs) and T follicular helper cells (Tfh)[18]. Each subset has its own distinct effector functions, releasing different cytokines that lead to a number of pro- or anti-inflammatory functions, and their differentiation is mediated by transcription factors specific to each subset[19](Figure 1.1). Effector Th cells can further differentiate to have two memory phenotypes: effector memory (TEM) and central memory (TCM) cells. Memory T cells reside either in recently infected tissue or in secondary lymphoid organs, and their main function is to rapidly expand with a stronger effector response when re-exposure to an antigen occurs, making up a central tenet of the immunological response[20, 21]. CD8 T cells, known as cytotoxic T cells, do not have multiple effector subsets like Th cells. They do, however, similarly differentiate into several memory phenotypes: TCM, TEM, and stem cell memory (TSCM) cells[18].

A key difference between CD4 and CD8 cells is how they are presented antigen. As mentioned above, double positive T cells differentiate into either CD4 or CD8 depending on which class of MHC they interact with: CD8 T cells recognize antigen presented by MHC-I, while CD4 T cells are presented antigen by MHC-II[22]. Nearly all nucleated cells express some level of MHC-I,

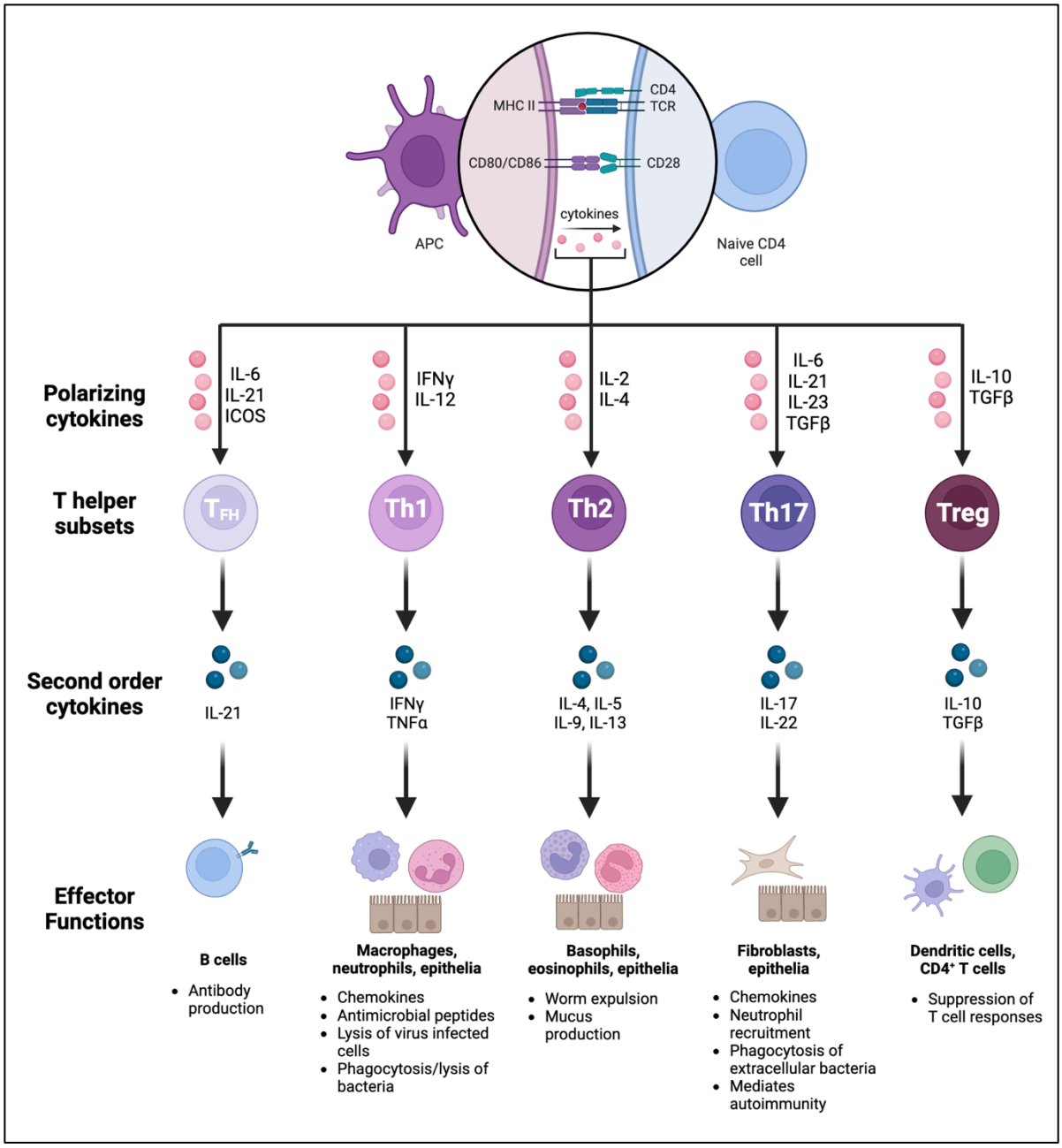

Figure 1.1. Polarization of CD4$^+$ T cell subsets. Naïve CD4$^+$ T cells can differentiate into 5 effector subsets depending on the cytokine signals received upon interaction with an antigen-presenting cell. These subsets have varying roles in regulating the immune response and secrete unique sets of cytokines to execute their effector functions on other immune, stromal, and epithelial cells.

which predominantly presents peptides of proteins that are found in the cytosol of the cell[23]. MHC-II is mostly found on B cells, dendritic cells, and macrophages and present antigen that has been internalized and processed in intracellular vesicles[24, 25]. For example, B cells internalize antigen-bound surface antibodies which are processed to present the antigenic peptide on MHC-II, while dendritic cells and macrophages can phagocytose pathogens and express peptide fragments on MHC-II. However, interferon-γ (IFN-γ) signaling can induce the expression of MHC-II on non-immune cells via the class II transactivation (CIITA) gene[26]. Notably, activated T cells express high levels of MHC-II in a CIITA-dependent manner, and it is believed that MHC-II on T cells may serve a role in signal transduction as well as antigen presentation[27-29]. An important caveat of MHC expression is the notion of cross-presentation, where MHC-I is able to present exogenous peptides, a mechanism that was conventionally reserved for MHC-II, on specialized subsets of APCs to $CD8^+$ T cells[30, 31]. By design, MHC-I displays peptides derived from proteins synthesized from a cell's own genes, thus allowing $CD8^+$ T cells to identify and eliminate cells with abnormal genes[32]. The mechanism of cross-presentation allows for the direct engagement of $CD8^+$ T cells with exogenous antigen rather than relying on signals received from $CD4^+$ T cells, but also helps to regulate the presence of self-reactive $CD8^+$ T cells in the periphery[33].

To understand the full scope of the immunological response, we must consider the important roles of cytokines. Cytokines are a large group of diverse soluble and membrane-bound proteins that are the mediators of cellular communication[34]. The major cytokine families include the interleukins (IL), interferons (IFN), colony-stimulating factors (CSF), and tumor necrosis factors (TNF). There are remarkably few similarities among cytokines in these families, in terms of both structure and function, but further subgroups within cytokine families can have overlapping functions[35, 36]. Cytokines can be pleiotropic or redundant, meaning that one cytokine can interact

with many cell types, or many cytokines execute the same functions[37]. Cytokines have roles in nearly every aspect of cell communication, including regulating gene expression, the cell cycle, cell death and apoptosis, and cellular lineage commitment and differentiation[34]. All nucleated cells are able to produce and respond to cytokines, but each cell lineage can be defined by unique cytokine profiles that determine the overall cell differentiation and activity. Cytokines are sometimes grouped together with chemokines, which mediate cellular movement, and growth factors, which stimulate cell proliferation and other healing mechanisms. However, each of these categories of signaling molecules have distinct and non-overlapping roles in the immune response.

The human immune system is comprised of an elaborate network of mechanisms that protect the body from infection and damage. The basic components described above have evolved to recognize and eliminate a vast array of foreign pathogens and aid in tissue repair, but the immune system has also developed to recognize and target threats from within the body, especially the malignant transformation of human cells into cancer. To understand how tumors develop in spite of the immune response, we must investigate the mechanisms of resistance to immunologic control and develop new strategies to reignite the immune response for the treatment of cancer.

1.3. Inflammation-mediated tumorigenesis and evasion of the immune response

Early theories regarding the development of cancer postulated that immunodeficiency disorders are largely responsible for tumor growth. In fact, many studies provide supportive evidence for this by demonstrating that patients with primary immunodeficiency disorders (PIDD) have significantly elevated risks of cancer development[38, 39]. Additionally, organ transplant patients who receive immunosuppressive regimens are predisposed for cancer development[38]. Notably, a large majority of these cases in immunosuppressed transplant patients result from viral-induced cancers,

suggesting impaired immunity limits the ability to control cancer-causing viruses. Overall, approximately 15% of all human cancers can be linked to only roughly a half-dozen viruses, including Epstein-Barr virus, hepatitis B and C, and human papilloma virus[40-43]. Cancers not linked to viral infections, including breast, ovarian, brain, and prostate cancers, do not display an increased incidence in immunosuppressed patients, indicating that links to immunodeficiency and tumor development may only be restricted to certain types of cancer[39].

While viruses can alter the DNA of the cells they infect, leading to cancer-causing mutations, other viral infections contribute to inflammatory changes in organ systems. This constitutes another significant risk factor and hallmark of cancer[44-46]. The connection between inflammation and cancer progression has long been recognized, especially following Rudolf Virchow's observance of leukocytes in tumors in the 19th century[47]. In a general sense, inflammation is the body's response to tissue damage, via either infection or physical injury[45, 48, 49]. Leukocytes are recruited to the site of damage to eliminate any invading pathogens where they produce cytokines and growth factors that support tissue repair[49]. These factors also trigger and support angiogenesis, which is the growth of new blood vessels, and is yet another key component to supporting cancer growth[50]. Normally, the immune system is able to return to homeostasis as inflammatory cells undergo apoptosis and reduce their production of pro-inflammatory cytokines. When inflammation persists, and the mechanisms supporting cellular proliferation are sustained for an extended time, the once-beneficial leukocytes and cytokines become damaging and contribute to an immunosuppressive and tumor supportive microenvironment.

1.3.1. Evasion of the immune system for tumorigenesis

Evasion of the immune response is one of the most important characteristics that defines cancer, described as a hallmark of cancer by Hanahan and Weinberg[51]. Under normal circumstances,

immune cells can recognize malignantly transformed cells as non-self, due to the expression of tumor-associated antigens (TAAs) and other molecular patterns[52]. In the innate immune response, early tumor development can induce an acute inflammatory response. The resulting damaged or necrotic tissues will release DAMPs, or damage associated molecular patterns, which are similar to PAMPs produced by foreign pathogens, and initiate the innate immune response[53, 54]. However, tumors can secrete pro-inflammatory cytokines that polarize innate immune cells to have tumor-promoting phenotypes, including IL-4 and TGF-β[55, 56]. This "alternative" polarization of innate cells like macrophages and neutrophils induce them to produce growth factors and angiogenic factors that cancer cells require for tumorigenesis, instead of cytokines like IFN-γ which enhances antigen presentation by macrophages to promote the cytotoxic activity of $CD8^+$ T cells against pathogens[57, 58]. Adaptive immune cells, especially T cells, can also recognize specific tumor antigens, as long as these are properly presented by an APC. However, not all tumors produce sufficient or specific enough of antigens that can be presented on APCs and subsequently recognized by T cells[59]. These mechanisms of immune scanning of human tissue and eliminating malignant cells early in tumorigenesis constitutes the theory of cancer immune surveillance[60]. Unfortunately, the interplay between the immune system and tumorigenesis is extremely complex, and many factors often accumulate into an environment that supports tumor formation, growth, and survival.

Cancer development is largely supported by tumor-intrinsic mechanisms that modulate the inflammatory response, as tumors frequently mutate to promote pro-inflammatory responses and inhibit the activity of adaptive immune cells. Through a process termed "cancer immunoediting", interactions between the tumor and the immune system are sculpted by progressive changes in tumor antigens and the ability of cancer cells to become less immunogenic[61-63]. The cancer

immunoediting theory describes three distinct phases: elimination, equilibrium, and escape[64]. The elimination phase overlaps with the roles of immunosurveillance, where the innate and adaptive immune response controls the growth of malignant cells. As mentioned above, this phase involves recognizing tumor antigens, mounting an inflammatory response, recruiting cytotoxic and phagocytic cells, and producing soluble factors that stimulate tissue repair to restore a homeostatic balance[62, 65]. This stage is thought to control the outgrowth of many tumors prior to detection in the body. However, tumors are, by their nature, genetically unstable and highly heterogeneous, meaning that even a small number of cells that may have developed with the right set of mutations can survive immunosurveillance mechanisms[62]. These cells persist quietly into the equilibrium phase of immunoediting, appearing healthy enough to not be eliminated, but steadily accumulating mutations to resist further mechanisms of the immune response[66, 67]. At this stage, low level chronic inflammation fosters continued production of cytokines and growth factors intended to support tissue repair. Yet, these inflammatory cytokines and growth factors also stimulate tumor progression and metastasis[68]. Subsequently, many tumor cells become able to produce chemotactic factors, which stimulate the movement and recruitment of leukocytes, and pro-inflammatory cytokines themselves, further supporting the growth of the evolving tumor. Tumor cell clones will also begin to produce immunosuppressive cytokines like TGF-β or IL-10 and recruit immunomodulatory cells that typically serve to maintain homeostasis following an immune response[56]. Instead, these immunosuppressive cells, including Tregs and myeloid derived suppressor cells, will suppress the function of effector cells that would otherwise maintain immune homeostasis. Eventually, these tumors reach a critical point where they have amassed enough mechanisms to overcome the immune response altogether, in the final immunoediting phase

known as escape[63]. The tumor, having successfully evaded the host system's immunological defenses, will continue to grow in an uncontrolled manner, leading to malignant progression.

1.3.2. Immunosuppressive cells facilitate tumor progression

Tumors alone are not solely responsible for the mechanisms of immune evasion. Several subsets of immunosuppressive cells populate the tumor microenvironment and support cancer development, progression, and metastasis. An important cell population are T regulatory cells (Tregs), which are a subset of $CD4^+$ T cells that secrete IL-10 and TGF-β, and the immunomodulatory activity of these cells is critical in the normal immune response to maintaining homeostasis and preventing autoimmunity[69-71]. Aside from regulating the activity, proliferation, and cytokine production of CD4 and CD8 T cells, Tregs also suppress several other immune cell activities, including B cell proliferation, NK cell cytotoxicity, and DC maturation[72-74]. Tregs have significant roles in the TME, as evidenced by an increase in antitumor activity following Treg depletion, and the elevated presence of Tregs among tumor infiltrating lymphocytes (TILs) in several cancers[75-77]. Another set of immunomodulatory cells are myeloid derived suppressor cells (MDSCs), which are a heterogeneous group of precursor and progenitor myeloid cells that largely function to limit T cell activity and proliferation through deprivation of amino acids, secretion of reactive oxygen species (ROS), and production of immunosuppressive cytokines IL-10 and TGF-β[78, 79]. These cells are highly prevalent in tumors, and their abundance correlates significantly with tumor progression. Tumor associated macrophages (TAMs) are present in high numbers in tumors as well and produce immunosuppressive cytokines and chemokines to limit $CD8^+$ T cells activity and recruit Tregs. These macrophages were described above as undergoing "alternative" polarization as a result of pro-inflammatory factors secreted by tumors to induce TAMs to produce growth factors and further inflammatory cytokines[55]. Finally, stromal cells, including cancer

associated fibroblasts (CAFs), in the TME are non-immune cells that have significant roles in providing a structural framework for tumors and in supporting pro-tumorigenic activities like angiogenesis and metastasis through pro-inflammatory cytokine production[80]. In some ways, the prevalence of immunosuppressive cells in the TME has challenged our understanding of tumor immune evasion. Particularly in cancers with a dense stromal component of their TME, tumors are often almost completely devoid of TILs, and their inability to infiltrate is mediated by TAMs and MDSCs[81, 82]. The concept of cancer immune privilege argues that immunomodulatory leukocytes are present early in tumor and TME development, that tumor antigen-specific T cells are functionally suppressed before they are able to experience their cognate antigen[82]. When tumors develop in response to these immunosuppressive conditions, they prove to be exceedingly complicated to target clinically, but new strategies have emerged that are more able to target these suppressive features[83, 84].

The human immune system is largely responsible for eliminating threats to the body, whether it be foreign pathogens or our own cells undergoing malignant transformation. However, a key hallmark of cancer development is the ability to evade the immune response. Many components of the immune system that are required in a normal immune response for clearing immune cells that have completed their function or suppressing excess inflammation is damaging to healthy tissue are beneficial to the survival of cancer cells, many of which develop mechanisms to utilize these components to their benefit. Inhibiting these necessary immunosuppressive components can be dangerous to the overall function of the immune system, so understanding how to target the immune evasion mechanisms of tumor cells safely and effectively is an important field in the progression of cancer therapeutics research.

1.4. Immune checkpoint blockade therapy and resistance mechanisms in cancer

1.4.1. Fundamentals of immune checkpoint blockade for the treatment of cancer

The immune system is tightly regulated by complex mechanisms that control proper immune cell activation, function, and eventual elimination following the execution of their effector activity. An important regulatory component of the immune system involves immune checkpoints (ICs), which are a class of receptor-ligand pairs that are expressed on immune cells, APCs, and other cell types. Several IC receptors have been well-characterized and targeted therapeutically in pre-clinical models or in patients. These include, but are not limited to, CTLA-4, PD-1, BTLA, TIM-3, and LAG-3, and they can have either inhibitory or stimulatory functions[85](Figure 1.2). ICs are an important component for maintaining another aspect of T cell tolerance by rendering T cells anergic that have been active for an extended time, which could otherwise eventually cause excessive inflammation and damage to healthy cells and tissues[86]. T cells are induced to express inhibitory immune checkpoint receptors following TCR activation, which can promote inhibitory signaling within the T cell upon interacting with their ligands. ICs can also compete with co-stimulatory receptors and ligands to further dampen T cell responses after activation[87]. The ligands for IC receptors can be ubiquitously expressed on APCs, as well as by tumor cells as a mechanism of immune evasion. Cancer immunotherapy was named Science Magazine's "Breakthrough of the Year" in 2013, highlighting the contributions of Steven Rosenberg and Carl June to chimeric antigen receptor (CAR) T cell therapy, and the successes of immune checkpoint blockade in clinical trials[88-94]. In 2018, the Nobel Prize in Physiology or Medicine was jointly

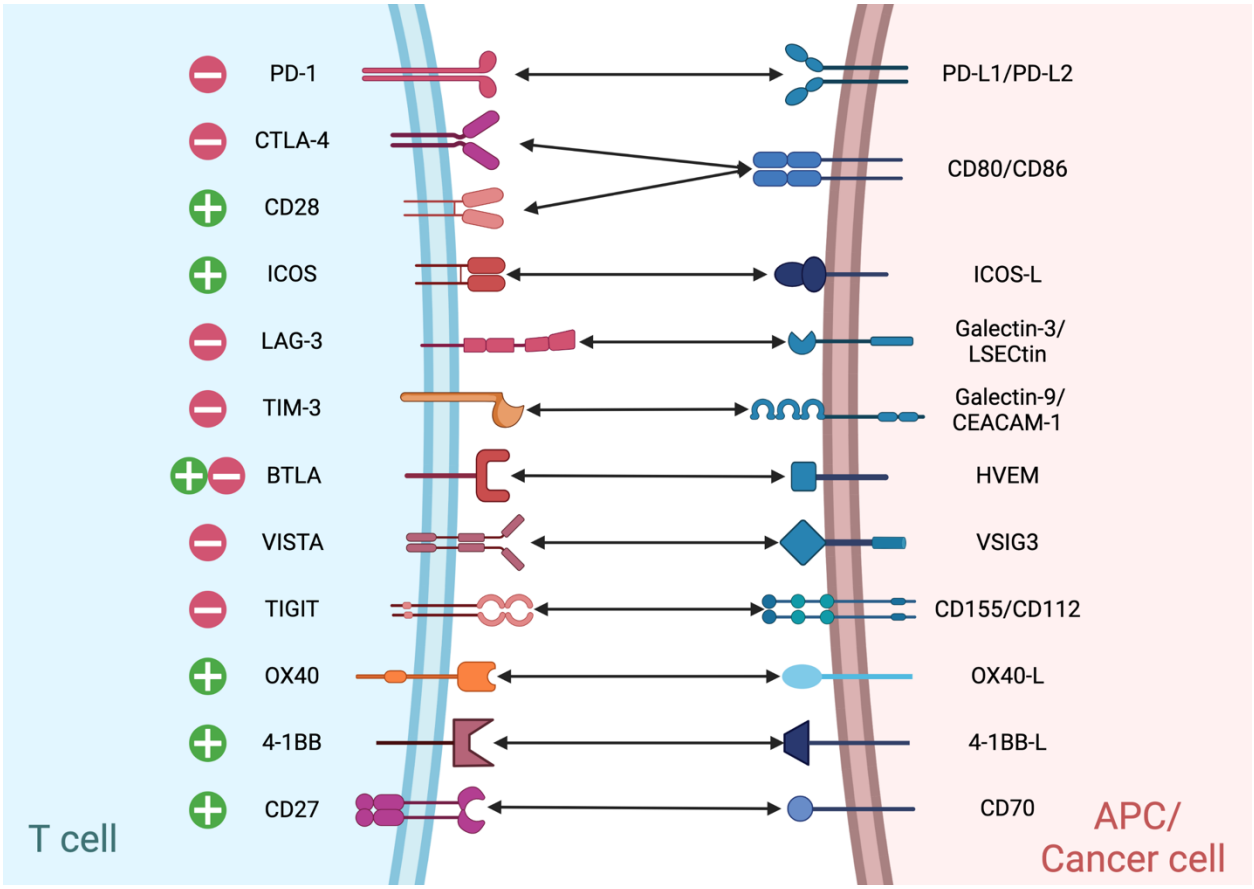

Figure 1.2. Immune checkpoints in the human immune response. T cell activation is mediated by receptor-ligand interactions with antigen-presenting cells. Interactions that stimulate T cells are indicated by a green plus sign, while interactions that suppress T cell activity are indicated by a red minus sign. The inhibitory receptor-ligand binding mediate self-tolerance and minimize tissue damage during normal immune responses, but many cancer cells upregulate these pathways to suppress antitumor T cell responses.

awarded to James Allison and Tasuku Honjo, who identified the functions of CTLA-4 and PD-1, respectively. Based on their work delineating the roles of these proteins in immune suppression, the field of immunotherapy was revolutionized[95, 96]. Targeting ICs therapeutically proved successful for patients in several solid tumors including non-small cell lung cancer (NSCLC), melanoma, and renal cancer[97, 98]. Many tumors use the expression of immune checkpoint ligands to prevent effector T cells from eliminating cancer cells by prematurely suppressing cytotoxic T cell activation and function. Fortunately, IC receptors and their ligands are surface-expressed and are easily targeted by blocking antibodies, which have become a mainstay for cancer immunotherapy in patients with various solid tumors.

Two of the most frequently targeted immune checkpoint receptors are CTLA-4 and PD-1[99]. Cytotoxic T-lymphocyte-associated antigen 4 (CTLA-4) was the first IC receptor to be targeted therapeutically, and functions to compete with the co-stimulatory receptor CD28. CD28 on T cells binding to CD80 or CD86 is a critical costimulatory signal required for T cell activation following TCR stimulation. When CTLA-4 out-competes CD28 for ligand binding, T cell activity is weakened. CTLA-4 is also constitutively present on immunosuppressive T regulatory cells (Tregs), which can inhibit effector T cells through release of immunomodulatory cytokines and direct induction of effector T cell apoptosis by cytolysis[100]. Although it is primarily a T cell surface receptor, CTLA-4 expression can also be expressed on malignant cells, NK cells, B cells, and monocytes, and cancer-induced inflammation can support an immunosuppressive microenvironment rich in CTLA-4-positive Tregs[101, 102]. CTLA-4^{+} Tregs also limit CD80/86 expression by APCs and promote dendritic cell apoptosis as methods of immune suppression[103-105]. Inhibition of CTLA-4 by receptor-blocking antibodies has demonstrated efficacy in melanoma, resulting in its FDA-approval for these tumors[90, 106].

The expression of programmed cell death protein-1 (PD-1) on T cells is induced following activation. When PD-1 interacts with its ligands PD-L1 or PD-L2, PD-1 disrupts signaling downstream of activated TCRs and co-stimulatory receptors, and T cells are driven to exhaustion, anergy, or apoptosis to clear the effector response[107]. PD-1 expression on T cells is induced following activation, and PD-1$^+$ Tregs are selectively increased among TILs[108-110]. PD-1 can also be found on B cells and monocytes[111]. The expression of PD-1 is higher on tumor-infiltrating T cells than T cells in the periphery and is much higher on tumor antigen-specific TILs than on T cells that infiltrate other normal tissues, which suggests that factors in the tumor microenvironment support enhanced PD-1 expression within tumors[110]. These cells are also typically functionally impaired, with upregulation of PD-1 contributing to decreased antigen-specific CD8$^+$ T cell production of IL-2, a cytokine that is necessary for T cell proliferation and function, leading to T cell anergy[107]. PD-L1 expression on APCs can be largely induced by cytokines including IFNγ, indicating that the PD-1/PD-L1 signaling axis is initiated following functional effector T cell activity[112]. However, many tumors can upregulate the expression of PD-L1 on their own as an immune evasion mechanism to stimulate PD-1 on effector T cells and prematurely attenuate antitumor activity. In addition to APCs and cancer cells, PD-L1 can be expressed on other components of the tumor microenvironment (TME), including suppressive myeloid cells and CAFs, in order to further limit T cell antitumor activity[113].

Increased expression of PD-1 and PD-L1, as well as other immune checkpoints, correlates with poor patient outcomes in many cancers, and several blocking antibodies targeting their interaction are available in the clinic. These antibodies have been critical for advancing immunotherapy, especially in tumors that are highly infiltrated by PD-1$^+$ lymphocytes. Antibodies that target either PD-1 or PD-L1 are both capable of inducing T cell mediated tumor clearance. PD-L2 is also a

ligand for PD-1 that can be targeted to sufficiently inhibit PD-1 signaling; however, even though it is expressed on tumors, activated T cells, stromal cells, and APCs, it is not as broadly expressed across tissue as PD-L1 and is therefore not as attractive of a target[112, 114, 115]. PD-L1 expression is also used as a biomarker to predict response to anti-PD-1 therapy, since patients with high PD-L1-expressing tumors like non-small cell lung cancer (NSCLC) are more likely to have better clinical responses to PD-1 or PD-L1 blockade[116].

1.4.2. Mechanisms of resistance to immune checkpoint blockade

While ICB has shown efficacy in a number of solid tumors, the success is still often limited to subsets of patients. For example, analysis of 428 metastatic melanoma patients who received ICB showed only 77 patients (18%) achieved ongoing complete response[117]. Unfortunately, there are many resistance mechanisms to ICB, both primary and acquired, that greatly limit the potential of these therapies for a broader patient population[118]. Patients with primary or intrinsic resistance either do not respond to ICB therapy or at best achieve partial response or stabilization of disease. Resistance to ICB is conferred by both tumor intrinsic and extrinsic mechanisms[119]. A significant hallmark of primary resistance to immunotherapy is the inability of activated tumor antigen-specific T cells to infiltrate the tumor and elicit their anti-tumor effector functions[120, 121]. $CD8^+$ T cells are an important target of ICB therapy, with the focus being on promoting tumor infiltration and restoring tumoricidal capabilities. Additional immune cells that are exploited during immune evasion can also be targeted by immunotherapeutic approaches, particularly by reducing the immunosuppressive mechanisms of MDSCs, macrophages, NK cells, and Tregs[122-124]. As previously described, Tregs regularly function to control $CD4^+$ and $CD8^+$ T cell responses to prevent autoimmunity, but increased populations of Tregs are often found in the TMEs and even within tumors of ICB-resistant cancers, including NSCLC and melanoma, where they secrete

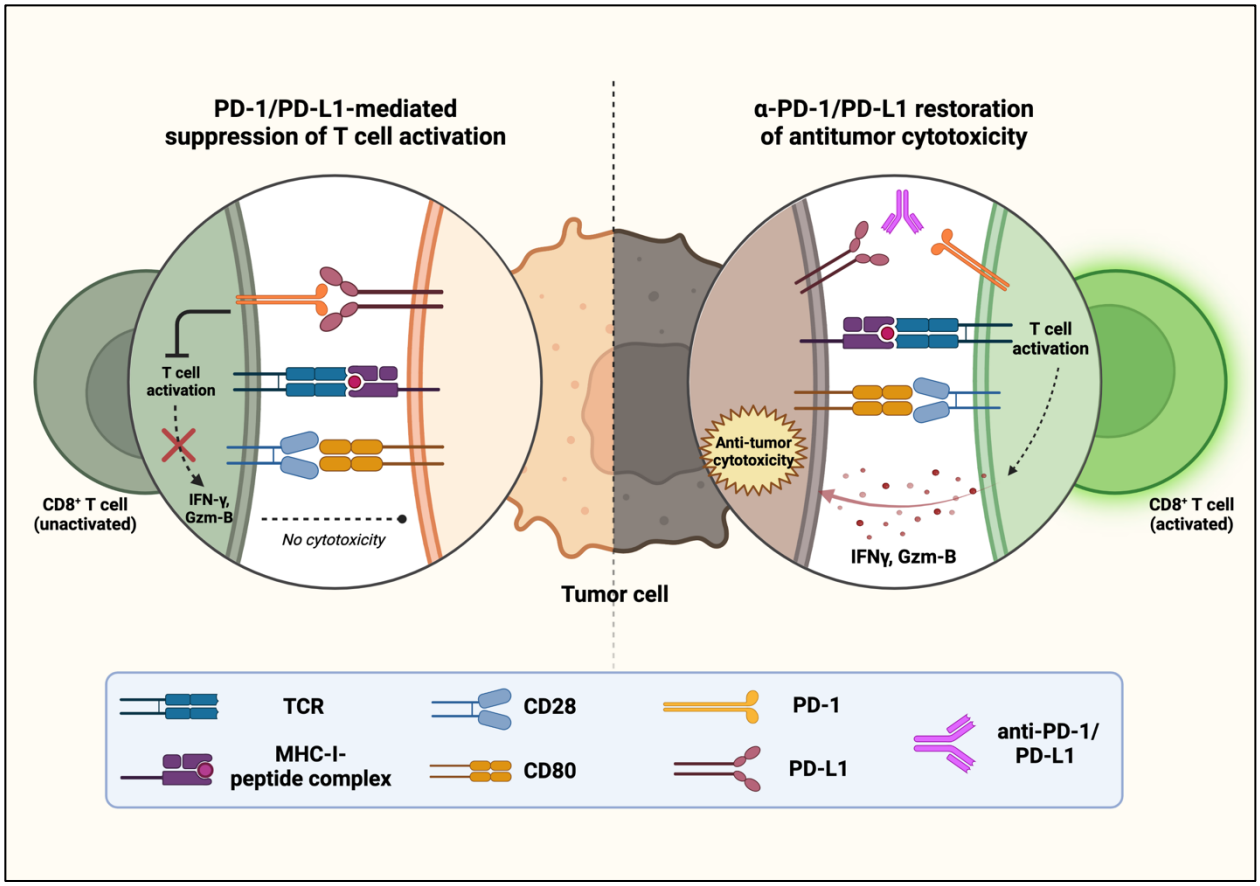

Figure 1.3. Immune checkpoint blocking antibodies for the treatment of cancer. The inhibitory immune checkpoint receptor PD-1 suppresses $CD8^+$ T cell activation following TCR stimulation, limiting the production of cytotoxic cytokines like IFN-γ and granzyme B. Tumors upregulate the expression of the ligand PD-L1, contributing to premature suppression of antitumor T cell responses. A neutralizing antibody for either PD-1 or PD-L1 disrupts the interaction between this ligand and receptor pair, which can restore T cell effector function and tumor-directed cytotoxic activity.

immunosuppressive factors to inhibit T cell activity[123, 125]. Their role in suppression of immune responses to tumors has been confirmed in studies where depletion of Tregs contributes to better antitumor activity in a number of cancer models[80, 125, 126]. Given that an important goal of ICB is to reinvigorate dampened antigen-specific T cell activity, these suppressive cells and other tumor-intrinsic properties create an environment that excludes functional effector T cells that must be present in order for ICB therapy to be effective.

Patients who develop acquired resistance to immune checkpoint blockade will initially experience response to therapy followed inevitably by progression of disease. Even in melanoma, which is arguably the most treatable cancer by ICB, only around one-third of patients receiving anti-PD-1 therapy have an objective response rate, and in one study only 44% of patients had a durable response lasting greater than one year[127]. A type of acquired resistance, sometimes known as adaptive resistance, is somewhat unique to immunotherapy[121]. Regarding PD-1/PD-L1 targeted therapy, the expression of these markers is not uniform across cells, both tumor cells and immune cells. Varied expression of PD-L1 among tumor cells, for example, will limit the efficacy of anti-PD-L1 therapy, as it cannot target cells that lack adequate PD-L1 expression. Therefore, unaffected cells are able to survive and repopulate a tumor after treatment-sensitive cells are cleared[128]. Additionally, some immunotherapies induce further cellular changes that limit treatment efficacy, including upregulation of additional checkpoint molecules as an inhibitory feedback mechanism, and IFN-γ produced by re-activated $CD8^+$ T cells contributing to modified gene expression in tumor cells[129]. Most importantly, effector T cells reinvigorated by ICB therapy are often epigenetically unstable, leading to deficiencies in the development of effector memory cells that are necessary for durable responses[130]. Effector T cells will only be reactivated for the duration of therapy, which can have potent anti-tumor effects, but without the establishment of a population

of memory cells, T cells will become exhausted again and be unable to control the outgrowth of persistent tumor cell subclones.

Due to tumor heterogeneity and the rate of mutation in some cancers, it has become increasingly apparent that complete elimination of most tumors cannot be accomplished with one line of treatment. Immunotherapy alone does have potential for durable complete responses in some patients, but the addition of other forms of therapy to target specific resistance mechanisms or molecular characteristics have been widely investigated in the clinic[95, 131-134]. In addition to ICB, patients may also require further immune stimulatory agents, drugs targeting specific genetic mutations or signaling pathways, or standard chemotherapeutic and radiation treatments. Development of these combinations is largely supported by the growing field of personalized medicine, and individuals that relapse with the same cancer type can receive different courses of treatment depending on the mechanisms of resistance that they experience. This has especially been made possible with advanced diagnostic and sequencing techniques that allow for the identification of the vast array of unique characteristics that a tumor can possess.

1.5. Biliary Tract Cancers – Epidemiology, molecular basis, tumor microenvironment

Biliary tract cancers (BTCs) are a heterogenous group of malignancies originating in the bile ducts, gallbladder, and liver. BTCs are comprised of cholangiocarcinomas (CCA), which arise in the intrahepatic, perihilar, or distal biliary tree, and gallbladder cancer (GBC). Cholangiocarcinomas account for 3% of all gastrointestinal malignancies and are the second most common class of liver cancers[135]. Overall, biliary tract cancers are rare, but incidence varies widely by geographic location due to a range of risk factors and has increased globally. Incidence and severity also vary by anatomic subtype, but collectively BTCs have only a 5-year survival rate of less than 10% in

the United States. Surgery remains the only curative treatment option for patients with BTC, however nearly three quarters of patients present with unresectable or metastatic disease, and patients eligible for surgery are highly susceptible to relapse[136, 137]. Systemic treatments have been difficult to develop for BTC due to mutational variation among the patient population, heterogeneity of tumor subtypes, and tendencies for chemoresistance.

1.5.1 Physiological classification and risk factors

Genetic predisposition contributes to BTC development in some patients. However, there are few genetic signatures common among patients that could define BTC, with substantial heterogeneity present among BTC anatomic subtypes and geographic distribution of patients (Figure 1.3)[138-140]. Several studies have utilized next-generation sequencing techniques for the genetic profiling of biliary tract tumors and have found aberrations in many key oncogenic pathways. Variants of TP53, KRAS, CDKN2A/B, and PIK3CA have been identified across all subtypes of BTC, but the frequencies at which they occur vary widely across studies and subtypes[141-143]. Other genetic alterations are more common in one or some subsets of BTC, but not distinctly enough to be diagnostic. However, certain signatures like BRAF and KRAS mutations have been used to distinguish BTC from hepatocellular carcinoma (HCC), which rarely present with these mutations themselves[144, 145]. Two highly prevalent genetic aberrations in BTC, IDH1/2 mutations and FGFR2 fusions, are found almost exclusively in intrahepatic cholangiocarcinoma (iCCA) [146, 147]. They are among the most recognized mutations in BTCs, since iCCA is the predominant subtype, but with IDH1/2 mutations occurring in less than 30% of patients and FGFR2 fusions in only 15% they are infrequent enough for consideration as defining mutations in iCCA[148].

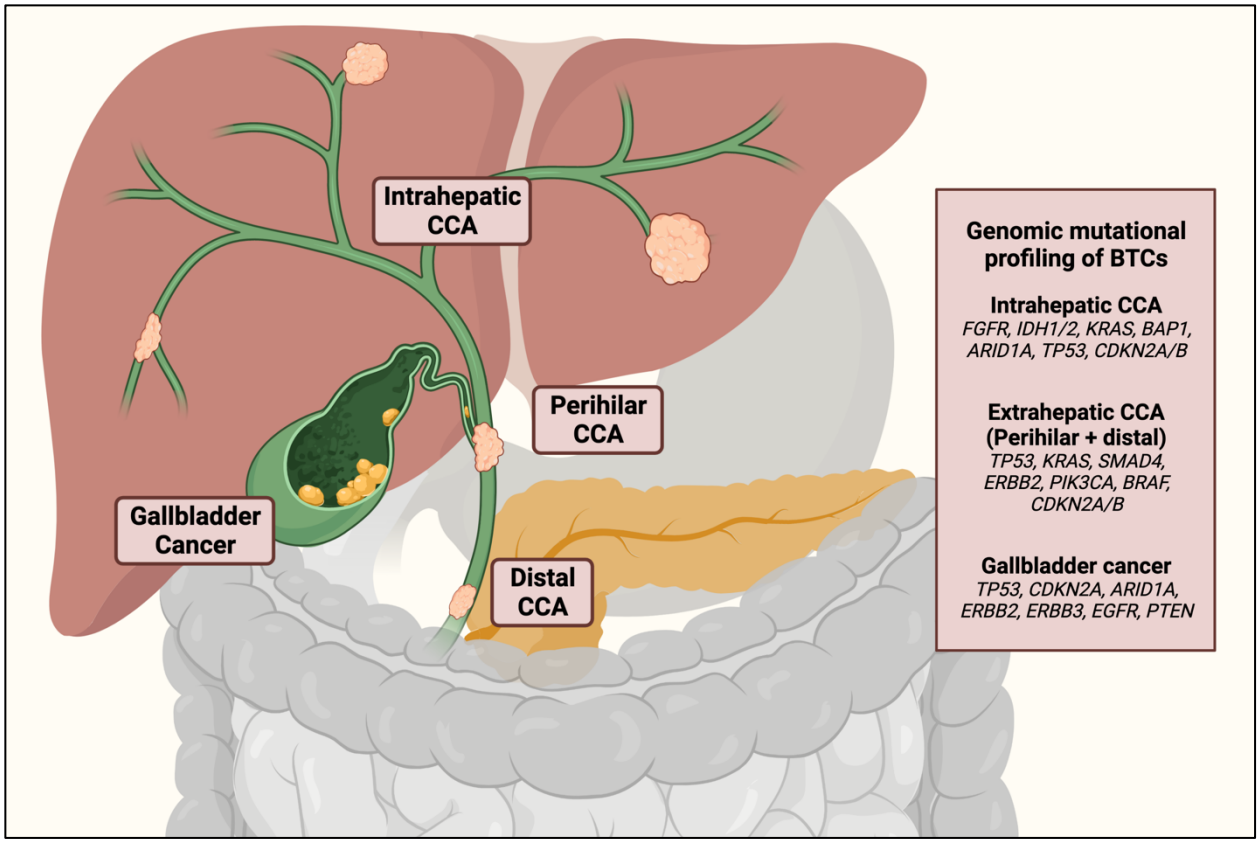

Figure 1.4. Anatomic subtypes of biliary tract cancer. Biliary tract cancers are classified by the location in the biliary tract from which tumors arise. Intrahepatic cholangiocarcinoma (CCA) develops in the second-order bile ducts within the liver, perihilar CCA develops in the common hepatic ducts, and distal CCA develops in the common bile duct. Each subtype has distinct morphological and epidemiological characteristics, as well as mutational profiles. Some genetic aberrations can be found across all biliary tract cancer subtypes, while others are restricted to the anatomical classification, like IDH1/2 mutations and FGFR2 fusions which are nearly exclusive to intrahepatic CCAs.

More recently, understanding the heterogeneity among and even within subtypes of BTCs is further complicated by the finding that BTCs can arise from multiple cells of origin, leading to several physiologically distinct classifications[149, 150]. Initially, classification of biliary tract cancers was based on the region of the biliary tree the disease arose from, with the three main subtypes being iCCA, eCCA, and GBC. Over time, biliary tract cancers have been reclassified several times. Within extrahepatic CCAs, for example, distinct pathophysiological profiles were observed in even more specific areas of the biliary tract that they were further subdivided into perihilar (pCCA) and distal (dCCA). Intrahepatic CCAs have a number of subclassifications based on various features, though it is increasingly agreed upon that there are two distinct subtypes supported by pathophysiological features, genetic signatures, and immunophenotyping[151-153]. The first subtype, called large bile duct type, are mucin-producing tumors that harbor KRAS mutations and grow in a periductal infiltrating or intraductal growing pattern. The second subtype, called small bile duct type, are primarily mass forming tumors that arise from cholangiocytes and can be almost exclusively characterized by IDH1/2 mutations and FGFR2 fusions, but not KRAS mutations[73]. This subtype is also linked to viral infections and chronic liver disease, while the large bile duct subtype typically presents with more oncogenic mutations.

For patients without a clear genetic predisposition to BTC, there are several risk factors that contribute to an inflammatory microenvironment in the biliary tract. These risk factors can promote development of some or all subtypes of BTC, but there is significant geographical disparity in their prevalence that impacts the global incidence of BTC[154, 155]. Infections with liver flukes contribute to the substantial incidence of BTCs in Asian countries, where the rates of cholangiocarcinoma are as high as 113 per 100,000 people[156]. In contrast, patients in Western countries do not share a distinct environmental risk factor resulting in less frequent disease in these

regions. For example, Opisthorchis viverrini and Clonorchis sinensis are endemic liver fluke infestations in Thailand and other regions of Southeast Asia and result predominantly from the prolonged ingestion of raw or undercooked fish and shellfish[157, 158]. Persistent or repeated infections cause pathogenic changes to the biliary tract, chronic inflammation, and accumulation of fibrosis, all of which drive the malignant transformation of biliary epithelia[159].

While it is well known that liver fluke infestations account for a large majority of inflammation-related cholangiocarcinoma cases, Hepatitis C virus (HCV) infections have been linked to increasing incidence rates of cholangiocarcinoma worldwide[154, 160, 161]. The mechanisms by which HCV leads to CCA development have yet to be clearly defined, but a few theories have emerged following meta-analyses of CCA patients[162]. HCV primarily infects hepatocytes, but it is believed that hepatocytes and cholangiocytes arise from a common hepatic progenitor, which may explain the susceptibility for CCA development[149, 163]. Viral-associated chronic liver injury is also typically linked to the epithelial-mesenchymal transition (EMT) mechanism, which is the process by which an epithelial cell undergoes several biological changes to morphologically adopt a mesenchymal-like phenotype, with an increased ability to migrate, replicate, and invade[164]. EMT is a significant component for the "activating invasion and metastasis" hallmark of cancer and has been found to be induced in hepatocytes by HCV infection[51, 165].

1.5.2. Tumor immune microenvironment of BTC

BTC development and progression is largely supported by the unique immune microenvironment of the liver. The liver has its own complex immune features and plays a dominant role in combating foreign pathogens, especially since it processes both arterial and venous blood. Blood also tends to flow quite slowly through the liver, passing through the capillary-like vessels called sinusoids, which allows for more prolonged interactions between pathogens and immune cells. The liver is

home to unique subsets of innate and adaptive immune cells, including natural killer cells, dendritic cells, liver sinusoidal endothelial cells (LSECs), and tissue-resident macrophages called Kupffer cells[166]. The liver is not typically considered a secondary lymphoid organ but has a pivotal role in supporting the adaptive immune response. Most of the previously mentioned cell types serve as antigen presenting cells (APCs) and produce large amounts of chemokines to recruit adaptive immune cells, neutrophils, and monocytes rapidly into the liver. However, millions of non-pathogenic microbes enter through the gut and are filtered through the liver that the immune response in the liver which remains tolerant toward their presence, carefully selecting only for pathogenic antigens. Unfortunately, this bias toward tolerance and immunosuppression creates an ideal microenvironment to support tumorigenesis and poor outcomes once tumors reach this organ as an end destination. In addition to HCC, the most common cause of cancer-related deaths worldwide, colorectal cancer (CRC) and other gastrointestinal cancers preferentially metastasize to the liver, likely due to its location downstream of blood flow and drainage from the colon as well as the slow movement of blood through the sinusoids that may trap cancer cells within the liver[167]. The liver is also prone to chronic inflammation and tissue damage, which can further exacerbate the immunosuppressive tendencies of the liver microenvironment that are ideal for tumorigenesis and metastasis.

Cholangiocarcinoma, especially iCCA, is largely supported by the immunosuppressive properties of the liver, as well as the highly dense desmoplastic TME associated with this tumor[168]. Desmoplasia is characterized by the presence of fibrous stromal cells and innate immune cells that produce many pro-tumorigenic factors to create an ideal environment for cancer development and progression. One features of the BTC TME is its exclusion of T lymphocytes from infiltrating tumors – a hallmark of tumor immune evasion described earlier. In general, BTCs have less

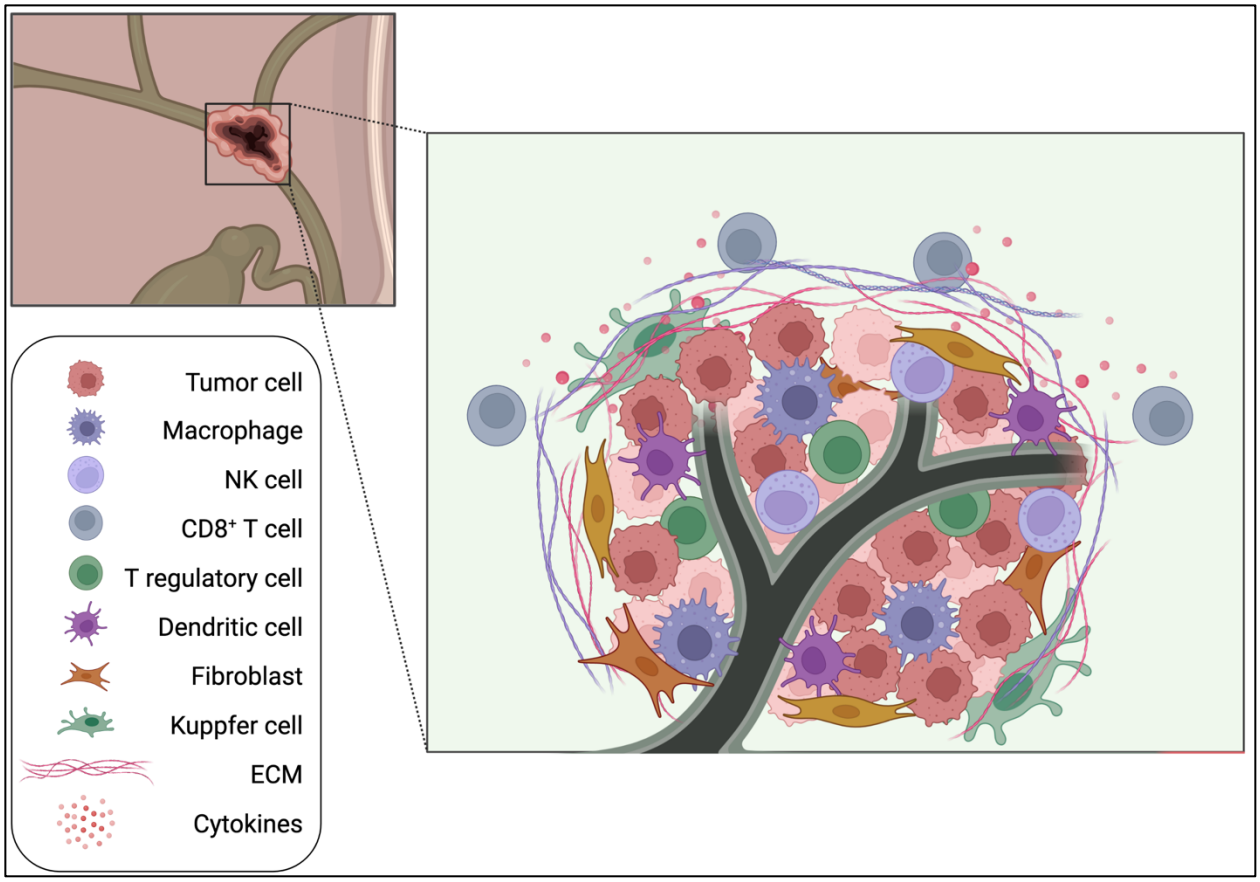

Figure 1.5. The tumor microenvironment of biliary tract cancer. Immunosuppressive cells, including T regulatory cells and tumor-associated macrophages, as well as a dense, fibrotic stromal compartment are characteristic of biliary tract cancers. This suppressive microenvironment largely excludes antigen-specific $CD8^+$ T cells, which are commonly found around the margins of these tumors. Thus, biliary tract cancers are difficult to manage with immune checkpoint blockade therapy, which requires close interactions between $CD8^+$ T cells and antigen-presenting tumor cells.

abundant $CD8^+$ T cells, but conversely prominent Tregs, and the ratio of $CD8^+$ T cells to Tregs is much lower than in normal surrounding tissue[169]. BTCs are also characterized by increased populations of MDSCs and TAMs, and few conventional dendritic cells (cDCs), which correlate with reduced clinical outcomes[170-173]. BTC tumor cells themselves can produce cytokines and other molecular signals to support the desmoplastic TME and recruit the immunosuppressive cells that promote the exclusion of cytotoxic T cells. Advanced therapeutic approaches in addition to immune checkpoint blockade are currently being investigated to target these immunosuppressive cell populations and restore cytotoxic T cell infiltration for durable antitumor responses in advanced BTC.

Success has been limited in the development of effective treatment strategies for advanced biliary tract cancers. BTCs have a dense stroma and immunosuppressive tumor microenvironment that is characteristically difficult to access and overcome, but successes in other malignancies have paved the way for new therapeutic strategies to be explored in this disease. Progress has especially increased in the investigation of targeted therapies as the field moves toward a more personalized approach for treatment and clinical management, with particular focus on oncogenic pathways that contribute to BTC tumorigenesis.

1.6. Ras/Raf/MEK/ERK Pathway in cancer development, progression, and anti-tumor immune responses

Mitogen activated protein kinase (MAPK) signaling cascades play vital roles in many cell survival and proliferation pathways. There are four canonical MAPK pathways, each made up of three-tiered kinase cascades: Jun N-terminal kinase (JNK) 1/2/3, p38/Akt, ERK1/2, and ERK5[174]. These kinase cascades are often initiated downstream of growth factor receptor tyrosine kinase (RTK)

binding of a mitogenic substrate, and successive phosphorylation events activate each step of the pathway (Figure 1.6). A mitogen is a small peptide or protein that initiates the process of cell division known as mitosis. The ERK pathways function primarily in cell growth, differentiation, and proliferation, while the JNK and p38 pathways are activated as stress responses and function in inflammatory and apoptotic pathways. The Ras/Raf/MEK/ERK cascade is notable in tumor development and progression, where approximately one-third of all cancers harbor activating mutations in this pathway[175]. A prominent example of a cancer-related RTK that has downstream Ras/Raf/MEK/ERK signaling is the epidermal growth factor receptor EGFR. Activation of the receptor stimulates the activation of the Ras family of small guanosine triphosphatases (GTPases), which mediates the activation of Raf serine/threonine kinases. Raf subsequently phosphorylates MEK1 and MEK2, whose activation initiates the phosphorylation of the ERK1 and ERK2 MAPKs[176]. These MAPKs either remain in the cytoplasm or translocate into the nucleus and have a plethora of functions critical to cell development, growth, and survival, since there are several hundred direct phosphorylation targets of ERK1/2 that have been identified to date[177-180].

1.6.1. Functions of oncogenic Ras signaling in tumor development

The Ras/Raf/MEK/ERK signaling axis has become one of the most well-characterized oncogenic pathways in several tumor types. For example, aberrant activating mutations in this pathway are found in more than 90% of pancreatic cancers and 70% of melanomas[181]. The constitutive activation of MEK and ERK are often associated with human cancer progression, but the mechanisms leading to this phenotype are complex given that activating mutations in these two proteins that impact their function as kinases have yet to be identified. Rather, genetic mutations in genes encoding upstream pathway components like Ras, Raf, and other signaling proteins are

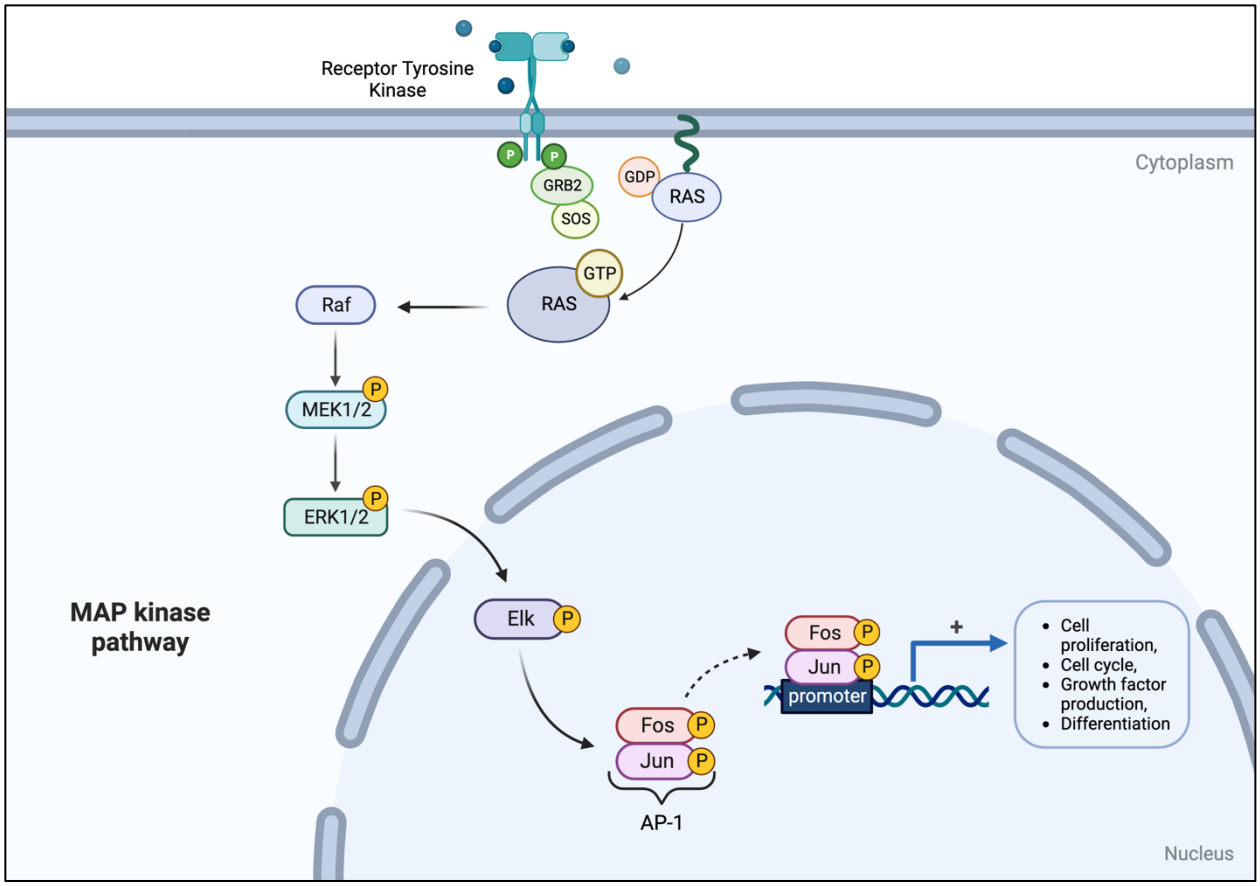

Figure 1.6. The Ras-Raf-MEK-ERK signaling pathway. The canonical Ras-MAPK signaling pathway is a kinase cascade that controls cellular proliferation and survival. Ras signaling is initiated at receptor tyrosine kinases, G-protein coupled receptors, or integrin receptors by guanine exchange factors, which exchange GDP for GTP. Ras then activates Raf, which initiates a phosphorylation cascade of MEK1 and MEK2 to ERK1 and ERK2. Activated ERK can translocate into the nucleus, where it phosphorylates a large number of transcription factors that regulate the expression of genes required for cell proliferation, differentiation, metabolism, and survival.

responsible for the aberrant activation in this pathway. To target the uncontrolled signaling, Raf and MEK inhibitors have long been used clinically with some success, while until recently, Ras has traditionally been considered to be undruggable. As a result, inhibition of MEK has emerged as a viable strategy for controlling ERK activation as its only known kinase. Ras/MAPK-dependent cancers are highly susceptible to the development of resistance to Raf- and MEK-targeted therapies, due to the nature of this pathway to utilize feedback mechanisms and interactions with other pathways that compensate for any loss of signaling. The ERK/MAPK pathway is also not as isolated and linear as is often depicted, with frequent cross-talk occurring with the PI3K/AKT and the JAK/STAT signaling pathways, which are also subject to oncogenic mutations that may influence the downstream activation of MAPKs. Combinations of PI3K and MEK pathway inhibitors have been investigated as a method of controlling resistance to MAPK pathway inhibition – with promising in vitro evidence – but these combinations have yet to progress past phase I clinical trials[182, 183].

Given that the primary functions of MAPKs are regulation of cell proliferation and survival, this signaling pathway provides immense benefit for many cancers when commandeered by tumors for uncontrolled growth and survival. This pathway directly supports several of the hallmarks of cancer, including sustaining proliferative signaling, resisting cell death, and evading growth suppressors[51]. More specifically, ERK signaling is required for the G1/S phase transition of the cell cycle due to the direct role for ERK on activating transcription factors, ultimately leading to the production of Cyclin D1[184]. Raf kinases also have direct roles in controlling cell survival, independent of MEK/ERK activation, including preventing apoptosis through inhibition of the degradation of Mcl-1 in CCA[185]. Generally, however, upregulation of this pathway is seen as an

initiating step to further mechanisms of tumorigenesis, particularly due to the role that phosphorylated ERK has on activating a diverse set of transcription factors.

1.6.2. Immunological implications of MEK/ERK signaling

Aside from the importance of Ras-MAPK signaling in tumor cell proliferation and survival, MEK/ERK activation is also essential to cells involved in the immune response. While this pathway is ubiquitous to all mammalian cells, Ras/Raf/MEK/ERK signaling is certainly initiated by TCR stimulation in T cells and is crucial to their proliferation and activation. ERK also activates Nur77, a transcription factor that mediates T cell apoptosis following TCR stimulation[186]. This is critical in the process of negative selection of naïve T cells that exhibit excessive affinity for TCR ligands, as well as regulating the clearance of exhausted activated T cells, with the latter having an important role in the immune response to cancer. As previously discussed, chronic antigen stimulation is a key characteristic of tumor immune evasion, but MEK inhibition has been shown to limit Nur77-mediated T cell apoptosis to potentially retain antigen-experienced T cells in the tumor microenvironment to support immunotherapeutic approaches[187]. Dysregulated MAPK signaling has also been linked to a loss of tumor control mechanisms in the immune response, with activating genomic alterations in this pathway correlating with increased metastasis and reduced TILs in breast cancer[188]. Most notably, MEK mediates MHC-I and PD-L1 expression and the production of immunosuppressive factors via IFN-γ, which has been observed in several tumor models investigating MEK inhibition[133, 189-192]. While MEK inhibition can restore T cell responses, it can also have negative effects on T cells as well, including limiting the production of IFN-γ and inhibiting $CD8^+$ T cell priming[193]. These diverse roles of MAPK signaling in the immune response add complexity to the use of pathway inhibitors in the treatment of MAPK-driven cancers, especially those supported by an immunosuppressive microenvironment.

1.7. Therapeutic development in BTC – clinical trials and roadblocks to overcome

Biliary tract cancer is frequently diagnosed at advanced stages when potentially curative surgical resection is not possible. For more than a decade, first line treatment for advanced BTC consisted of a combination of gemcitabine and cisplatin (GemCis), a chemotherapy combination used in treating several other cancers. GemCis was shown to be superior to gemcitabine alone in the phase III ABC-02 trial, with tumor control achieved in 81.4% of combination treated patients versus 71.8% of single agent treated patients[194]. However, the median overall survival rate for this combination in advanced BTC is still less than one year[195]. Recently, the addition of durvalumab to GemCis earned FDA approval as the new standard of care for advanced BTC patients[196, 197]. Other chemotherapy regimens have also been investigated as first line treatments for advanced BTC in several clinical trials, including FOLFIRINOX and GemCis plus nab-paclitaxel, but disease progression is still frequent and further investigation into improving the standard of care is ongoing[198, 199].

1.7.1. Molecular targeted treatment strategies for BTC

The substantial genetic basis for biliary tract cancer development has enabled significant investigation into targeted therapies. Most of the frequently identified genetic aberrations in BTCs have not been successfully targeted by molecular therapeutic approaches. To date, the only candidates with FDA-approved precision medicine therapies for cholangiocarcinoma are IDH1/2 and FGFR2-fusions, but these mutations are almost exclusive to iCCA and present in only relatively small subsets of patients[200]. Around 15% of BTC patients have mutations in DNA damage repair pathway genes that can be best targeted using PARP inhibitors, though investigations into these drugs in BTC are still premature[201]. Additional genetic alterations targeted

by clinically available drugs but have had limited success in BTC management include HER2 (ERBB2), members of the PI3K/Akt/mTOR pathway, and members of the Ras/Raf/MEK/ERK pathway, with the latter receiving the most notable attention and potential for improvement[141, 202, 203].

MAPK signaling is frequently dysregulated in BTCs and has emerged as an attractive target for molecular therapy. KRAS mutations are present in up to 19% of iCCA and have been identified in all anatomic subtypes of BTC[204]. TGFβ-mediated ERK1/2 activation has been associated with epithelial to mesenchymal transition in BTC cell lines, contributing to tumor growth and invasiveness[205]. Constitutive activation of the Ras-MAPK pathway is a feature of many tumors that confers resistance to TGF-β induced cell cycle arrest[206]. In BTC, MEK inhibitors have enabled durable partial responses and stable disease and combining MEK and BRAF inhibitors have resulted in objective response rates of approximately 50%[207-210]. Additionally, selumetinib was found to reverse cancer cachexia related muscle loss in BTC patients, despite low tumor responses[211]. Many further clinical trials have either been conducted or are ongoing that investigate the use of MEK inhibitors in combination with other targeted therapies or immunotherapy in order to improve overall response in BTC patients (Table 1.1).

1.7.2. Progress in immune checkpoint blockade development for advanced BTC

The most important therapeutic developments for biliary tract cancer management utilize immune checkpoint inhibitors. As single agents, immune checkpoint inhibitors have been largely disappointing in the control of advanced BTCs, unless patients were preselected for certain characteristics like microsatellite instability (MSI)[212, 213]. PD-L1 expression is variable in BTC tumors and is commonly used as a biomarker for response to ICB in some cancer models, but has not emerged as a reliable marker in BTC[214]. For example, out of 104 patients enrolled in the

KEYNOTE-158 trial investigating PD-1 blockade in BTC, 58.7% of patients had PD-L1-expressing tumors, but less than 6% of all patients had an objective response to treatment[212]. With the significant exclusion of effector T cells from BTC tumors, ICB has very little room to elicit effective anti-tumor responses. Fortunately, combination treatment strategies with immunotherapy and chemotherapy or molecular targeted therapy have exhibited more promise for controlling advanced BTC (Table 1.2)[215]. There is evidence to support that chemotherapy may enhance immunotherapy in tumors with dense stroma by reducing immunosuppressive cells like Tregs and promoting immune cell infiltration into tumors[216]. This was recently confirmed in the TOPAZ-1 trial where advanced BTC patients receiving durvalumab (anti-PD-1) with GemCis had a 26.7% ORR compared to 18.7% ORR with GemCis alone, potentially giving rise to a new standard of care for advanced BTC[197].

With the knowledge that overactive MEK/ERK signaling contributes to an immunosuppressive TME, combinations of Raf and MEK inhibitors with immunotherapy have been of interest in several tumor models, including BTC[188, 217-221]. The rationale for combining these inhibitors with ICB is supported by a number of preclinical studies, both in BTC and related malignancies. In a murine model of colorectal cancer (CRC), the MEK inhibitor cobimetinib induces $CD8^+$ T cell infiltration into tumors, limits Nur77-mediated T cell apoptosis, and synergizes with PD-L1 blockade to significantly reduce tumor burden[187]. In a KRAS-wild type model of iCCA, the MEK inhibitor trametinib upregulates MHC-I and PD-L1 expression, increases effector $CD8^+$ T cells in the liver, and significantly improves tumor burden and survival when combined with PD-1 blockade[222]. This study also demonstrated that combination MEK and immune checkpoint inhibition can be effective regardless of activating KRAS mutational status, a key indication for introducing this therapeutic combination to a broader BTC patient population. In the clinic, these

combinations have only produced modest results across tumor types. For BRAFV600-mutant melanoma, a triple combination of durvalumab, dabrafenib, and trametinib had a nearly 70% objective response rate with evidence of improved immune cell tumor infiltration[223]. The phase III IMblaze 370 clinical trial in metastatic CRC utilized atezolizumab with or without cobimetinib and did not observe any significant differences in overall response or ORR between groups, a disappointing result in the progression of combining MEK inhibitors with ICB[218]. Excitingly, however, the same combination was investigated by our group in patients with advanced BTC and met its primary endpoint of improved progression-free survival (PFS) in those receiving the combination of atezolizumab and cobimetinib versus atezolizumab alone, although OS was not improved in either group[221]. Exploratory analysis of paired tumor biopsy samples showed that combination treatment increased CD8 T cell/Treg ratios, demonstrating an improvement to cytotoxic T cell infiltration over immunosuppressive Tregs. Interestingly, analysis of peripheral blood mononuclear cells (PBMCs) revealed that combination treatment limited $CD8^+$ T cell activation compared to PD-L1 blockade alone, with no fold change in T cell activation phenotypic markers from baseline to day 15 of treatment, indicating that systemic MEKi limits T cell activation[224]. Fortunately, this effect can be overcome with the addition of a T cell agonist against 4-1BB or CD27, which can promote enhanced T cell activation when combined with MEKi and ICB compared to dual MEK/PD-1 inhibition[224]. A follow up clinical trial is ongoing that investigates the addition of an agonist for CD27, a costimulatory molecule similar to CD28 that supports T cell expansion and survival following TCR engagement, to the dual blockade of MEK and PD-L1 (NCT04941287).

Based on the available data, biliary tract cancers continued to be difficult to manage, especially when reaching advanced disease stages. Encouraging results have emerged in recent clinical

investigations highlighting that effective therapeutic strategies are on the horizon, especially in the field of combination immunotherapy. BTCs have garnered significantly more attention in recent years despite its reputation as a rare and untreatable group of malignancies, with a new first-line therapy finally emerging after over a decade without improvement. BTCs do harbor many resistance mechanisms that are still yet to be overcome, but understanding the drawbacks of previous clinical trials will help to guide the future development of successful treatment strategies.

1.8. Summary, scope, and goals for dissertation

In summary, understanding how to overcome immune evasion is an important area of research, especially in the context of treating rare malignancies like biliary tract cancers. BTCs are a notoriously "immunologically cold" cancer, with a highly immunosuppressive tumor microenvironment that is devoid of effector T lymphocytes. Immunotherapeutic strategies alone have not been widely successful across cancer types, but combinatorial approaches are of significant interest. For advanced BTC patient populations, targeting the Ras/Raf/MEK/ERK signaling pathway has been promising, regardless of genetic aberrations within this pathway, and combinations with immune checkpoint blockade have also been successful for some patient populations over single agent therapy. However, systemic administration of MEK inhibitors have uncovered unintended effects on immune cells that hamper their potential anti-tumor activity.

This dissertation investigates the role of MEK inhibition in the treatment of biliary tract cancers and the effects on the immune response, especially when combined with ICB. MEK inhibition promotes anti-tumor responses in other gastrointestinal cancers and mediates T cell infiltration into tumors, circumventing an immunosuppressive TME. However, MEK inhibitors can limit the function of T cells that are required for an effective response. Using both clinical and preclinical

approaches, we seek to identify and understand the mechanisms by which MEK inhibitors can elicit anti-tumor responses and synergize with anti-PD-L1 blockade therapy in the context of BTC. We find that the dual blockade of MEK and PD-L1, though modestly effective, uncovers additional targets for molecular therapy to develop more advanced combination therapies. Treatment options for advanced BTCs are extremely limited, but we anticipate that this work will support critical advances in the development of effective treatment strategies for these patients.

1.9. Tables

Table 1.1. Completed clinical trials investigating MEK inhibitors in advanced biliary tract cancers

Study	Interventions (Target)	Disease Status	Phase	Size	Outcomes
NCT02042443/SWOG S1310[225]	Trametinib (MEK)	Advanced, refractory biliary tract cancer	II	24	ORR: 8% PFS: 1.4 months OS: 4.3 months
NCT01943864[226]	Trametinib (MEK)	Refractory biliary tract cancer	II	20	ORR: 0% PFS: 10.6 weeks OS: N/R
NCT00959127[209]	Binimetinib (MEK)	Unresectable, metastatic biliary tract cancer	I	26	ORR: 8% PFS: 2.1 months OS: 4.8 months
NCT02151084[227]	A: GemCis + selumetinib (MEK) (cont.) B: GemCis + selumetinib (MEK) (seq.) C. GemCis	Unresectable, metastatic biliary tract cancer	II	A: 15 B: 17 C: 15	PR: 35% (A), 35% (B), 29% (C) PFS: 6.0 months (A), 7.0 months (B), 6.3 months (C) OS: 11.7 months (A), 11.7 months (B), 12.8 months (C)
NCT01828034[228]	Binimetinib (MEK) + GemCis	Unresectable, metastatic biliary tract cancer	I/II	35	ORR: 36% PFS: 6 months OS: 13.3 months
NCT00553332[208]	Selumetinib (MEK)	Advanced biliary tract cancer	II	28	ORR: 12% PFS: 3.7 months OS: 9.8 months
NCT032101458[221]	Atezolizumab (PD-L1) +/- cobimetinib (MEK)	Unresectable, metastatic biliary tract cancer	II	77	ORR: 2.8% (A), 3.3% (A+C) PFS: 1.87 months (A), 3.65 months (A+C) OS: N/R

GemCis: Gemcitabine + cisplatin; **ORR**: Objective response rate; **PFS**: Progression-free survival; **OS**: Overall survival; **N/R**: Not reported.

Table 1.2. Completed clinical trials investigating immune checkpoint blockade in advanced biliary tract cancers

Study	Interventions (Target)	Disease Status	Phase	Size	Outcomes
NCT02628067/KEYNOTE-158[229]	Pembrolizumab (PD-1)	Chemotherapy-refractory, MSI-H solid tumors	II	22	ORR: 40.9% PFS: 4.2 months OS: 24.3 months
NCT02628067/KEYNOTE-158[212]	Pembrolizumab (PD-1)	Chemotherapy-refractory, MSS solid tumors	II	104	ORR: 5.8% PFS: 2 months OS: 7.4 months
NCT02054806/KEYNOTE-028[212]	Pembrolizumab (PD-1)	Chemotherapy-refractory, PD-L1-positive tumors	Ib	24	ORR: 13% PFS: 1.8 months OS: 5.7 months
NCT02829918[213]	Nivolumab (PD-1)	Chemotherapy-refractory biliary tract cancer	II	54	ORR: 22% PFS: 3.68 months OS: 14.2 months
NCT01938612[230]	Durvalumab (PD-L1) +/- tremelimumab (CTLA-4)	Chemotherapy-refractory biliary tract cancer	I	42	ORR: 4.8% (D), 10.8% (D+T) PFS: 1.5 months (D), 1.6 months (D+T) OS: 8.1 months (D), 10.1 months (D+T)
NCT02923934[231]	Nivolumab (PD-1) + ipilimumab (CTLA-4)	Chemotherapy-refractory biliary tract cancer	II	39	ORR: 23% PFS: 2.9 months OS: 5.7 months
NCT03311789[232]	Nivolumab (PD-1) + GemCis	Unresectable or metastatic biliary tract cancer	II	32	ORR: 55.6% PFS: 6.1 months OS: 8.5 months
NCT03875235/TOPAZ-1[197]	GemCis +/- durvalumab (PD-1)	Unresectable biliary tract cancer	III	685	ORR: 26.7 (D+GC), 18.7% (GC) PFS: 7.2 months (D+GC), 5.7 months (GC) OS: 12.8 months (D+GC), 11.5 months (GC)
NCT03486678[233]	Camrelizumab (PD-1) + GemOx	Unresectable, metastatic biliary tract cancer	II	37	ORR: 54% PFS: 6.1 months OS: 11.8 months
NCT03796429/JS001-ZS-BC001[234]	Toripalimab (PD-1) + GemS-1	Unresectable, metastatic biliary tract cancer	II	48	ORR: 27.1% PFS: 7.0 months OS: 16.0 months
NCT02443324[235]	Pembrolizumab (PD-1) + Ramucirumab (VEGFR-2)	Unresectable, metastatic biliary tract cancer	I	26	ORR: 4% PFS: 1.6 months OS: 6.4 months
NCT03797326/LEAP-005[236]	Pembrolizumab (PD-1) + Lenvatinib (multi-TKI)	Unresectable, metastatic biliary tract cancer	II	31	ORR: 10% PFS: 6.1 months OS: 8.6 months
NCT03082895[237]	Camrelizumab (PD-1) + FOLFOX4 or GemOx	Unresectable, metastatic biliary tract cancer	II	92	ORR: 16.3% PFS: 5.3 months OS: 12.4 months

MSI-H: Microsatellite instability-high; **MSS**: Microsatellite stable; **ORR**: Objective response rate; **PFS**: Progression-free survival; **OS**: Overall survival; **GemCis**: Gemcitabine + cistplatin; **GemOx**: Gemcitabine + oxaliplatin; **GemS-1**: Gemcitabine + S-1; **FOLFOX4**: 5-fluorouracil, leucovorin, + oxaliplatin.

Chapter 2: Combined MEK/PD-L1 inhibition alters peripheral cytokines and lymphocyte populations correlating with improved clinical outcomes in advanced biliary tract cancer

2.1. Author's Contribution and Acknowledgements of Reproduction

This chapter is reproduced with minor edits from Amanda N. Ruggieri[1], Mark Yarchoan[2], Subir Goyal[3], Yuan Liu[3], Elad Sharon[4], Helen X. Chen[4], Brian M. Olson[1], Chrystal M. Paulos[5], Bassel F. El-Rayes[6], Shishir K. Maithel[5], Nilofer S. Azad[2], Gregory B. Lesinski[1], Combined MEK/PD-L1 inhibition alters peripheral cytokines and lymphocyte populations correlating with improved clinical outcomes in advanced biliary tract cancer. *Clinical Cancer Research*, 2022. doi: 10.1158/1078-0432.CCR-22-1123.

A.N.R., M.Y., N.S.A., and G.B.L. conceived and designed the study. A.N.R. and G.B.L. composed the manuscript. A.N.R. and G.B.L. designed experiments. B.M.O. assisted with flow cytometry panel design. A.N.R. collected and analyzed flow cytometry data. E.S. and H.X.C. provided support and guidance on clinical trial registration administration. A.N.R., S.G., and Y.L. conducted and assisted with biostatistical analysis. C.M.P. provided human blood samples. A.N.R. and M.Y. collected and organized clinical data. B.F.E., S.K.M., and N.S.A. provided clinical guidance and expertise. All authors reviewed the manuscript.

Affiliations:

[1]Department of Hematology and Medical Oncology, Winship Cancer Institute of Emory University, Atlanta, GA, USA

[2]Department of Oncology, Johns Hopkins University Sidney Kimmel Comprehensive Cancer Center, Baltimore, MD, USA

[3]Biostatistics Shared Resource, Winship Cancer Institute of Emory University, Atlanta, GA, USA

[4]National Cancer Institute (NCI) Cancer Therapy Evaluation Program (CTEP), Bethesda, MD, USA

[5]Department of Surgery, Winship Cancer Institute of Emory University, Atlanta, GA.

[6]O'Neal Comprehensive Cancer Center of the University of Alabama at Birmingham, Birmingham, AL, USA

2.2 Abstract

Biliary tract cancers (BTCs) are aggressive malignancies refractory to chemotherapy and immunotherapy. MEK inhibitor (MEKi)-based regimens may have utility in this disease when combined with PD-L1 blockade. We hypothesize that dual MEK/PD-L1 inhibition alters circulating soluble and cellular immune mediators to improve clinical outcomes in patients with advanced BTC. We examined immune features in peripheral blood from 77 patients with advanced BTC enrolled in a Phase II clinical trial investigating atezolizumab with or without cobimetinib. Plasma and PBMCs were isolated from whole blood to evaluate soluble factors and immune cell populations. Baseline blood samples were additionally compared with healthy donors to identify immune signatures unique to BTC. At baseline, the soluble factors PDGF-BB, PlGF-1, IL-5, and IL-17A were elevated in BTC patients compared to healthy adult donors, and higher baseline frequencies of $CD8^+BTLA^+$ T cells correlated with better overall survival in this trial. There were also significant treatment-related alterations in several factors, including decreased PDGF-BB following combination treatment, that correlated with improved OS and PFS. Higher baseline levels of IL-23 and RANTES corresponded to improved clinical outcomes following combination

treatment. Dual MEKi/PD-L1 inhibition increased populations of $CD4^+TIM3^+$ and decreased $CD8^+VISTA^+$ T cells, correlating with worse OS and better PFS, respectively. This work represents a comprehensive analysis of peripheral immune features in BTC patients and systemic responses to dual MEK/PD-L1 inhibition. These data support further investigation to understand how MEKi combines with immunotherapeutic approaches to improve clinical outcomes for advanced BTC patients.

2.3. Introduction

Biliary tract cancers (BTC) are a rare group of aggressive malignancies that include gallbladder cancer (GBC), intrahepatic cholangiocarcinoma (ICC), and extrahepatic cholangiocarcinoma (ECC). Biliary tract cancers collectively have a 5-year median survival rate of less than 10% and are typically diagnosed at advanced stage when curative surgical resection is not possible. These tumors are also refractory to most systemic treatment options. Precision medicine approaches in subsets of patients with tumors harboring FGFR2 fusions or IDH1/2 mutations offer promise, but other targeted therapies have not shown substantial benefit over chemotherapy[148, 202, 238-240]. In considering pathways consistently altered in BTC, constitutive activation of Ras/Raf/MEK/ERK signaling is frequent in tumors from BTC patients[205]. Activating KRAS mutations are present in approximately 22% of BTC cases, associating with poor prognosis and uncontrolled cell growth[241]. This has prompted investigations with inhibitors of MAPK/ERK Kinase (MEK), which limit disease progression as single agents in BTC and have been tested in combination with immunotherapy in patients with other solid tumors, including melanoma and breast cancer[205, 207, 208, 217, 241, 242].

Programmed cell death ligand 1 (PD-L1) is expressed on tumor cells heterogeneously among BTC patients, interacting with its receptor PD-1 to possibly limit cytotoxic T cell function and anti-tumor immunity[214]. Immune checkpoint inhibitor (ICI) therapies including PD-L1 blockade have limited activity historically against BTC[243, 244], but recent data from the phase III TOPAZ-1 trial show that adding durvalumab, a PD-L1-targeted antibody, to standard of care gemcitabine and cisplatin improves overall survival in the first-line for advanced BTC patients[197]. As a result, immunotherapy has garnered major attention in the context of BTC, and further investigation of systemic immune features in these patients can inform future therapeutic strategies.

Previous pre-clinical studies demonstrate that MEK inhibition (MEKi) can enhance $CD8^+$ T cell infiltration into tumors, while PD-L1 blockade invigorates $CD8^+$ T cell mediated antitumor activity. Furthermore, MEKi synergizes with PD-L1 blockade to improve anti-tumor responses in several solid tumor models[187, 223]. Building off these studies, we recently published results from a clinical trial investigating atezolizumab (anti-PD-L1) with or without the MEK inhibitor cobimetinib in patients with advanced BTC (NCT03201458). This trial met its primary endpoint of improved progression-free survival (PFS), with a median PFS of 3.65 months in combination-treated patients, versus 1.87 months in patients receiving atezolizumab monotherapy[221].

In this study, we address the hypothesis that dual MEK/PD-L1 inhibition alters circulating soluble and cellular immune mediators to improve clinical outcomes in advanced BTC. Using a unique collection of peripheral blood samples from advanced BTC patients undergoing therapy with atezolizumab with or without cobimetinib, we provide a comprehensive analysis of immune features. Our data encompasses cytokines, chemokines, and phenotypically-defined immune cell subsets from a large cohort of patients, informing our understanding of how dual MEK/PD-L1 inhibition impacts immune markers during treatment. Finally, using baseline blood samples from

patients and a cohort of healthy adult donors, we identify novel immune features prominent in BTC patients, suggesting potential avenues for future investigations of therapeutic targets.

2.4. Results

2.4.1. Differential production of cytokines, chemokines, and growth factors in the blood of BTC patients compared to healthy donors

To define prominent immune features in patients with BTC, independent of treatment, we compared biomarker data at baseline from this patient cohort with that of healthy donors. We analyzed a panel of 45 soluble factors in peripheral plasma samples, which evaluated cytokines regulating T cell differentiation and function, inflammatory cytokines, chemokines, and growth factors. Fifteen markers, including a subset of pro-inflammatory cytokines, were below the detectable assay threshold in >50% of all plasma samples and concentrations could not be accurately determined. Therefore, these fifteen factors were excluded from further analyses. Of the remaining 30 soluble factors, 21 were significantly elevated among BTC patients (Figure 2.1A, Table 2.3). In particular, PDGF-BB, IL-5, IL-17A, and PlGF-1 were all elevated five-fold more than what was observed in healthy donors ($p \leq 0.002$) (Figure 2.1B-E). The remaining 9 factors were not present at concentrations significantly different from healthy donors. Independent of treatment effect from the clinical trial, there were no correlations between any soluble factors at baseline with clinical outcomes (data not shown).

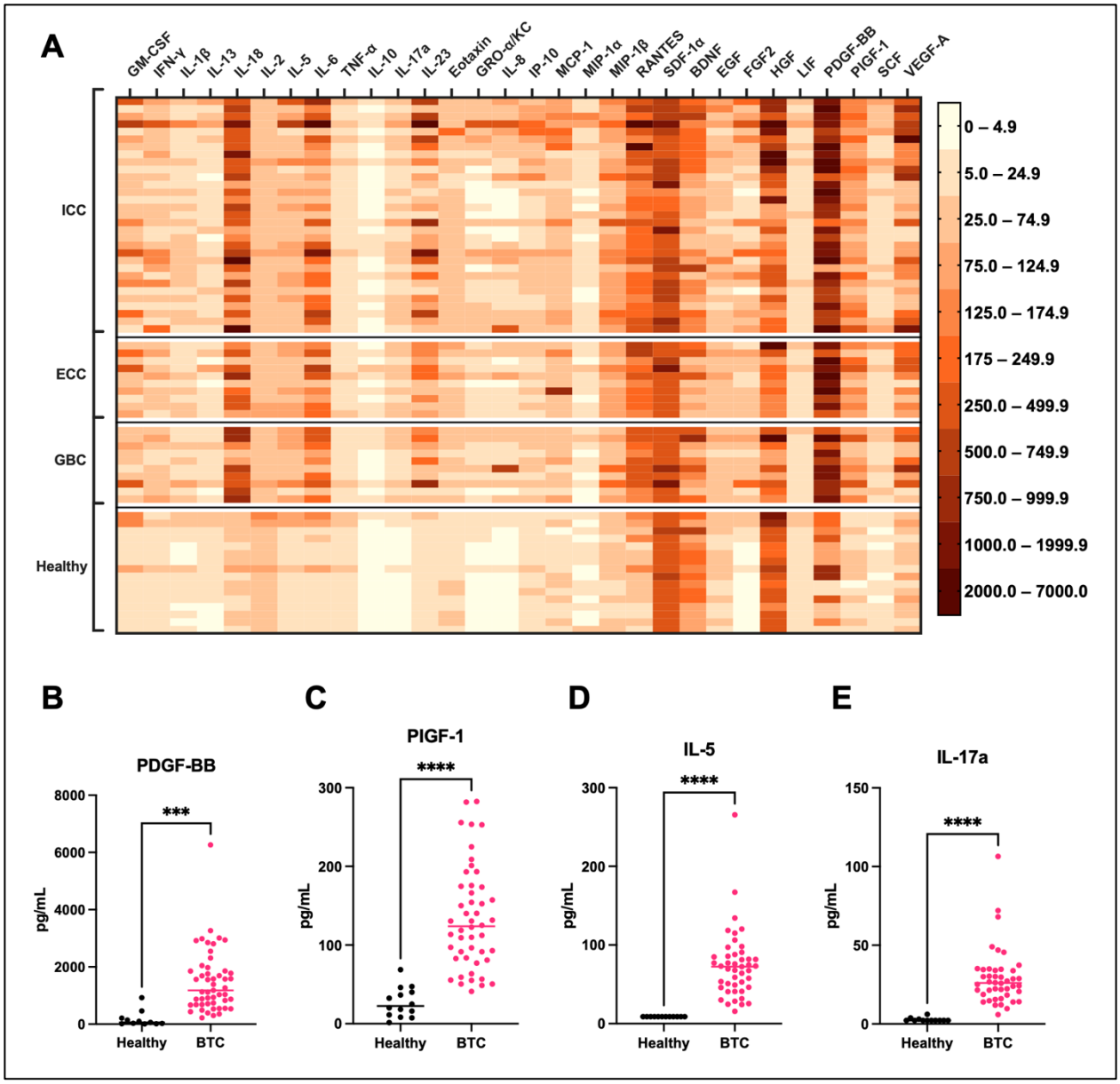

Figure 2.1. Biliary tract cancer patients have distinct soluble factor signatures compared to healthy donors. (A) Heat map of cytokines, chemokines, and growth factors among BTC anatomic subtypes that are differentially expressed from healthy donors. Several factors are significantly elevated in BTC patients compared to healthy donors across all disease subtypes, including (B) PDGF-BB, (C) PlGF-1, (D) IL-5, and (E) IL-17a. Comparisons between BTC patients and healthy donors were evaluated by Student's t tests. ***P<0.001 ****P<0.0001.

2.4.2. PD-1 and BTLA-expressing T cells are elevated in BTC patients

Multiparameter 23-color flow cytometric analysis of PBMCs was used to interrogate unique immune landscapes in blood of advanced BTC patients (Figure 2.6). Our analysis encompassed 19 phenotypically distinct populations including lymphocytes, myeloid cells, and cells expressing immune checkpoint proteins. We also used this flow panel to conduct analysis of a separate cohort of 12 healthy adult PBMCs and found that 9 phenotypically-defined cell populations were significantly different between BTC patients and healthy donors (Table 2.4). Circulating total $CD8^+$ T cells were lower overall in BTC patient samples ($p=0.003$), but of those $CD8^+$ T cells, BTC patients had higher frequencies of cells expressing inhibitory checkpoint ligands. Notably, $CD8^+PD\text{-}1^+$ ($p=0.007$) and $CD8^+BTLA^+$ ($p=0.016$) cells were present at higher frequencies in BTC patients. Additionally, $CD4^+PD\text{-}1^+$ ($p=0.001$) and $CD4^+BTLA^+$ ($p=0.001$) T cells were higher in BTC patients, as well as $PD\text{-}1^+TIM3^-$ activated $CD8^+$ T cells ($p=0.004$) (Figure 2.2A-E, Table 2.4). In contrast, $CD4^+$ and $CD8^+$ T cells expressing TIM3, LAG3, and VISTA were not present in BTC patients at frequencies different from healthy donors. We also assessed relationships between distinct immune phenotypes identified and clinical parameters in this cohort of metastatic BTC patients. We postulated peripheral biomarkers may emerge to predict overall survival and signify more aggressive disease. Interestingly, the frequency of $BTLA^+CD8^+$ T cells correlated with OS, where patients with above-median population frequencies had longer OS, regardless of treatment received on the clinical trial ($p=0.036$) (Figures 2.2E, Figure 2.2F, Table 2.4).

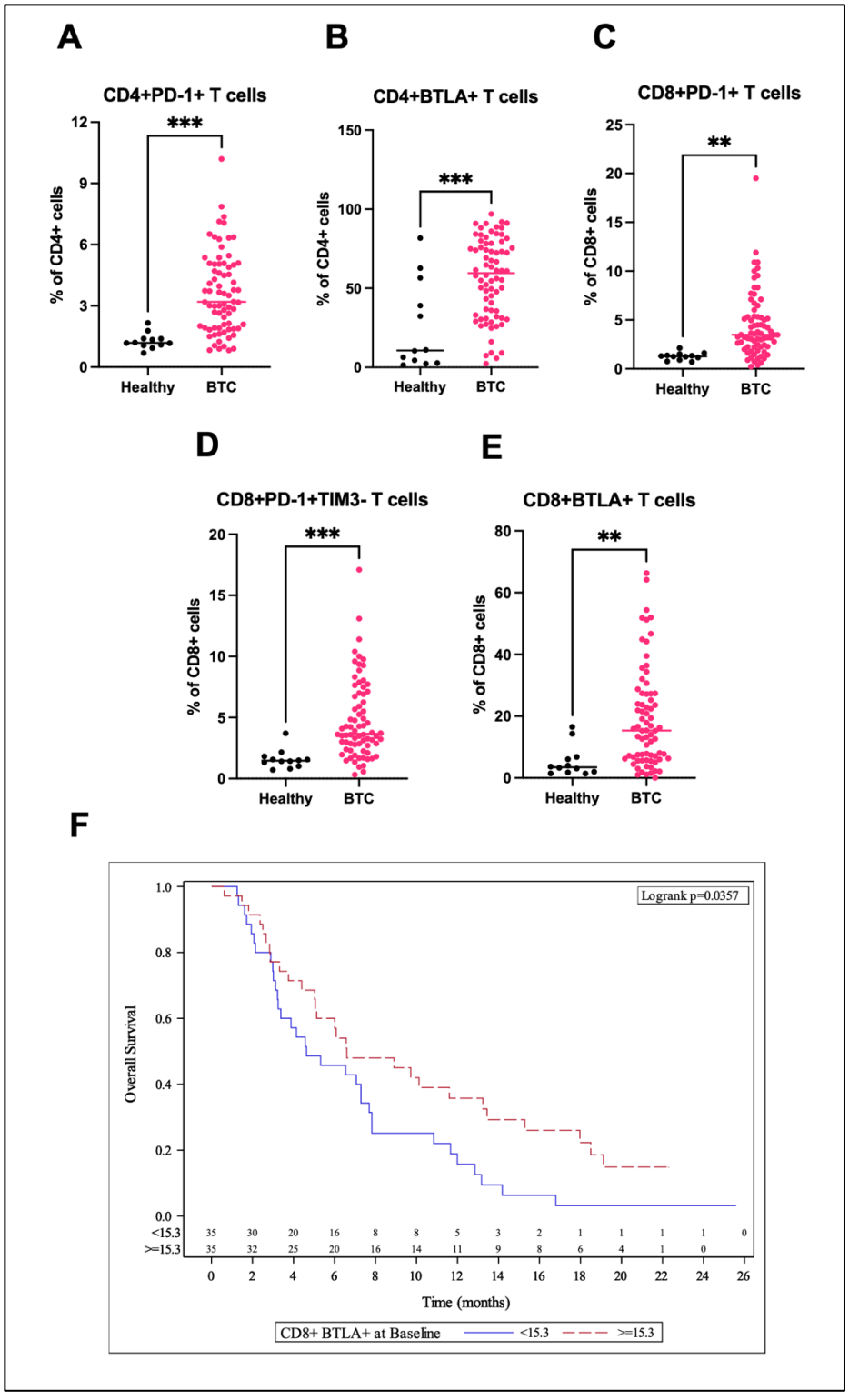

Figure 2.2. T cells with an activated phenotype are significantly elevated in BTC patients, and BTLA^{+}CD8^{+} T cells elevated above median at baseline correlate with better overall

survival. Baseline populations of (A) $CD4^+PD\text{-}1^+$, (B) $CD4^+BTLA^+$, (C) $CD8^+PD\text{-}1^+$, and (D) $CD8^+PD\text{-}1^+TIM3^-$ T cells are elevated in BTC patients compared to healthy donors. (E) $BTLA^+CD8^+$ T cells are significantly elevated in BTC patients compared to healthy donors. (F) Kaplan-Meier curve of BTC patients stratified by median population of $CD8^+BTLA^+$ T cells depicting that above-median populations at baseline are associated with better overall survival. Comparisons between BTC patients and healthy donors were evaluated by Student's t tests. Association with overall survival was explored by the Cox proportional hazard model and significance determined by log-rank test. **P<0.01, ***P<0.001.

2.4.3. MEK inhibition significantly alters growth factor levels when combined with anti-PD-L1 therapy in advanced BTC that correlate with improved clinical outcomes

To assess the effect of both single-agent treatment with atezolizumab and dual therapy with cobimetinib, we calculated percent change of plasma concentrations of soluble factors from baseline to C2D1 (Figure 2.3A). We stratified all patients by median percent change for each soluble factor, then evaluated correlations between percent change and clinical outcomes within each treatment group (Table 2.5, Table 2.6). For patients in Arm B, dual treatment with atezolizumab and cobimetinib significantly decreased plasma concentrations of PDGF-BB ($p=0.0456$), BDNF ($p=0.0036$), and PlGF-1 ($p<0.0001$) from baseline to C2D1, while patients in Arm A receiving atezolizumab monotherapy had no significant changes in plasma concentration for these analytes (Figure 2.3B-D). Of these factors, the decrease in plasma concentrations of PDGF-BB in Arm B was associated with improved OS (UVA $p=0.023$, FDR=0.345; MVA $p=0.084$, FDR=0.921) and PFS (UVA $p=0.040$, FDR=0.360; MVA $p=0.067$, FDR=0.395) on exploratory univariate analysis and in multivariable analysis. Given the limited sample size however, these trends were no longer statistically significant upon false discovery rate (FDR) adjustment for multiple comparisons (Figure 2.3E, Table 2.5, Table 2.6). Changes in concentration of other soluble factors correlated with improved clinical outcomes for patients in Arm A and Arm B, but could not be directly associated with treatment effects following two-way ANOVA (Table 2.5, Table 2.6). We next evaluated baseline plasma concentrations of soluble factors as predictors of response to cobimetinib and atezolizumab combination therapy (Table 2.7, Table 2.8). Baseline levels were stratified by median concentration of each analyte as a whole, then evaluated for correlations with clinical outcomes within each treatment group. Higher baseline concentrations of IL-23 in Arm B patients correlated with improved overall survival (UVA $p<0.001$, FDR=0.03;

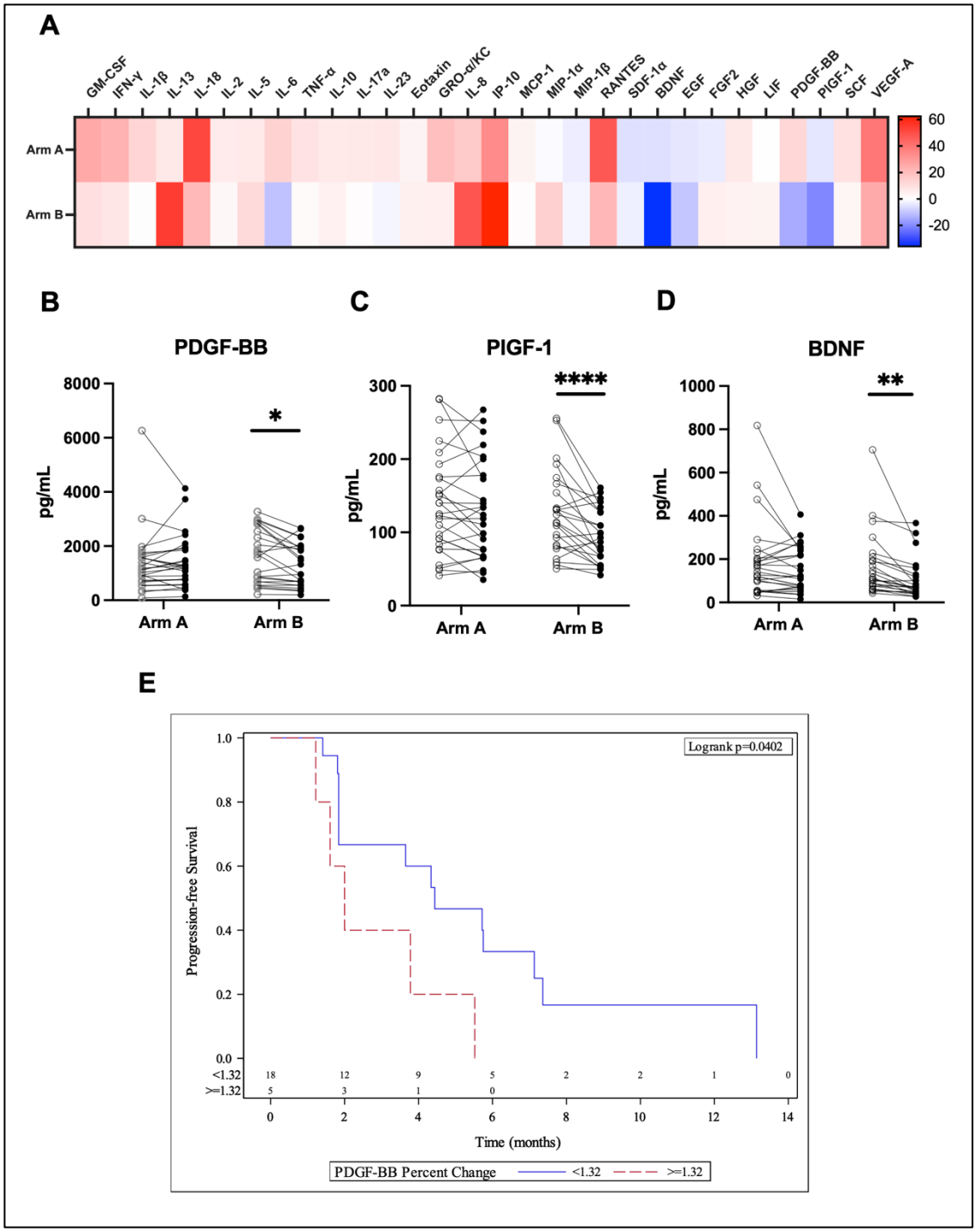

Figure 2.3. Dual MEK/PD-L1 inhibition alters soluble factor levels that correlate with clinical outcomes. (A) Heat map depicting mean percent change in soluble factor plasma concentrations from baseline to C2D1 across all patients within each treatment arm (Arm A n=28,

Arm B n=23). Changes in soluble factor concentrations from baseline to C2D1 for (B) PDGF-BB, (C) PlGF-1, and (D) BDNF. (E) Kaplan-Meier plot of PFS for Arm B patients stratified by median percent change in PDGF-BB concentration from baseline to C2D1, where patients with a decrease in PDGF-BB had improved PFS. Comparisons between treatment arms and changes in soluble factor concentrations were evaluated by two-way repeated measures ANOVA. Association with PFS was explored using the Cox proportional hazard model and significance was determined by log-rank test. *P<0.05, **P<0.01, ****P<0.0001.

MVA p=0.02, FDR=0.60), while higher baseline concentrations of BDNF (UVA p=0.063, FDR=0.330; MVA p=0.017, FDR=0.170), IL-8 (UVA p=0.005, FDR=0.075; MVA p=0.013, FDR=0.170) and RANTES (UVA p<0.001, FDR=0.030; MVA p=0.001, FDR=0.030) indicated better PFS (Table 2.7, Table 2.8), both in univariate exploratory analysis and after adjusting for multiple comparisons. Baseline plasma concentrations of other soluble factors in both Arm A and Arm B had relationships to clinical outcomes that trended toward significance by UVA and/or MVA (Table 2.7, Table 2.8). Measurement of these factors at baseline may be predictive of how advanced BTC patients respond to dual blockade of MEK and PD-L1.

2.4.4. Regulation of T lymphocyte populations with an exhausted phenotype by dual MEK/PD-L1 blockade correlates with improved clinical outcomes

From baseline to C2D1, combination therapy was associated with an increase in $CD4^+TIM3^+$ T cells, as evidenced by a notable interaction via two-way ANOVA (pint=0.032, Figure 2.4B). However, this increase correlated with worse overall survival for these patients (UVA p=0.015, FDR=0.285; MVA p=0.016, FDR=0.219); Figure 2.4C; Table 2.9, Table 2.10). Both overall survival and progression-free survival were improved for single-agent treated patients with increasing populations of $CD4^+BTLA^+$ (UVA_{OS} p=0.006, FDR=0.057, MVA_{OS} p=0.013, FDR=0.247; UVA_{PFS} p=0.003, FDR=0.029, MVA_{PFS} p=0.002, FDR=0.038) and $CD8^+BTLA^+$ T cells (UVA_{OS} p=0.005, FDR=0.057, MVA_{OS} p=0.060, FDR=0.418; UVA_{PFS} p=0.003, FDR=0.029, MVA_{PFS} p=0.02, FDR=0.019). Additionally, Arm A patients with an increase in $CD4^+LAG3^+$ T cells from baseline to C2D1 also had improved OS (UVA p=0.014, FDR=0.089; MVA p=0.066, FDR=0.418), while decreasing $CD8^+VISTA^+$ T cells correlated with improved PFS for Arm B patients (UVA p=0.001, FDR=0.019; MVA p=0.003, FDR=0.057). Changes in

other immune populations from baseline to C2D1 had correlations with clinical outcomes trending toward significance (Table 2.9, Table 2.10).

2.4.5. High baseline CD8$^+$ T cells correlate with improved overall survival following dual MEK/PD-L1 blockade

The predictive value of baseline populations of peripheral immune cells on clinical outcomes was next evaluated (Table 2.11, Table 2.12). Baseline populations of immune cells were stratified by median percent of parent population. In Arm B patients, higher peripheral CD8$^+$ T cells (UVA p=0.016, FDR=0.304; MVA p=0.138, FDR=0.836) and CD8$^+$ cells that were BTLA$^+$ (UVA p=0.061, FDR=0.5795; MVA p=0.092, FDR=0.836) correlated with improved OS. Patients in this arm with fewer peripheral CD8$^+$VISTA$^+$ T cells also had better OS (UVA p=0.036, FDR=0.228; MVA p=0.125, FDR=0.497) and improved PFS (UVA p=0.018, FDR=0.342; MVA p=0.09, FDR=0.656). Above-median populations of intermediate monocytes in single-agent treated Arm A patients also correlated with better OS (UVA p=0.027, FDR=0.228; MVA p=0.013, FDR=0.247). These findings were significant upon exploratory univariate and multivariate analyses, but due to small sample size were no longer significant when adjusted for multiple comparisons.

2.5. Discussion

This study provides a comprehensive profile of the systemic immune landscape of advanced BTC and evaluates how MEK inhibition and anti-PD-L1 therapy modulate systemic immune factors and their relationship to clinical outcomes. We assess peripheral immune biomarkers in pretreatment samples to profile the immune landscapes of a large cohort of advanced BTC

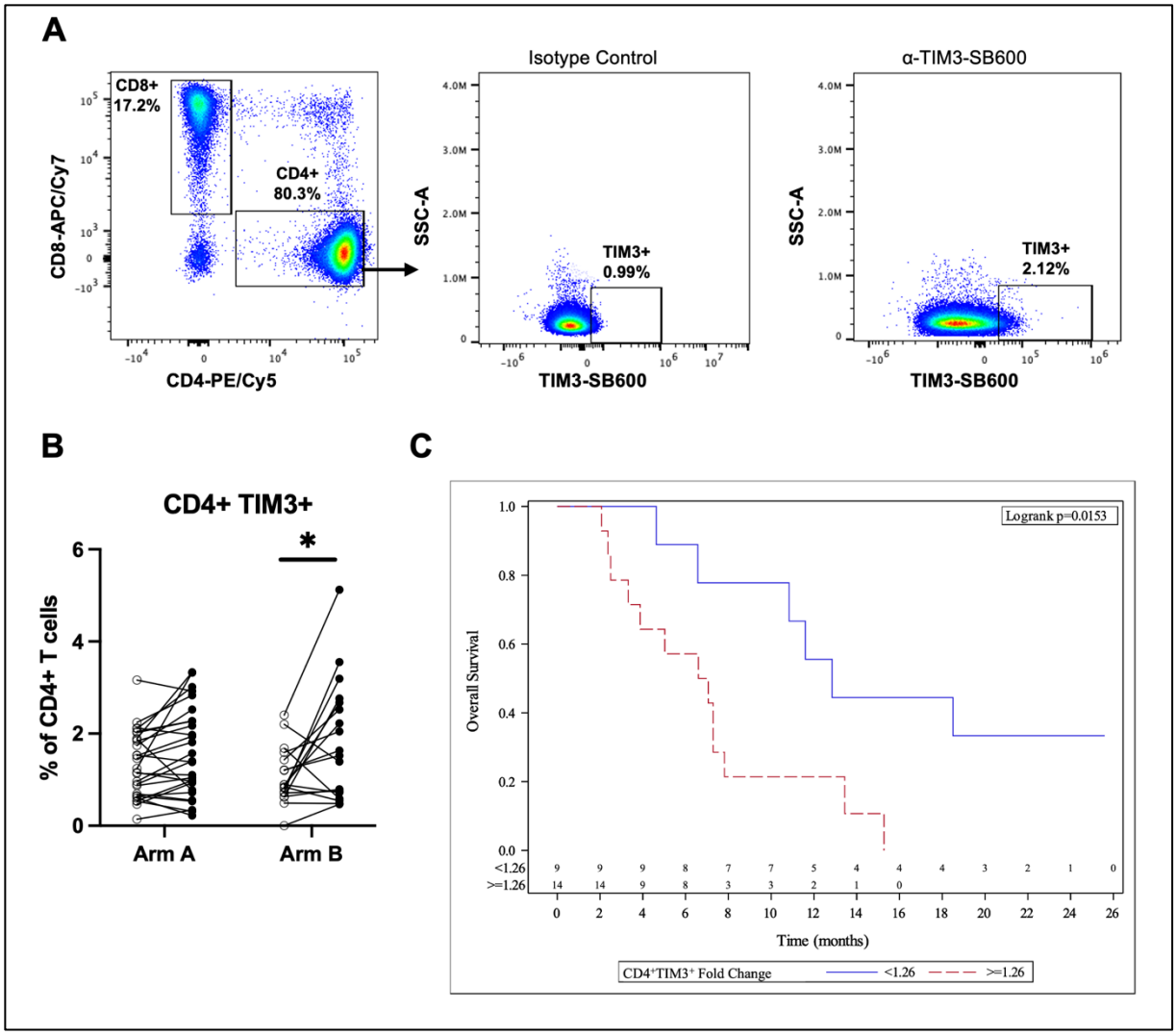

Figure 2.4. Inhibition of MEK and PD-L1 promotes increased populations of TIM3-expressing CD4 lymphocytes but leads to worse overall survival. (A) Gating schema for identifying $CD4^{+}TIM3^{+}$ T cells. (B) Changes in populations of $CD4^{+}TIM3^{+}$ T cells as percent of $CD4^{+}$ T cells from baseline to C2D1. (C) Kaplan-Meier plot of OS for Arm B patients stratified by median fold change in $CD4^{+}TIM3^{+}$ T cell populations from baseline to C2D1, where increased populations correlate with worse OS. Comparisons between treatment arms and changes in immune cell populations were evaluated by two-way repeated measures ANOVA. Association

with OS was explored using the Cox proportional hazard model and significance was determined by log-rank test. *P<0.05.

patients. We identified several soluble factors, including PDGF-BB, IL-5, IL-17A, and PlGF-1, that are elevated in plasma of BTC patients when compared to healthy donors, as well as $CD4^+$ and $CD8^+$ T cells expressing PD-1 and BTLA. In our clinical trial, dual MEK/PD-L1 blockade altered production of soluble factors in patient plasma compared to PD-L1 blockade alone, including a decrease in PDGF-BB that correlated with improved PFS. Further, changes in several T cell populations expressing immune checkpoint markers were observed in patients receiving combined MEK/PD-L1 inhibitors and correlated with improved clinical outcomes.

The use of MEK inhibition (MEKi) to enhance PD-1/PD-L1-targeted immunotherapy has been investigated in various preclinical tumor models and in clinical trials. While we observed correlations between important immune factors and survival outcomes, our overall clinical experience with dual MEK/PD-L1 inhibition in advanced BTC patients revealed a modest extension of PFS compared to PD-L1 blockade alone. The low objective response rate in both treatment arms in this study reflect the immune resistant nature of BTC and the need to understand mechanisms of response and resistance to immunotherapy in BTC patients. Although MEKi has been shown to promote $CD8^+$ T cell infiltration and limit TCR-mediated exhaustion, previous work from our group shows systemic MEK administration can also inhibit T cell activation and function. In particular, the addition of MEKi to PD-L1 blockade in this trial limited expansion of T cell populations with activated phenotypes, whereas anti-PD-L1 alone increased these cells[224]. Fortunately, subsequent preclinical studies showed that this could be overcome through co-treatment with antibodies that act as agonists to T cell function, such as 4-1BB[224]. Inspired by these results, we have initiated a follow-up randomized trial investigating the combination of cobimetinib and atezolizumab with varlilumab, an agonistic mAb for CD27, to restore T cell activation (NCT04941287). MEKi and PD-L1 blockade have distinct functions in controlling the

immune response to solid tumors, which may explain why specific correlations to OS and PFS were evident that were not related to overall response rates. We hope our work interrogating other immune features associated with clinical benefit will guide development of future treatment options for these patients[221].

Cytokine signatures have been surveyed to predict responders to immunotherapy in other tumor models and may have utility in advanced BTC patients[245]. Several factors, including PlGF-1 and PDGF-BB, that are markedly higher in plasma from BTC patients compared to healthy individuals, also have an established relationship with the biology of BTC tumors[246-248]. For example, placental growth factor (PlGF-1) is present at high levels in blood from ICC patients and associated with desmoplasia and disease progression[247]. Collectively this factor promotes aggressive disease, and its inhibition limits progression in hepatocellular carcinoma (HCC) and cholangiocarcinoma (CCA) tumor models[247, 249]. Like PlGF-1, platelet derived growth factor B (PDGF-BB) is prominently produced by myofibroblasts in hepatobiliary tumors and promotes pro-survival signaling in BTC[130]. Plasma levels of PDGF-BB were substantially reduced in BTC patients receiving cobimetinib with atezolizumab versus atezolizumab alone, and this decrease correlated with improved PFS in combination treated patients. PDGF-BB signals exclusively through the PDGFRβ receptor, activating downstream MEK/ERK and PI3K/AKT signaling[248, 250, 251]. PDGFRβ is associated with epithelial-to-mesenchymal transition (EMT) to promote invasion and metastasis in colorectal cancer[252]. To further support a relationship between MEK signaling and PDGF-BB, this growth factor has a critical mitogenic role in fibroblasts and other stromal cells in the tumor microenvironment, promoting stromal cell activation and angiogenesis[253, 254]. Since peripheral PDGF-BB was also elevated at baseline in BTC patients versus healthy donors, and PDGFRβ is expressed in human CCA tumors, targeting of the PDGF-BB/PDGFRβ axis likely has

a role in controlling BTC. Previous studies have demonstrated genetic and pharmacologic inhibition of PDGFRβ promotes apoptosis and reduces tumor growth in in vivo models of BTC[130]. However, further investigation is necessary to elucidate mechanistic relationships between PDGF-BB and BTC for potential use in future therapeutic strategies.

Analysis of peripheral immune populations showed notable changes in both $CD4^+$ and $CD8^+$ T cells expressing immune checkpoint proteins associating with clinical outcomes in patients receiving combination therapy. Atezolizumab alone led to higher $LAG3^+$ and $BTLA^+$ T cell populations correlating with better OS and PFS, while atezolizumab and cobimetinib combination therapy led to fewer $CD8^+VISTA^+$ T cells that correlated with improved PFS. Conversely, combination therapy significantly increased the frequency of $CD4^+TIM3^+$ T cells, correlating with worse PFS. These data were consistent with prior studies in melanoma whereby MEKi also increased TIM3 expression on lymphocytes, and higher TIM3 expression frequently correlates with poor clinical outcomes in several other cancer models[255, 256]. Further investigations following this clinical trial may benefit from addition of agents targeting TIM3, which could be more effective in combination with other checkpoint inhibitors[256]. In addition to treatment-related changes in T cell populations, analysis of peripheral immune cells at baseline revealed higher frequency of $CD8^+BTLA^+$ T cells versus healthy donors, which correlated with increased overall survival in this BTC patient cohort. These results prompt further questions related to the role of BTLA on peripheral T cells as a reflection of BTC progression. BTLA is a co-stimulatory molecule in the CD28 immunoglobulin superfamily that harbors classical inhibitory signaling motifs[85, 257]. However, the role of BTLA as a regulator of T cell mediated immune responses to cancer is not straightforward. Regulation of immune checkpoint expression and function is key to controlling the immune response in many cancers, but there has been little investigation into associations

between MEKi and BTLA, LAG3, or VISTA expression. Indeed, there are documented molecular connections between activation of ERK with downstream transcription factors that control expression of genes encoding checkpoint proteins, though further investigation is required to fully characterize the relationship between MEKi and immune checkpoint expression on immune cells.

While this study lends meaningful insight into systemic immune features in BTC patients, it does have limitations. Since the trial was open at multiple sites and patients had unresectable metastatic disease, the feasibility of obtaining tissue to probe intratumoral immune features was limited, with a greater sample size of peripheral blood specimens. Our data suggest peripheral blood is useful for understanding systemic immune alterations that accompany advanced cancer and may reveal provocative differences for further study. Although our patient population was substantial for biliary tract cancer studies, sample sizes in our analyses were much smaller than other clinical trials. In particular, data in our analyses of treatment effects was dichotomized by the median value of each analyte before stratification by treatment arm for correlation with clinical outcomes. Furthermore, to make our conclusions more succinct, we describe changes in immune factors from baseline to C2D1 as either increases or decreases depending on which side of the median they fall on. This simplifies some quantitative details where the median is not precisely at no fold or percent change but makes our conclusions more concise overall. We also acknowledge this study was only conducted in the United States, and therefore does not encapsulate the pathological manifestations of BTC common in other regions such as liver fluke infection. Additionally, our comparison of baseline samples to healthy donors does not account for inflammatory diseases of the liver and biliary tract, including hepatitis, primary sclerosing cholangitis, and gallbladder disease, that could influence the peripheral immune factors in our patient population. Finally, targeted therapy against FGFR2 fusions and IDH alterations are among the most promising areas of clinical development

for BTC, but we did not have extensive genome-level data on tumors from patients enrolled in this trial to consider for advancing this line of study[136, 258]. Despite these understandable limitations, our comprehensive analysis of immune cell and soluble factor signatures in the blood of advanced BTC patients is of value to the field.

Overall, this study investigates how MEKi combines with anti-PD-L1 to modulate clinically-relevant, systemic soluble factors and immune populations in a large cohort of patients with advanced metastatic BTC. We have also delineated differences in peripheral immune markers of BTC patients compared to healthy individuals. This work advances our understanding of how MEKi synergizes with immune checkpoint blockade and has uncovered factors that merit additional study for a disease with few effective treatment options.

2.6. Materials and Methods

2.6.1. Patients and Treatment

Peripheral blood was collected from 77 patients with metastatic, pathologically confirmed ICC, ECC, or GBC following informed consent (Table 2.1). Patients were enrolled in a randomized, national Phase II clinical trial (NCT03201458) of atezolizumab with or without cobimetinib[221]. Patients randomized to Arm A received atezolizumab every two weeks, while patients randomized to Arm B received cobimetinib daily (21 days on/7 days off) alongside atezolizumab every two weeks. This work was carried out under a protocol approved by the National Cancer Institute's (NCI) Cancer Therapy Evaluation Program (CTEP) and the central and local institutional review boards (IRBs). All patients were enrolled between February 2018 and October 2018. Whole blood samples were collected prior to treatment and on treatment at the start of cycle 2 (C2D1), then

transported overnight to Winship Cancer Institute for processing and analysis. Due to the aggressive nature of BTC, we collected patient correlative samples at this time point to avoid missing samples from patients with disease progression or treatment intolerance. From a biologic standpoint, prior work suggests that early immune responses (within 4 weeks) are important indicators of favorable clinical outcomes to PD-1/PD-L1 targeted therapies [259]. PBMCs and plasma were isolated from whole blood via density gradient centrifugation using Ficoll-Paque (GE Healthcare Bio-Sciences AB, Uppsala, Sweden). Additionally, we obtained samples from two cohorts of de-identified healthy donors, collecting 12 PBMC samples from buffy coats (Sylvan N. Goldman Oklahoma Blood Institute, Oklahoma City, OK) and 16 plasma samples from whole blood (Emory University Hospital, Atlanta, GA), used as comparators for our baseline data. Normal donor blood samples were processed similarly to patient samples by density gradient centrifugation. All patient and normal donor plasma were cryopreserved at -80°C until analysis, and all PBMCs were cryopreserved in liquid nitrogen prior to analysis. Blood samples received more than 2 days after collection were not used for PBMC isolation to ensure consistent quality but were still processed for plasma via centrifugation and used for bioplex analysis. As a result, some patients did not have viable samples at all timepoints, and hence data were collected using samples from 70 patients for PBMC analysis and 51 patients for plasma analysis. Patient sample exclusion criteria is detailed in Figure 2.5.

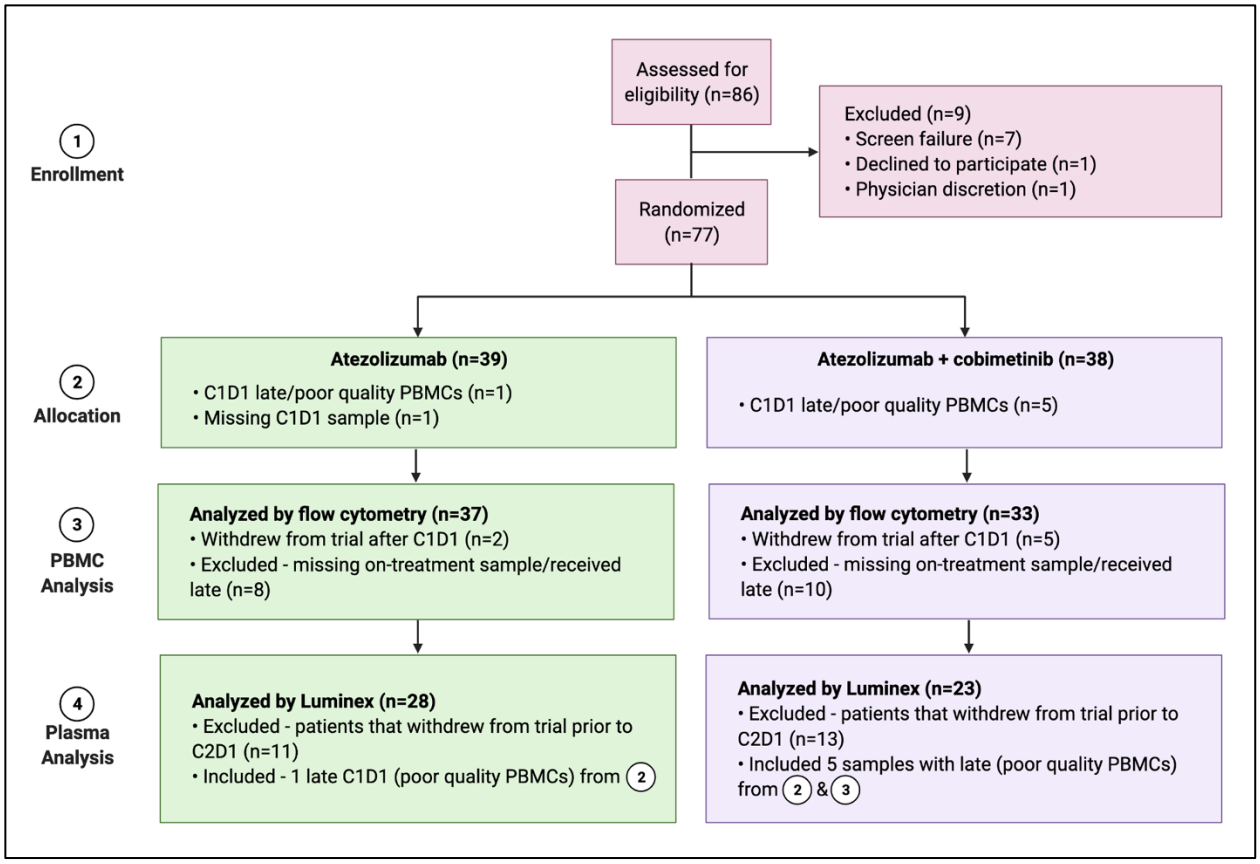

Figure 2.5. Patient sample exclusion diagram. Number of samples excluded and reasons for exclusion at each step of analysis.

2.6.2. Cytokine, chemokine, and growth factor analysis

Plasma samples were analyzed using a panel of 45 cytokines, chemokines, and growth factors on a Luminex magnetic bead-based platform according to manufacturer protocol (ProcartaPlex Cytokine/Chemokine/Growth Factor Panel 1, EPX450-12171-901, ProcartaPlex Immunoassays, Invitrogen; Waltham, MA). Samples were analyzed in duplicate and batch-run on a Luminex 100 instrument and quantified using analyte-specific standard curves for each batch. Only 51 patients who remained on treatment through C2D1 blood collection were analyzed. Quality filtering based on a coefficient of variation of >15% was performed for each analyte. Fifteen analytes were excluded from analyses for >50% of measurements falling below the detectable assay threshold across patient samples.

2.6.3. Flow cytometry

Comprehensive phenotypic analysis of peripheral immune cells was conducted via 23-color flow cytometry. Antibodies are detailed in Table 2.2. Cryopreserved PBMCs were thawed at 37°C, washed, centrifuged, and resuspended in FACS buffer (PBS + 3% FBS + 0.05 mM EDTA). Cells were incubated with surface antibody for 30 min at 4°C, washed, permeabilized and fixed overnight using the FoxP3/Transcription Factor Staining Buffer set (00-5523-00, eBioscience). Cells were incubated with intracellular antibodies for one hour at room temperature, washed, and resuspended in FACS buffer for analysis. Flow cytometric analysis was conducted on a Cytek Aurora (Cytek Biosciences, Fremont, CA). Compensation controls were generated using UltraComp eBeads Compensation Beads (01-2222-41, Invitrogen; Waltham, MA). Data were analyzed using FlowJo software version 10.7.2 (FlowJo, LLC; Ashland, OR).

2.6.4. Statistical analyses

Descriptive statistics were used to summarize patients' demographics and disease characteristics. Biomarker values at baseline and their changes to C2D1 were first summarized and associated with treatment group, then further linked with clinical outcomes (e.g., OS, PFS). To account for data dependency rooted in repeated samples from the same patients, two-way repeated measures ANOVA test, along with Šídák's multiple comparisons test, was used to test the interaction effect between percent change and treatment groups. This approach permits determination of whether combination treatment leads to more change in biomarker measurements than single agent treatment (Arm B vs Arm A). All biomarker measurements were compared between patient and healthy donor samples using two-sided Student's t-test. For either baseline biomarker levels or their changes to C2D1, univariate (UVA) and multivariate (MVA) associations with clinical outcomes (OS, PFS) in each treatment arm were explored using the Cox proportional hazards model, illustrated using the Kaplan-Meier method, and significance was determined by log-rank test. The measures of all biomarkers were dichotomized on the entire sample (< median vs. >= median) for univariate and multivariate analyses. Soluble factors were dichotomized by percent change, and immune populations were dichotomized by fold change. Multivariate analyses were adjusted simultaneously for age, sex, and anatomic tumor subtype as relevant clinical variables. To correct for multiple testing, the Benjamini and Hochberg method was used to control the false discovery rate (FDR) on both UVA and MVA, with a cut-off value of $p<0.25$ for significance. Significance was adjusted separately for soluble factors and for immune cell populations. Due to limited statistical power from a small sample size, significance for multivariate analyses was determined as $p<0.1$, while significance of all other analyses was determined as $p<0.05$.

2.7. Acknowledgements

We would like to acknowledge the cores at Winship Cancer Institute and Emory University that made this research possible including the Pediatric/Winship Flow Cytometry Core, the Winship Biostatistics and Bioinformatics Core, under NIH/NCI award number P30CA138292. In addition, sample collection at enrolling sites was supported by the NCI ETCTN UM1 grants. The content is solely the responsibility of the authors and does not necessarily represent the official views of the National Institutes of Health. This work is supported by NIH grants R01CA228414, R01CA208253, R01CA228406, and P30CA006973. The clinical study from which samples were derived was coordinated by the National Cancer Institute (NCI) Experimental Therapeutics Clinical Trials Network (ETCTN), and supported by F. Hoffmann-La Roche, Ltd. and the National Cancer Institute of the National Institutes of Health under the award number UM1CA186691.

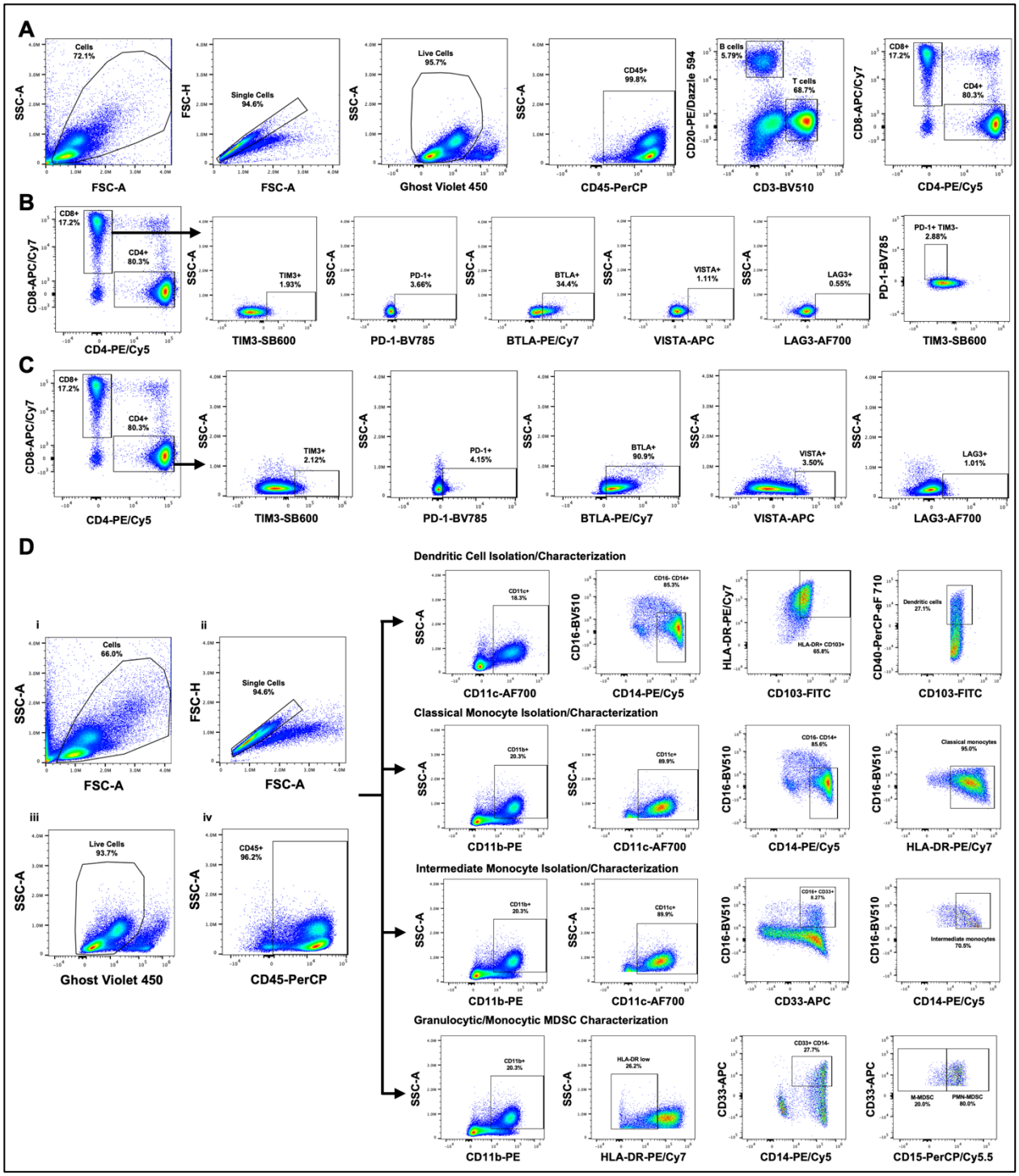

Figure 2.6. Representative gating schema for flow cytometry of lymphocyte and myeloid immune cell populations. (A) Lymphocyte events were gated successively from left to right. $CD4^+$ and $CD8^+$ T cells are gated from within the previous plot's T cell gate. Immune checkpoint

molecules are each shown as percent of (B) $CD8^+$ T cells or (C) $CD4^+$ T cells. (D) Myeloid events were gated similarly to lymphocytes (i-iv) then divided into four main gating strategies. For each population, events were gated successively; values represent the percent of events from the previous graph's gate.

2.8. Tables

Table 2.1. NCT03201458 patient demographics

Patient Characteristics	N=77
Age	
>=44, <65	43
>=65, <86	34
Sex	
Female	48
Male	29
Tumor Type	
Extrahepatic cholangiocarcinoma (ECC)	14
Intrahepatic cholangiocarcinoma (ICC)	43
Gallbladder carcinoma (GBC)	20
Prior Therapies	
1	47
2	30

Table 2.2. Antibodies for flow cytometry

Antibody	Fluorophore	Clone	Vendor
Ghost Dye Violet 450			Tonbo Biosciences
CD45	PerCP	HI30	Biolegend
CD3	BV510	UCHT1	Biolegend
CD8	APC-Cy7	SK1	Biolegend
CD4	PE-Cy5	RPA-T4	Invitrogen
PD-1	BV785	EH12.2H7	Biolegend
CD38	BV650	HB-7	Biolegend
TIM3	SB600	F38-2E2	Invitrogen
LAG3	AF700	3DS223H	Invitrogen
BTLA	PE-Cy7	MIH26	Biolegend
VISTA	APC	B7H5DS8	Invitrogen
CD33	APC	WM53	Invitrogen
CD11b	PE	CBRM1/5	Biolegend
CD11c	AF700	3.9	Invitrogen
CD15	PerCP-Cy5.5	W6D3	Biolegend
HLA-DR	PE-Cy7	LN3	Invitrogen
CD14	PE-Cy5	61D3	Invitrogen
CD103	FITC	B-Ly7	Invitrogen
CD40	PerCP-eFluor 710	5C3	Invitrogen
HLA-DR	BV750	L243	Biolegend

Table 2.3. Soluble factor concentrations in BTC patients at baseline and in healthy donors

Soluble Factor	Healthy donor (HD) samples (N=16)		BTC patient samples (N=51)		
	Mean ± SD (pg/mL)	Median (pg/mL)	Mean ± SD (pg/mL)	Median (pg/mL)	P-value BTC vs. HD
Th1/Th2 cytokines					
GM-CSF	36.85 ± 49.84	14.02	93.84 ± 117.70	58.11	0.0651
IFN-γ	17.04 ± 4.62	15.21	61.02 ± 59.90	45.27	***0.0048***
IL-1β	16.06 ± 20.75	8.44	29.09 ± 20.47	23.91	***0.0303***
IL-2	55.99 ± 38.67	44.56	55.01 ± 14.91	53.38	0.8818
IL-5	23.74 ± 33.33	8.97	81.20 ± 78.57	70.45	***0.0061***
IL-6	33.31 ± 44.84	9.68	279.09 ± 464.73	173.37	***0.0395***
IL-8	3.73 ± 2.17	2.80	55.40 ± 94.71	24.96	***0.0336***
IL-13	12.33 ± 10.13	7.94	23.98 ± 27.02	14.50	0.0977
IL-18	33.60 ± 17.18	27.59	456.73 ± 453.61	342.35	***0.0004***
TNF-α	17.01 ± 13.49	12.48	19.21 ± 8.14	18.00	0.4279
Th9/Th17/Th22/Treg					
IL-10	2.20 ± 1.19	1.68	6.31 ± 6.56	4.72	***0.0158***
IL-17A	3.76 ± 3.37	2.20	30.95 ± 21.43	26.62	***<0.0001***
IL-23	19.26 ± 4.02	18.25	234.94 ± 389.09	97.68	***0.0309***
Chemokines					
Eotaxin/CCL11	23.35 ± 16.47	15.12	45.59 ± 26.23	42.23	***0.0022***
GRO-α/KC/CXCL1	5.32 ± 3.63	3.16	30.97 ± 42.64	20.67	***0.0197***
IP-10/CXCL10	19.93 ± 13.37	16.83	48.71 ± 43.54	33.78	***0.0117***
MCP-1/CCL2	21.87 ± 11.06	20.82	84.12 ± 123.13	54.85	***0.0487***
MIP-1α/CCL3	8.13 ± 8.14	6.36	17.76 ± 26.63	7.74	0.1607
MIP-1β/CCL4	33.38 ± 9.92	32.19	103.34 ± 54.80	92.00	***<0.0001***
RANTES/CCL5	50.57 ± 45.55	26.86	366.10 ± 568.18	223.35	***0.0308***
SDF-1α	429.69 ± 69.17	435.75	532.51 ± 314.05	440.96	0.2003
Growth Factors					
BDNF	187.38 ± 108.14	169.05	176.80 ± 161.70	123.34	0.8075
EGF	31.25 ± 17.70	26.81	52.35 ± 31.61	43.62	***0.0135***
FGF-2	8.32 ± 12.40	2.33	59.89 ± 63.52	43.65	***0.0021***
HGF	381.08 ± 232.45	310.07	643.04 ± 1107.14	208.57	0.3531
PDGF-BB	238.32 ± 291.98	121.11	1484.78 ± 1082.34	1182.70	***<0.0001***
PIGF-1	27.82 ± 18.39	22.56	128.26 ± 60.63	122.77	***<0.0001***
SCF	8.39 ± 4.91	6.18	29.10 ± 23.00	21.41	***0.0007***
VEGF-A	47.75 ± 24.24	50.42	272.28 ± 373.76	132.33	***0.0198***
LIF	16.03 ± 7.96	13.90	20.02 ± 15.19	16.06	0.3181

Table 2.4. Peripheral immune cell populations in BTC patients at baseline and in healthy donors

Immune Cells	Healthy donor (HD) samples (N=12)		BTC patient samples (N=74)		
	Mean ± SD	Median	Mean ± SD	Median	P-value BTC vs. HD
CD4+ T cells					
Total	60.73 ± 17.84	64.65	72.89 ± 12.79	74.00	***0.0117***
PD-1+	1.28 ± 0.39	1.19	3.63 ± 1.99	3.20	***0.0005***
TIM3+	0.79 ± 0.31	0.77	1.37 ± 1.25	0.94	0.2752
BTLA+	25.92 ± 28.00	10.70	56.03 ± 25.15	58.20	***0.0007***
LAG3+	1.20 ± 0.32	1.11	2.07 ± 3.07	1.09	0.6644
VISTA+	1.43 ± 0.62	1.26	1.22 ± 1.07	0.94	0.8671
CD8+ T cells					
Total	34.14 ± 17.04	31.15	22.04 ± 10.97	20.90	***0.0033***
PD-1+	1.28 ± 0.39	1.28	4.34 ± 3.25	3.48	***0.0068***
TIM3+	0.62 ± 0.21	0.61	1.29 ± 1.38	0.86	0.2587
BTLA+	5.35 ± 5.01	3.47	19.19 ± 16.22	15.30	***0.0163***
LAG3+	0.92 ± 0.37	0.97	0.89 ± 0.66	0.75	0.9998
VISTA+	0.70 ± 0.29	0.70	1.64 ± 2.82	0.96	0.5559
PD-1+TIM3-	1.59 ± 0.78	1.47	4.67 ± 3.08	3.62	***0.0036***
Myeloid					
Classical monocytes	7.30 ± 4.82	8.42	12.90 ± 8.37	11.60	0.0801
Intermediate monocytes	0.62 ± 0.36	0.63	1.22 ± 0.97	1.06	0.1062
M-MDSC	1.94 ± 1.71	1.48	3.00 ± 4.03	1.17	0.7240
PMN-MDSC	0.38 ± 0.43	0.25	2.22 ± 3.36	1.13	0.1780
Dendritic cells	0.45 ± 0.41	0.42	1.20 ± 1.50	0.66	0.2459

Table 2.5. Soluble factor percent change from baseline to C2D1: Univariate analysis

Soluble Factor Percent Change from Baseline to C2D1		Overall Survival						Progression-Free Survival					
		Univariate Analysis						Univariate Analysis					
Soluble Factor	Median % change (Range)	Atezolizumab (Arm A)			Atezolizumab + Cobimetinib (Arm B)			Atezolizumab (Arm A)			Atezolizumab + Cobimetinib (Arm B)		
		Hazard Ratio (95% CI)	HR p-value	Log-rank p-value	Hazard Ratio (95% CI)	HR p-value	Log-rank p-value	Hazard Ratio (95% CI)	HR p-value	Log-rank p-value	Hazard Ratio (95% CI)	HR p-value	Log-rank p-value
Th1/Th2 cytokines													
GM-CSF	0.01 (-87.90 - 553.30)	0.94 (0.41-2.12)	0.877	0.877	1.05 (0.43-2.57)	0.920	0.919	1.10 (0.50-2.43)	0.817	0.815	5.47 (1.48-20.19)	***0.011***	***0.004***
IFN-γ	0.00 (-74.03 - 400.83)	0.85 (0.36-1.97)	0.700	0.700	3.25 (1.12-9.45)	***0.031***	***0.023***	1.01 (0.45-2.27)	0.986	0.986	0.60 (0.24-1.52)	0.280	0.265
IL-1β	2.20 (-75.71 - 98.46)	0.74 (0.32-1.71)	0.482	0.480	0.79 (0.33-1.93)	0.610	0.608	0.68 (0.30-1.55)	0.361	0.352	1.94 (0.72-5.20)	0.189	0.173
IL-2	4.7 (-42.95 - 61.68)	0.65 (0.28-1.49)	0.306	0.303	1.04 (0.43-2.53)	0.937	0.936	0.81 (0.36-1.84)	0.618	0.614	1.42 (0.55-3.69)	0.473	0.462
IL-5	1.82 (-61.83 - 113.26)	0.86 (0.38-1.98)	0.731	0.731	0.80 (0.32-1.98)	0.627	0.625	1.00 (0.45-2.25)	0.995	0.995	3.90 (1.33-11.40)	***0.013***	***0.007***
IL-6	-9.16 (-79.97 - 184.42)	0.69 (0.30-1.59)	0.382	0.380	0.85 (0.35-2.06)	0.723	0.721	0.91 (0.41-2.03)	0.814	0.812	1.33 (0.51-3.45)	0.565	0.556
IL-8	-7.83 (-98.47 - 1218.95)	0.66 (0.28-1.55)	0.340	0.336	1.82 (0.65-5.12)	0.258	0.249	1.03 (0.44-2.44)	0.945	0.945	0.77 (0.28-2.13)	0.611	0.603
IL-13	5.11 (-82.44 - 1095.80)	0.37 (0.14-0.97)	***0.044***	***0.037***	0.93 (0.38-2.24)	0.865	0.865	0.72 (0.32-1.62)	0.423	0.415	0.85 (0.33-2.14)	0.722	0.717
IL-18	-10.80 (-79.78 - 847.33)	1.05 (0.47-2.35)	0.913	0.913	1.18 (0.48-2.91)	0.727	0.725	0.87 (0.39-1.95)	0.739	0.736	0.63 (0.23-1.68)	0.354	0.339
TNF-α	3.77 (-55.91 - 84.71)	0.64 (0.28-1.47)	0.291	0.288	0.67 (0.27-1.67)	0.395	0.390	0.84 (0.37-1.91)	0.677	0.673	2.60 (0.91-7.47)	0.076	0.060
Th9/Th17/Th22/Treg													
IL-10	0.01 (-67.53 - 139.01)	0.39 (0.16-0.94)	***0.037***	***0.033***	1.21 (0.49-3.01)	0.681	0.680	0.58 (0.24-1.37)	0.211	0.201	2.04 (0.70-6.00)	0.193	0.176
IL-17A	8.11 (-57.23 - 135.68)	0.67 (0.29-1.56)	0.357	0.355	0.76 (0.31-1.83)	0.539	0.536	0.74 (0.33-1.68)	0.471	0.464	2.72 (0.93-7.89)	0.067	0.052
IL-23	-8.66 (-75.40 - 327.85)	0.78 (0.34-1.79)	0.552	0.551	0.87 (0.36-2.13)	0.763	0.762	0.68 (0.30-1.54)	0.354	0.345	0.83 (0.24-1.61)	0.332	0.318
Chemokines													
Eotaxin/CCL11	-0.90 (-43.70 - 120.21)	0.77 (0.34-1.72)	0.519	0.517	1.27 (0.51-3.12)	0.608	0.605	1.57 (0.68-3.66)	0.292	0.283	0.86 (0.34-2.18)	0.747	0.742
GRO-α/KC/CXCL1	-6.15 (-87.47 - 672.56)	0.91 (0.40-2.08)	0.816	0.816	0.91 (0.37-2.23)	0.832	0.831	1.14 (0.50-2.65)	0.752	0.749	0.91 (0.35-2.37)	0.850	0.847
IP-10/CXCL10	17.58 (-33.91 - 398.77)	0.57 (0.25-1.29)	0.178	0.173	1.07 (0.44-2.65)	0.875	0.875	0.70 (0.32-1.56)	0.383	0.376	0.75 (0.29-1.99)	0.569	0.561
MCP-1/CCL2	-6.21 (-68.37 - 171.81)	1.47 (0.65-3.32)	0.358	0.356	0.49 (0.19-1.23)	0.130	0.122	1.68 (0.75-3.77)	0.207	0.196	1.08 (0.42-2.77)	0.869	0.866
MIP-1α/CCL3	4.10 (-81.47 - 168.58)	0.79 (0.34-1.79)	0.565	0.564	1.15 (0.47-2.84)	0.761	0.760	0.90 (0.40-1.99)	0.792	0.790	0.72 (0.27-1.90)	0.511	0.501
MIP-1β/CCL4	-5.15 (-74.89 - 84.48)	0.24 (0.09-0.66)	***0.006***	***0.003***	1.15 (0.47-2.81)	0.760	0.758	0.85 (0.38-1.92)	0.698	0.694	0.80 (0.31-2.06)	0.647	0.640
RANTES/CCL5	-5.57 (-85.08 - 759.83)	0.68 (0.30-1.56)	0.367	0.365	1.47 (0.58-3.74)	0.416	0.411	1.08 (0.48-2.43)	0.846	0.845	0.47 (0.18-1.27)	0.139	0.122
SDF-1α	-5.07 (-82.62 - 47.74)	0.69 (0.31-1.55)	0.366	0.364	1.15 (0.47-2.81)	0.760	0.758	1.38 (0.61-3.11)	0.434	0.427	0.80 (0.31-2.06)	0.647	0.640
Growth Factors													
BDNF	-25.63 (-72.04 - 69.63)	1.25 (0.53-2.95)	0.603	0.603	0.90 (0.37-2.20)	0.824	0.824	1.76 (0.78-3.95)	0.171	0.161	1.51 (0.58-3.98)	0.400	0.387
EGF	-11.40 (-67.05 - 133.20)	0.92 (0.40-2.12)	0.851	0.850	0.69 (0.27-1.77)	0.442	0.438	1.26 (0.54-2.92)	0.597	0.593	0.96 (0.36-2.58)	0.941	0.940
FGF-2	0.02 (-93.65 - 310.44)	0.23 (0.08-0.65)	***0.006***	***0.003***	0.88 (0.34-2.29)	0.792	0.791	0.60 (0.26-1.35)	0.214	0.204	1.51 (0.52-4.36)	0.450	0.440
HGF	-4.06 (-78.61 - 314.96)	0.42 (0.17-1.04)	0.060	0.053	0.92 (0.38-2.23)	0.853	0.853	0.59 (0.26-1.34)	0.211	0.201	1.51 (0.58-3.92)	0.397	0.384
PDGF-BB	1.32 (-59.19 - 101.34)	1.07 (0.43-2.65)	0.882	0.882	*0.29 (0.09-0.91)*	***0.033***	***0.023***	1.55 (0.66-3.67)	0.315	0.307	0.34 (0.11-1.03)	0.056	***0.040***
PlGF-1	-11.87 (-65.17 - 88.76)	1.18 (0.50-2.79)	0.705	0.704	0.95 (0.36-2.52)	0.918	0.918	1.98 (0.87-4.52)	0.104	*0.095*	1.29 (0.45-3.65)	0.636	0.630
SCF	1.00 (-50.33 - 114.38)	0.57 (0.25-1.33)	0.194	0.189	0.51 (0.20-1.26)	0.145	0.136	0.47 (0.20-1.10)	0.082	0.072	0.75 (0.29-1.95)	0.552	0.543
VEGF-A	-0.21 (-88.55 - 1049.73)	0.93 (0.41-2.09)	0.855	0.855	1.49 (0.61-3.62)	0.378	0.373	1.12 (0.50-2.54)	0.783	0.780	0.71 (0.28-1.81)	0.470	0.459
LIF	1.58 (-48.55 - 87.41)	0.70 (0.31-1.60)	0.398	0.396	1.01 (0.42-2.44)	0.985	0.985	0.82 (0.36-1.84)	0.627	0.622	1.11 (0.43-2.86)	0.822	0.819

Table 2.6. Soluble factor percent change from baseline to C2D1: Multivariate analysis

Soluble Factor Percent Change from Baseline to C2D1		Overall Survival						Progression-Free Survival					
		Multivariate Analysis						Multivariate Analysis					
Soluble Factor	Median % change (Range)	Atezolizumab (Arm A)			Atezolizumab + Cobimetinib (Arm B)			Atezolizumab (Arm A)			Atezolizumab + Cobimetinib (Arm B)		
		Hazard Ratio (95% CI)	HR p-value	Overall p-value	Hazard Ratio (95% CI)	HR p-value	Overall p-value	Hazard Ratio (95% CI)	HR p-value	Overall p-value	Hazard Ratio (95% CI)	HR p-value	Overall p-value
Th1/Th2 cytokines													
GM-CSF	0.01 (-87.90 - 553.30)	0.65 (0.24-1.76)	0.393	0.393	0.86 (0.31-2.34)	0.762	0.762	0.87 (0.34-2.22)	0.764	0.764	9.87 (2.04-47.69)	***0.004***	***0.004***
IFN-γ	0.00 (-74.03 - 400.83)	0.64 (0.25-1.64)	0.351	0.351	2.07 (0.60-7.20)	0.250	0.250	0.98 (0.39-2.49)	0.974	0.974	0.49 (0.16-1.52)	0.216	0.216
IL-1β	2.20 (-75.71 - 98.46)	0.81 (0.32-2.01)	0.647	0.647	1.46 (0.49-4.33)	0.492	0.492	0.72 (0.29-1.77)	0.471	0.471	2.93 (0.92-9.33)	*0.068*	*0.068*
IL-2	4.7 (-42.95 - 61.68)	0.68 (0.29-1.58)	0.365	0.365	0.89 (0.31-2.54)	0.827	0.827	0.82 (0.36-1.90)	0.650	0.650	2.21 (0.69-7.00)	0.180	0.180
IL-5	1.82 (-61.83 - 113.26)	0.92 (0.39-2.14)	0.844	0.844	1.51 (0.52-4.37)	0.450	0.450	1.07 (0.46-2.47)	0.883	0.883	11.86 (2.62-53.66	***0.001***	***0.001***
IL-6	-9.16 (-79.97 - 184.42)	0.39 (0.13-1.15)	*0.087*	*0.087*	0.79 (0.29-2.19)	0.656	0.656	0.64 (0.24-1.71)	0.377	0.377	1.45 (0.46-4.60)	0.528	0.528
IL-8	-7.83 (-98.47 - 1218.95)	0.71 (0.28-1.76)	0.456	0.456	1.54 (0.51-4.59)	0.443	0.443	1.28 (0.50-3.25)	0.608	0.608	0.74 (0.25-2.19)	0.583	0.583
IL-13	5.11 (-82.44 - 1095.80)	0.44 (0.16-1.25)	0.123	0.123	0.54 (0.19-1.51)	0.242	0.242	0.87 (0.36-2.10)	0.756	0.756	0.90 (0.31-2.58)	0.843	0.843
IL-18	-10.80 (-79.78 - 847.33)	0.70 (0.25-1.98)	0.501	0.501	1.86 (0.65-5.29)	0.245	0.245	0.68 (0.24-1.93)	0.470	0.470	0.81 (0.29-2.28)	0.685	0.685
TNF-α	3.77 (-55.91 - 84.71)	0.67 (0.28-1.56)	0.348	0.348	0.94 (0.34-2.65)	0.910	0.910	0.85 (0.37-1.97)	0.708	0.708	2.89 (0.89-9.41)	*0.079*	*0.079*
Th9/Th17/Th22/Treg													
IL-10	0.01 (-67.53 - 139.01)	0.19 (0.06-0.61)	***0.005***	***0.005***	1.31 (0.44-3.91)	0.632	0.632	0.41 (0.15-1.11)	*0.080*	*0.080*	2.16 (0.63-7.44)	0.223	0.223
IL-17A	8.11 (-57.23 - 135.68)	0.72 (0.30-1.74)	0.462	0.462	0.86 (0.31-2.41)	0.776	0.776	0.78 (0.33-1.82)	0.562	0.562	4.34 (1.25-15.02)	***0.021***	***0.021***
IL-23	-8.66 (-75.40 - 327.85)	0.90 (0.36-2.22)	0.813	0.813	0.33 (0.08-1.38)	0.128	0.128	0.74 (0.31-1.77)	0.493	0.493	0.42 (0.08-2.10)	0.289	0.289
Chemokines													
Eotaxin/CCL11	-0.90 (-43.70 - 120.21)	0.51 (0.20-1.33)	0.169	0.169	1.08 (0.40-2.91)	0.871	0.871	1.36 (0.55-3.37)	0.508	0.508	0.73 (0.26-2.03)	0.552	0.552
GRO-α/KC/CXCL1	-6.15 (-87.47 - 672.56)	0.98 (0.39-2.47)	0.958	0.958	1.00 (0.35-2.82)	0.997	0.997	1.28 (0.53-3.05)	0.581	0.581	0.89 (0.28-2.80)	0.841	0.841
IP-10/CXCL10	17.58 (-33.91 - 398.77)	0.77 (0.24-2.41)	0.652	0.652	0.74 (0.26-2.13)	0.577	0.577	1.24 (0.40-3.88)	0.711	0.711	0.51 (0.17-1.54)	0.231	0.231
MCP-1/CCL2	-6.21 (-68.37 - 171.81)	2.83 (0.91-8.75)	*0.071*	*0.071*	0.49 (0.18-1.35)	0.167	0.167	2.38 (0.80-7.07)	0.120	0.120	1.08 (0.39-3.01)	0.876	0.876
MIP-1α/CCL3	4.10 (-81.47 - 168.58)	0.99 (0.40-2.50)	0.990	0.990	1.83 (0.68-4.93)	0.230	0.230	1.39 (0.55-3.52)	0.491	0.491	0.84 (0.29-2.42)	0.749	0.749
MIP-1β/CCL4	-5.15 (-74.89 - 84.48)	0.18 (0.06-0.56)	***0.003***	***0.003***	1.38 (0.51-3.72)	0.522	0.522	0.91 (0.40-2.09)	0.829	0.829	0.87 (0.33-2.34)	0.790	0.790
RANTES/CCL5	-5.57 (-85.08 - 759.83)	0.48 (0.18-1.28)	0.144	0.144	1.07 (0.35-3.24)	0.904	0.904	1.21 (0.47-3.10)	0.695	0.695	0.40 (0.13-1.22)	0.107	0.107
SDF-1α	-5.07 (-62.62 - 47.74)	0.48 (0.19-1.23)	0.127	0.127	1.38 (0.51-3.72)	0.522	0.522	1.36 (0.56-3.30)	0.493	0.493	0.87 (0.33-2.34)	0.790	0.790
Growth Factors													
BDNF	-25.63 (-72.04 - 69.63)	0.93 (0.36-2.37)	0.872	0.872	0.91 (0.33-2.55)	0.864	0.864	1.50 (0.64-3.56)	0.353	0.353	1.31 (0.44-3.90)	0.633	0.633
EGF	-11.40 (-67.05 - 133.20)	1.18 (0.44-3.17)	0.747	0.747	0.53 (0.16-1.77)	0.303	0.303	1.78 (0.65-4.86)	0.261	0.261	0.70 (0.21-2.42)	0.578	0.578
FGF-2	0.02 (-93.65 - 310.44)	0.14 (0.05-0.45)	***<.001***	***<.001***	0.66 (0.21-2.02)	0.461	0.461	0.50 (0.20-1.21)	0.123	0.123	2.01 (0.56-7.27)	0.286	0.286
HGF	-4.06 (-78.61 - 314.96)	0.45 (0.13-1.55)	0.206	0.206	0.89 (0.21-3.73)	0.872	0.872	0.91 (0.28-3.03)	0.883	0.883	0.70 (0.18-2.64)	0.593	0.593
PDGF-BB	1.32 (-59.19 - 101.34)	1.08 (0.40-2.93)	0.877	0.877	0.29 (0.07-1.18)	*0.084*	*0.084*	1.57 (0.63-3.89)	0.330	0.330	0.30 (0.08-1.09)	*0.067*	*0.067*
PlGF-1	-11.87 (-65.17 - 88.76)	0.80 (0.29-2.18)	0.666	0.666	1.46 (0.47-4.53)	0.510	0.510	1.73 (0.69-4.33)	0.241	0.241	0.97 (0.27-3.47)	0.967	0.967
SCF	1.00 (-50.33 - 114.38)	0.39 (0.14-1.07)	*0.067*	*0.067*	0.39 (0.13-1.20)	0.101	0.101	0.34 (0.12-1.00)	***0.049***	***0.049***	0.75 (0.26-2.20)	0.605	0.605
VEGF-A	-0.21 (-88.55 - 1049.73)	0.64 (0.24-1.67)	0.359	0.359	1.30 (0.48-3.55)	0.606	0.606	0.93 (0.38-2.28)	0.874	0.874	0.53 (0.19-1.52)	0.240	0.240
LIF	1.58 (-48.55 - 87.41)	0.77 (0.30-1.98)	0.593	0.593	1.42 (0.50-4.07)	0.513	0.513	0.92 (0.37-2.27)	0.852	0.852	1.92 (0.47-7.93)	0.367	0.367

Table 2.7. Soluble factor baseline concentration: Univariate analysis

Soluble Factor Baseline Concentration		Overall Survival						Progression-Free Survival					
		Univariate Analysis						Univariate Analysis					
Soluble Factor	Median (Range) (pg/mL)	Atezolizumab (Arm A)			Atezolizumab + Cobimetinib (Arm B)			Atezolizumab (Arm A)			Atezolizumab + Cobimetinib (Arm B)		
		Hazard Ratio (95% CI)	HR p-value	Log-rank p-value	Hazard Ratio (95% CI)	HR p-value	Log-rank p-value	Hazard Ratio (95% CI)	HR p-value	Log-rank p-value	Hazard Ratio (95% CI)	HR p-value	Log-rank p-value
Th1/Th2 cytokines													
GM-CSF	58.12 (9.42 - 612.86)	0.93 (0.41-2.08)	0.851	0.851	2.09 (0.85-5.13)	0.107	0.098	0.83 (0.37-1.85)	0.652	0.648	1.18 (0.46-3.01)	0.732	0.727
IFN-γ	45.30 (14.26 - 353.87)	1.09 (0.48-2.47)	0.840	0.840	1.20 (0.47-3.03)	0.702	0.700	1.25 (0.56-2.80)	0.585	0.580	1.03 (0.40-2.67)	0.954	0.953
IL-1β	23.92 (9.60 - 138.97)	1.45 (0.64-3.32)	0.375	0.373	2.26 (0.93-5.52)	0.073	0.065	1.41 (0.63-3.18)	0.406	0.398	1.04 (0.39-2.80)	0.941	0.939
IL-2	53.38 (26.59 - 91.34)	1.01 (0.45-2.29)	0.981	0.981	2.20 (0.90-5.36)	0.083	0.075	1.11 (0.50-2.49)	0.799	0.797	1.14 (0.45-2.90)	0.786	0.782
IL-5	70.46 (15.76 - 548.92)	0.95 (0.42-2.12)	0.897	0.897	2.69 (1.05-6.92)	***0.040***	***0.032***	0.94 (0.42-2.12)	0.887	0.885	0.79 (0.30-2.05)	0.626	0.619
IL-6	173.46 (25.37 - 3210.05)	1.16 (0.52-2.59)	0.723	0.723	0.91 (0.38-2.21)	0.844	0.843	0.91 (0.41-2.03)	0.820	0.819	2.89 (0.98-8.52)	0.055	***0.041***
IL-8	24.97 (2.47 - 543.31)	1.00 (0.45-2.24)	0.998	0.998	1.26 (0.52-3.05)	0.611	0.609	1.36 (0.62-3.01)	0.442	0.436	4.62 (1.42-15.03)	***0.011***	***0.005***
IL-13	14.50 (2.40 - 113.01)	1.05 (0.47-2.36)	0.904	0.904	1.32 (0.54-3.26)	0.540	0.537	0.99 (0.44-2.21)	0.983	0.983	0.64 (0.25-1.65)	0.356	0.342
IL-18	342.37 (38.82 - 2316.06)	1.31 (0.57-3.02)	0.524	0.523	0.76 (0.30-1.93)	0.564	0.561	1.47 (0.65-3.29)	0.353	0.344	1.81 (0.64-5.11)	0.262	0.246
TNF-α	18.00 (9.89 - 49.26)	0.83 (0.37-1.85)	0.645	0.645	1.65 (0.68-4.04)	0.269	0.262	0.85 (0.38-1.89)	0.691	0.687	1.50 (0.58-3.84)	0.402	0.389
Th9/Th17/Th22/Treg													
IL-10	4.72 (1.79 - 41.93)	1.85 (0.82-4.19)	0.141	0.135	1.37 (0.56-3.33)	0.489	0.485	1.32 (0.59-2.94)	0.496	0.490	1.31 (0.51-3.38)	0.576	0.568
IL-17A	26.62 (5.97 - 116.65)	1.04 (0.46-2.35)	0.916	0.916	2.49 (0.95-6.53)	0.063	0.053	1.02 (0.45-2.27)	0.970	0.970	0.89 (0.35-2.26)	0.799	0.795
IL-23	97.71 (14.31 - 2220.66)	0.85 (0.37-1.95)	0.698	0.698	6.20 (2.10-18.25)	***<.001***	***<.001***	0.76 (0.32-1.78)	0.522	0.517	2.00 (0.71-5.60)	0.189	0.170
Chemokines													
Eotaxin/CCL11	42.24 (14.05 - 185.71)	0.92 (0.40-2.09)	0.838	0.838	1.01 (0.41-2.51)	0.982	0.982	1.86 (0.82-4.22)	0.140	0.130	1.42 (0.54-3.71)	0.475	0.464
GRO-α/KC/CXCL1	20.69 (2.05 - 286.26)	0.84 (0.36-1.94)	0.678	0.678	1.54 (0.63-3.78)	0.343	0.338	0.93 (0.41-2.12)	0.863	0.862	2.81 (0.98-8.07)	0.055	***0.040***
IP-10/CXCL10	35.80 (13.82 - 226.23)	0.59 (0.25-1.36)	0.213	0.209	0.84 (0.34-2.03)	0.692	0.690	1.09 (0.48-2.45)	0.842	0.840	1.42 (0.56-3.65)	0.462	0.451
MCP-1/CCL2	54.90 (18.84 - 881.59)	2.08 (0.90-4.82)	0.087	0.081	1.30 (0.54-3.13)	0.562	0.559	1.85 (0.83-4.14)	0.134	0.124	2.23 (0.86-5.77)	0.100	*0.085*
MIP-1α/CCL3	7.74 (1.40 - 143.94)	1.36 (0.60-3.06)	0.460	0.459	2.54 (0.95-6.82)	0.063	0.054	1.18 (0.52-2.66)	0.694	0.690	0.44 (0.16-1.18)	0.104	*0.088*
MIP-1β/CCL4	92.00 (31.49 - 269.17)	0.81 (0.35-1.87)	0.624	0.624	1.19 (0.49-2.87)	0.705	0.703	0.75 (0.33-1.70)	0.497	0.491	1.63 (0.60-4.42)	0.338	0.323
RANTES/CCL5	223.51 (106.61 - 3088.76)	0.77 (0.34-1.77)	0.543	0.542	0.83 (0.33-2.11)	0.697	0.695	0.98 (0.42-2.27)	0.961	0.961	7.19 (2.06-25.00)	***0.002***	***<.001***
SDF-1α	436.45 (170.98 - 1803.65)	0.72 (0.32-1.65)	0.443	0.441	1.81 (0.74-4.41)	0.190	0.182	0.93 (0.41-2.12)	0.862	0.861	1.45 (0.54-3.89)	0.461	0.449
Growth Factors													
BDNF	126.66 (31.11 - 818.14)	0.96 (0.43-2.16)	0.919	0.920	1.57 (0.65-3.83)	0.317	0.311	1.21 (0.55-2.67)	0.638	0.634	2.40 (0.91-6.32)	0.077	0.063
EGF	43.63 (12.59 - 174.67)	0.90 (0.40-2.01)	0.796	0.796	0.98 (0.40-2.39)	0.964	0.964	1.00 (0.45-2.24)	0.992	0.992	1.78 (0.70-4.56)	0.228	0.213
FGF-2	46.38 (2.93 - 332.36)	1.12 (0.50-2.52)	0.789	0.789	1.42 (0.57-3.57)	0.450	0.446	1.24 (0.55-2.79)	0.602	0.597	1.10 (0.42-2.85)	0.850	0.847
HGF	226.52 (88.90 - 5799.44)	0.50 (0.21-1.17)	0.108	0.102	1.31 (0.54-3.18)	0.550	0.547	1.08 (0.48-2.45)	0.856	0.854	1.24 (0.48-3.17)	0.656	0.648
PDGF-BB	1182.98 (85.90 - 6266.65)	1.19 (0.52-2.68)	0.683	0.683	*0.94 (0.39-2.28)*	0.892	0.892	1.06 (0.47-2.37)	0.894	0.892	0.67 (0.26-1.75)	0.419	0.407
PlGF-1	122.79 (41.02 - 282.44)	0.89 (0.40-2.00)	0.778	0.778	2.11 (0.80-5.54)	0.130	0.120	0.92 (0.41-2.06)	0.841	0.839	0.73 (0.29-1.86)	0.510	0.500
SCF	21.42 (10.58 - 111.94)	0.76 (0.33-1.75)	0.515	0.514	0.71 (0.28-1.77)	0.461	0.457	1.13 (0.50-2.51)	0.772	0.770	0.75 (0.29-1.96)	0.558	0.549
VEGF-A	132.39 (5.53 - 2141.25)	0.47 (0.20-1.09)	0.079	0.073	1.02 (0.42-2.46)	0.973	0.973	0.93 (0.41-2.11)	0.862	0.861	2.41 (0.86-6.76)	0.094	0.079
LIF	16.07 (5.60 - 90.90)	0.57 (0.25-1.31)	0.186	0.180	2.42 (0.97-6.06)	0.058	***0.050***	0.77 (0.33-1.78)	0.545	0.541	1.03 (0.38-2.77)	0.951	0.950

Table 2.8. Soluble factor baseline concentration: Multivariate analysis

Soluble Factor Baseline Concentration		Overall Survival						Progression-Free Survival					
		Multivariate Analysis						Multivariate Analysis					
Soluble Factor	Median (Range) (pg/mL)	Atezolizumab (Arm A)			Atezolizumab + Cobimetinib (Arm B)			Atezolizumab (Arm A)			Atezolizumab + Cobimetinib (Arm B)		
		Hazard Ratio (95% CI)	HR p-value	Overall p-value	Hazard Ratio (95% CI)	HR p-value	Overall p-value	Hazard Ratio (95% CI)	HR p-value	Overall p-value	Hazard Ratio (95% CI)	HR p-value	Overall p-value
Th1/Th2 cytokines													
GM-CSF	58.12 (9.42 - 612.86)	1.26 (0.53-3.03)	0.599	0.599	2.03 (0.68-6.00)	0.202	0.202	1.19 (0.47-3.05)	0.715	0.715	0.82 (0.26-2.61)	0.742	0.742
IFN-γ	45.30 (14.26 - 353.87)	1.09 (0.36-3.28)	0.882	0.882	0.80 (0.27-2.43)	0.699	0.699	1.36 (0.43-4.31)	0.604	0.604	1.00 (0.31-3.19)	0.999	0.999
IL-1β	23.92 (9.60 - 138.97)	1.24 (0.51-3.05)	0.635	0.635	1.50 (0.54-4.15)	0.438	0.438	1.35 (0.53-3.44)	0.534	0.534	0.84 (0.29-2.49)	0.758	0.758
IL-2	53.38 (26.59 - 91.34)	1.22 (0.50-2.98)	0.669	0.669	2.69 (0.92-7.88)	*0.072*	*0.072*	1.38 (0.56-3.40)	0.481	0.481	0.79 (0.26-2.44)	0.686	0.686
IL-5	70.46 (15.76 - 548.92)	0.82 (0.35-1.91)	0.644	0.644	2.44 (0.85-6.98)	*0.098*	*0.098*	0.74 (0.30-1.82)	0.516	0.516	0.77 (0.26-2.31)	0.639	0.639
IL-6	173.46 (25.37 - 3210.05)	1.52 (0.64-3.58)	0.343	0.343	1.63 (0.49-5.36)	0.425	0.425	1.13 (0.46-2.80)	0.784	0.784	4.85 (1.19-19.70)	***0.027***	***0.027***
IL-8	24.97 (2.47 - 543.31)	0.75 (0.30-1.92)	0.556	0.556	1.10 (0.38-3.18)	0.860	0.860	1.18 (0.48-2.87)	0.722	0.722	5.83 (1.44-23.60)	***0.013***	***0.013***
IL-13	14.50 (2.40 - 113.01)	1.37 (0.57-3.25)	0.480	0.480	1.26 (0.40-3.90)	0.694	0.694	1.36 (0.51-3.62)	0.544	0.544	0.34 (0.11-1.06)	*0.063*	*0.063*
IL-18	342.37 (38.82 - 2316.06)	1.94 (0.70-5.40)	0.203	0.203	0.69 (0.19-2.55)	0.577	0.577	1.44 (0.59-3.54)	0.424	0.424	3.54 (1.00-12.61)	*0.051*	*0.051*
TNF-α	18.00 (9.89 - 49.26)	0.71 (0.30-1.66)	0.431	0.431	1.65 (0.60-4.51)	0.331	0.331	0.67 (0.28-1.65)	0.388	0.388	1.35 (0.46-3.92)	0.584	0.584
Th9/Th17/Th22/Treg													
IL-10	4.72 (1.79 - 41.93)	2.15 (0.91-5.06)	*0.080*	*0.080*	1.58 (0.55-4.57)	0.400	0.400	1.56 (0.66-3.67)	0.313	0.313	1.00 (0.31-3.29)	0.994	0.994
IL-17A	26.62 (5.97 - 116.65)	1.36 (0.58-3.24)	0.480	0.480	1.33 (0.47-3.79)	0.593	0.593	1.35 (0.54-3.35)	0.523	0.523	0.71 (0.24-2.08)	0.530	0.530
IL-23	97.71 (14.31 - 2220.66)	1.21 (0.47-3.07)	0.694	0.694	7.90 (1.39-45.04)	***0.020***	***0.020***	1.14 (0.39-3.38)	0.808	0.808	2.06 (0.60-7.13)	0.253	0.253
Chemokines													
Eotaxin/CCL11	42.24 (14.05 - 185.71)	0.64 (0.23-1.75)	0.380	0.380	1.16 (0.35-3.86)	0.811	0.811	1.69 (0.67-4.26)	0.268	0.268	1.38 (0.42-4.56)	0.601	0.601
GRO-α/KC/CXCL1	20.69 (2.05 - 286.26)	0.61 (0.23-1.59)	0.315	0.315	1.21 (0.44-3.37)	0.712	0.712	0.74 (0.29-1.92)	0.540	0.540	2.70 (0.79-9.22)	0.113	0.113
IP-10/CXCL10	35.80 (13.82 - 226.23)	0.39 (0.15-1.05)	*0.061*	*0.061*	0.78 (0.29-2.14)	0.629	0.629	0.93 (0.37-2.35)	0.882	0.882	1.18 (0.40-3.49)	0.769	0.769
MCP-1/CCL2	54.90 (18.84 - 881.59)	2.32 (0.92-5.83)	*0.073*	*0.073*	1.47 (0.50-4.31)	0.482	0.482	1.84 (0.81-4.15)	0.143	0.143	2.13 (0.69-6.55)	0.188	0.188
MIP-1α/CCL3	7.74 (1.40 - 143.94)	1.51 (0.64-3.55)	0.347	0.347	1.79 (0.65-4.93)	0.263	0.263	1.25 (0.53-2.94)	0.616	0.616	0.42 (0.15-1.16)	*0.094*	*0.094*
MIP-1β/CCL4	92.00 (31.49 - 269.17)	1.01 (0.41-2.45)	0.989	0.989	0.70 (0.25-1.96)	0.501	0.501	0.93 (0.39-2.21)	0.871	0.871	1.24 (0.42-3.71)	0.695	0.695
RANTES/CCL5	223.51 (106.61 - 3088.76)	0.86 (0.36-2.06)	0.730	0.730	1.26 (0.46-3.43)	0.650	0.650	0.90 (0.37-2.20)	0.826	0.826	11.65 (2.66-51.04	***0.001***	***0.001***
SDF-1α	436.45 (170.98 - 1803.65)	0.87 (0.36-2.10)	0.761	0.761	0.84 (0.28-2.51)	0.753	0.753	1.30 (0.51-3.31)	0.587	0.587	1.05 (0.34-3.23)	0.937	0.937
Growth Factors													
BDNF	126.66 (31.11 - 818.14)	0.76 (0.28-2.09)	0.599	0.599	1.45 (0.54-3.87)	0.455	0.455	1.07 (0.44-2.64)	0.879	0.879	4.31 (1.30-14.34)	***0.017***	***0.017***
EGF	43.63 (12.59 - 174.67)	0.70 (0.26-1.93)	0.496	0.496	1.50 (0.55-4.07)	0.425	0.425	0.83 (0.29-2.40)	0.730	0.730	2.98 (0.92-9.59)	*0.067*	*0.067*
FGF-2	46.38 (2.93 - 332.36)	1.41 (0.60-3.30)	0.433	0.433	1.19 (0.44-3.24)	0.729	0.729	1.67 (0.64-4.34)	0.296	0.296	0.83 (0.31-2.27)	0.724	0.724
HGF	226.52 (88.90 - 5799.44)	0.33 (0.12-0.91)	***0.033***	***0.033***	1.06 (0.38-2.92)	0.916	0.916	0.97 (0.38-2.48)	0.952	0.952	0.94 (0.30-2.93)	0.919	0.919
PDGF-BB	1182.98 (85.90 - 6266.65)	1.08 (0.45-2.57)	0.867	0.867	0.67 (0.16-2.85)	0.591	0.591	0.94 (0.41-2.19)	0.894	0.894	1.18 (0.36-3.93)	0.785	0.785
PlGF-1	122.79 (41.02 - 282.44)	1.18 (0.46-3.01)	0.736	0.736	0.54 (0.14-1.99)	0.351	0.351	1.22 (0.50-2.93)	0.663	0.663	0.42 (0.11-1.56)	0.195	0.195
SCF	21.42 (10.58 - 111.94)	0.91 (0.37-2.26)	0.838	0.838	0.58 (0.15-2.20)	0.420	0.420	1.34 (0.56-3.18)	0.507	0.507	0.33 (0.09-1.27)	0.107	0.107
VEGF-A	132.39 (5.53 - 2141.25)	0.54 (0.22-1.33)	0.184	0.184	0.83 (0.29-2.41)	0.737	0.737	1.12 (0.47-2.64)	0.800	0.800	2.13 (0.56-8.01)	0.265	0.265
LIF	16.07 (5.60 - 90.90)	0.67 (0.27-1.69)	0.399	0.399	1.62 (0.58-4.49)	0.357	0.357	0.81 (0.34-1.95)	0.640	0.640	0.97 (0.28-3.29)	0.957	0.957

Table 2.9. Immune cell fold change from baseline to C2D1: Univariate analysis

Immune Cell Population Fold Change from Baseline to C2D1		Overall Survival						Progression-Free Survival					
		Univariate Analysis						Univariate Analysis					
Immune Cells	Median Fold Change (Range)	Atezolizumab (Arm A)			Atezolizumab + Cobimetinib (Arm B)			Atezolizumab (Arm A)			Atezolizumab + Cobimetinib (Arm B)		
		Hazard Ratio (95% CI)	HR p-value	Log-rank p-value	Hazard Ratio (95% CI)	HR p-value	Log-rank p-value	Hazard Ratio (95% CI)	HR p-value	Log-rank p-value	Hazard Ratio (95% CI)	HR p-value	Log-rank p-value
CD4+ T cells													
Total	0.99 (0.87 - 1.24)	0.81 (0.36-1.81)	0.605	0.604	2.56 (0.83-7.95)	0.104	0.092	0.48 (0.21-1.14)	0.096	0.086	0.99 (0.35-2.82)	0.988	0.988
PD-1+	1.07 (0.39 - 1.07)	1.08 (0.48-2.46)	0.846	0.846	1.81 (0.73-4.47)	0.200	0.191	1.13 (0.51-2.50)	0.771	0.768	0.57 (0.22-1.48)	0.248	0.238
TIM3+	1.26 (0.35 - 4.86)	0.68 (0.29-1.60)	0.373	0.370	0.29 (0.10-0.84)	***0.022***	***0.015***	0.61 (0.27-1.39)	0.239	0.229	0.80 (0.31-2.12)	0.660	0.656
BTLA+	1.05 (0.05 - 3.42)	3.79 (1.38-10.41)	***0.010***	***0.006***	0.50 (0.20-1.24)	0.136	0.127	3.40 (1.46-7.90)	***0.004***	***0.003***	1.36 (0.53-3.49)	0.517	0.512
LAG3+	1.02 (0.04 - 2.66)	3.16 (1.22-8.22)	***0.018***	***0.014***	0.54 (0.22-1.33)	0.180	0.171	2.33 (1.02-5.34)	***0.045***	***0.037***	1.72 (0.63-4.68)	0.290	0.280
VISTA+	0.92 (0.05 - 16.33)	1.99 (0.77-5.13)	0.153	0.146	1.04 (0.42-2.58)	0.939	0.939	2.03 (0.85-4.83)	0.111	0.100	0.97 (0.36-2.64)	0.960	0.959
CD8+ T cells													
Total	1.06 (0.33 - 1.44)	1.27 (0.55-2.94)	0.575	0.574	0.91 (0.37-2.22)	0.833	0.832	1.86 (0.79-4.36)	0.153	0.141	1.51 (0.59-3.86)	0.387	0.380
PD-1+	1.28 (0.42 - 8.13)	0.95 (0.41-2.17)	0.896	0.896	0.87 (0.35-2.17)	0.761	0.760	0.62 (0.26-1.45)	0.268	0.258	1.10 (0.43-2.82)	0.844	0.843
TIM3+	1.18 (0.00 - 28.16)	0.65 (0.25-1.67)	0.371	0.368	0.48 (0.19-1.24)	0.132	0.123	0.64 (0.28-1.50)	0.307	0.298	0.81 (0.31-2.12)	0.669	0.666
BTLA+	0.99 (0.00 - 3.63)	3.83 (1.41-10.41)	***0.008***	***0.005***	0.81 (0.32-2.08)	0.666	0.664	3.45 (1.44-8.23)	***0.005***	***0.003***	1.80 (0.68-4.73)	0.236	0.225
LAG3+	0.89 (0.00 - 7.51)	2.62 (1.10-6.23)	***0.030***	***0.025***	0.60 (0.25-1.48)	0.267	0.261	1.79 (0.76-4.21)	0.182	0.174	1.76 (0.69-4.51)	0.240	0.230
VISTA+	0.93 (0.00 - 3.85)	2.25 (0.91-5.52)	0.078	0.071	1.47 (0.60-3.64)	0.401	0.399	1.92 (0.81-4.52)	0.138	0.129	0.15 (0.04-0.56)	***0.005***	***0.001***
CD38+HLA-DR+	1.09 (0.13 - 37.56)	1.05 (0.44-2.52)	0.905	0.905	2.88 (0.91-9.08)	0.071	0.059	1.23 (0.52-2.91)	0.637	0.633	2.08 (0.52-8.30)	0.301	0.286
PD-1+TIM3-	1.22 (0.41 - 6.97)	1.08 (0.48-2.47)	0.849	0.849	1.12 (0.46-2.75)	0.800	0.799	0.71 (0.31-1.64)	0.429	0.421	1.28 (0.48-3.43)	0.623	0.619
Myeloid													
Classical monocytes	0.85 (0.23 - 4.94)	1.28 (0.57-2.90)	0.549	0.548	0.98 (0.38-2.54)	0.971	0.971	1.35 (0.61-2.98)	0.459	0.451	0.72 (0.26-2.00)	0.527	0.521
Intermediate monocytes	0.99 (0.00 - 7.33)	0.87 (0.38-1.99)	0.737	0.737	0.47 (0.18-1.20)	0.113	0.103	0.97 (0.43-2.20)	0.944	0.943	0.97 (0.36-2.59)	0.945	0.944
M-MDSC	0.52 (0.00 - 24.03)	0.71 (0.31-1.61)	0.408	0.406	0.71 (0.28-1.84)	0.485	0.481	0.69 (0.31-1.55)	0.371	0.363	0.62 (0.23-1.67)	0.348	0.338
PMN-MDSC	0.86 (0.00 - 66.2)	0.91 (0.39-2.08)	0.816	0.816	1.32 (0.48-3.62)	0.587	0.586	0.88 (0.37-1.96)	0.716	0.712	0.59 (0.20-1.71)	0.330	0.317
Dendritic cells	1.09 (0.16 - 7.44)	1.34 (0.59-3.04)	0.492	0.490	1.27 (0.49-3.25)	0.623	0.621	1.18 (0.53-2.62)	0.686	0.683	1.67 (0.62-4.52)	0.315	0.304

Table 2.10. Immune cell population fold change from baseline to C2D1: Multivariate analysis

Immune Cell Population Fold Change from Baseline to C2D1		Overall Survival						Progression-Free Survival					
		Multivariate Analysis						Multivariate Analysis					
Immune Cells	Median Fold Change (Range)	Atezolizumab (Arm A)			Atezolizumab + Cobimetinib (Arm B)			Atezolizumab (Arm A)			Atezolizumab + Cobimetinib (Arm B)		
		Hazard Ratio (95% CI)	HR p-value	Overall p-value	Hazard Ratio (95% CI)	HR p-value	Overall p-value	Hazard Ratio (95% CI)	HR p-value	Overall p-value	Hazard Ratio (95% CI)	HR p-value	Overall p-value
CD4+ T cells													
Total	0.99 (0.87 - 1.24)	1.32 (0.52-3.35)	0.562	0.562	1.91 (0.57-6.41)	0.294	0.294	0.59 (0.24-1.44)	0.247	0.247	0.88 (0.26-2.97)	0.834	0.834
PD-1+	1.07 (0.39 - 1.07)	0.66 (0.24-1.80)	0.418	0.418	1.51 (0.48-4.73)	0.475	0.475	0.92 (0.36-2.34)	0.867	0.867	0.29 (0.09-0.97)	***0.045***	***0.045***
TIM3+	1.26 (0.35 - 4.86)	0.86 (0.33-2.22)	0.757	0.757	0.19 (0.05-0.74)	***0.016***	***0.016***	0.64 (0.27-1.52)	0.308	0.308	0.63 (0.17-2.31)	0.487	0.487
BTLA+	1.05 (0.05 - 3.42)	3.69 (1.32-10.35)	***0.013***	***0.013***	0.47 (0.14-1.59)	0.222	0.222	4.36 (1.69-11.25)	***0.002***	***0.002***	1.31 (0.41-4.20)	0.645	0.645
LAG3+	1.02 (0.04 - 2.66)	2.80 (0.93-8.43)	*0.066*	*0.066*	0.23 (0.06-0.81)	***0.023***	***0.023***	2.04 (0.84-4.95)	0.115	0.115	1.86 (0.61-5.70)	0.276	0.276
VISTA+	0.92 (0.05 - 16.33)	1.37 (0.43-4.41)	0.594	0.594	1.62 (0.52-5.02)	0.404	0.404	1.55 (0.64-3.79)	0.335	0.335	1.48 (0.38-5.81)	0.575	0.575
CD8+ T cells													
Total	1.06 (0.33 - 1.44)	0.84 (0.32-2.23)	0.727	0.727	1.26 (0.45-3.51)	0.656	0.656	1.47 (0.57-3.81)	0.431	0.431	1.28 (0.45-3.64)	0.648	0.648
PD-1+	1.28 (0.42 - 8.13)	1.29 (0.52-3.23)	0.584	0.584	1.64 (0.41-6.54)	0.481	0.481	0.66 (0.26-1.69)	0.387	0.387	0.87 (0.23-3.39)	0.844	0.844
TIM3+	1.18 (0.00 - 28.16)	0.91 (0.33-2.51)	0.854	0.854	0.45 (0.16-1.24)	0.122	0.122	0.70 (0.28-1.75)	0.443	0.443	1.00 (0.34-2.95)	0.999	0.999
BTLA+	0.99 (0.00 - 3.63)	2.95 (0.96-9.11)	*0.060*	*0.060*	1.00 (0.31-3.27)	0.997	0.997	2.94 (1.18-7.31)	***0.020***	***0.020***	1.60 (0.51-5.02)	0.420	0.420
LAG3+	0.89 (0.00 - 7.51)	1.76 (0.56-5.47)	0.330	0.330	0.43 (0.15-1.24)	0.119	0.119	1.11 (0.40-3.09)	0.844	0.844	1.48 (0.52-4.20)	0.465	0.465
VISTA+	0.93 (0.00 - 3.85)	1.21 (0.34-4.29)	0.770	0.770	1.53 (0.60-3.94)	0.373	0.373	1.27 (0.46-3.52)	0.644	0.644	0.10 (0.02-0.46)	***0.003***	***0.003***
CD38+HLA-DR+	1.09 (0.13 - 37.56)	1.35 (0.45-4.02)	0.589	0.589	3.47 (0.67-18.09)	0.139	0.139	1.69 (0.64-4.42)	0.288	0.288	1.23 (0.23-6.47)	0.808	0.808
PD-1+TIM3-	1.22 (0.41 - 6.97)	1.48 (0.59-3.71)	0.404	0.404	1.58 (0.51-4.93)	0.429	0.429	0.76 (0.31-1.91)	0.563	0.563	1.24 (0.36-4.29)	0.738	0.738
Myeloid													
Classical monocytes	0.85 (0.23 - 4.94)	0.88 (0.34-2.27)	0.798	0.798	1.23 (0.43-3.49)	0.697	0.697	1.16 (0.48-2.78)	0.747	0.747	0.54 (0.17-1.69)	0.290	0.290
Intermediate monocytes	0.99 (0.00 - 7.33)	0.48 (0.16-1.40)	0.177	0.177	0.39 (0.13-1.23)	0.110	0.110	0.94 (0.39-2.22)	0.880	0.880	0.91 (0.29-2.85)	0.871	0.871
M-MDSC	0.52 (0.00 - 24.03)	0.50 (0.20-1.28)	0.147	0.147	0.64 (0.21-1.95)	0.430	0.430	0.52 (0.21-1.31)	0.166	0.166	0.47 (0.15-1.44)	0.184	0.184
PMN-MDSC	0.86 (0.00 - 66.2)	0.88 (0.34-2.25)	0.791	0.791	2.81 (0.84-9.45)	*0.095*	*0.095*	0.98 (0.40-2.28)	0.923	0.923	0.43 (0.11-1.75)	0.239	0.239
Dendritic cells	1.09 (0.16 - 7.44)	1.44 (0.60-3.47)	0.416	0.416	2.91 (0.78-10.85)	0.111	0.111	1.16 (0.48-2.84)	0.739	0.739	3.06 (0.72-12.95)	0.129	0.129

Table 2.11. Immune cell populations at baseline: Univariate analysis

Immune Cell Baseline Populations		Overall Survival						Progression-Free Survival					
		Univariate Analysis						Univariate Analysis					
Immune Cells	Median (Range)	Atezolizumab (Arm A)			Atezolizumab + Cobimetinib (Arm B)			Atezolizumab (Arm A)			Atezolizumab + Cobimetinib (Arm B)		
		Hazard Ratio (95% CI)	HR p-value	Log-rank p-value	Hazard Ratio (95% CI)	HR p-value	Log-rank p-value	Hazard Ratio (95% CI)	HR p-value	Log-rank p-value	Hazard Ratio (95% CI)	HR p-value	Log-rank p-value
CD4+ T cells													
Total	74.00 (38.40 - 96.40)	0.92 (0.45-1.86)	0.813	0.814	0.57 (0.26-1.24)	0.159	0.152	1.01 (0.50-2.04)	0.982	0.982	1.14 (0.49-2.63)	0.761	0.759
PD-1+	3.20 (0.82 - 10.20)	0.99 (0.50-2.00)	0.988	0.988	0.84 (0.40-1.78)	0.649	0.648	1.36 (0.66-2.78)	0.403	0.392	0.93 (0.41-2.14)	0.869	0.867
TIM3+	0.94 (0.00 - 7.77)	1.33 (0.66-2.67)	0.422	0.421	1.30 (0.61-2.76)	0.496	0.494	1.22 (0.59-2.50)	0.590	0.582	1.81 (0.77-4.25)	0.174	0.164
BTLA+	58.21 (2.37 - 96.90)	1.15 (0.58-2.28)	0.694	0.694	1.25 (0.59-2.64)	0.557	0.555	0.85 (0.42-1.74)	0.665	0.659	0.71 (0.31-1.62)	0.415	0.408
LAG3+	1.09 (0.00 - 14.70)	1.03 (0.51-2.08)	0.927	0.927	1.24 (0.59-2.62)	0.574	0.572	1.37 (0.67-2.81)	0.390	0.380	1.46 (0.64-3.35)	0.368	0.361
VISTA+	0.94 (0.00 - 6.57)	1.36 (0.69-2.71)	0.377	0.376	1.32 (0.62-2.81)	0.474	0.471	1.72 (0.83-3.55)	0.145	0.133	0.87 (0.38-2.01)	0.751	0.749
CD8+ T cells													
Total	20.90 (3.06 - 56.60)	0.93 (0.47-1.85)	0.834	0.834	2.53 (1.16-5.53)	***0.020***	***0.016***	0.84 (0.41-1.71)	0.632	0.625	0.80 (0.35-1.84)	0.601	0.597
PD-1+	3.48 (0.23 - 19.50)	0.63 (0.32-1.25)	0.187	0.184	1.01 (0.48-2.14)	0.984	0.984	1.06 (0.52-2.16)	0.866	0.864	0.97 (0.41-2.28)	0.938	0.938
TIM3+	0.86 (0.00 - 7.14)	0.82 (0.41-1.64)	0.567	0.566	0.59 (0.28-1.26)	0.173	0.167	0.99 (0.49-2.02)	0.982	0.982	1.27 (0.55-2.95)	0.580	0.576
BTLA+	15.30 (0.00 - 66.30)	1.50 (0.73-3.07)	0.268	0.265	2.06 (0.95-4.45)	0.067	0.061	1.29 (0.62-2.67)	0.498	0.489	1.03 (0.45-2.36)	0.946	0.946
LAG3+	0.75 (0.00 - 3.13)	0.42 (0.19-0.91)	***0.028***	***0.024***	1.68 (0.78-3.65)	0.187	0.181	0.54 (0.26-1.16)	0.113	0.101	1.24 (0.54-2.86)	0.615	0.611
VISTA+	0.96 (0.00 - 19.30)	0.46 (0.22-0.97)	***0.04***	***0.036***	0.82 (0.39-1.72)	0.597	0.595	0.42 (0.20-0.89)	***0.024***	***0.018***	1.18 (0.52-2.69)	0.690	0.687
CD38+HLA-DR+	0.74 (0.00 - 17.60)	0.86 (0.42-1.75)	0.672	0.672	0.68 (0.30-1.51)	0.338	0.333	0.95 (0.46-1.96)	0.884	0.883	1.15 (0.49-2.73)	0.746	0.745
PD-1+TIM3-	3.62 (0.33 - 17.10)	0.61 (0.31-1.22)	0.164	0.160	0.93 (0.43-2.01)	0.860	0.859	1.06 (0.52-2.16)	0.866	0.863	0.99 (0.43-2.29)	0.989	0.989
Myeloid													
Classical monocytes	11.6 (0.00 - 55.40)	1.35 (0.65-2.79)	0.420	0.419	0.95 (0.45-2.03)	0.902	0.901	1.43 (0.68-3.00)	0.349	0.338	0.67 (0.29-1.57)	0.357	0.350
Intermediate monocytes	0.17 (0.00 - 4.90)	2.23 (1.08-4.60)	***0.030***	***0.027***	1.04 (0.49-2.19)	0.926	0.925	1.26 (0.61-2.58)	0.531	0.522	0.71 (0.31-1.65)	0.426	0.420
M-MDSC	1.12 (0.00 - 19.80)	1.40 (0.70-2.81)	0.345	0.343	1.28 (0.60-2.72)	0.520	0.518	1.29 (0.63-2.63)	0.480	0.471	0.87 (0.38-2.00)	0.735	0.733
PMN-MDSC	1.13 (0.00 - 6.94)	1.30 (0.66-2.60)	0.449	0.448	0.62 (0.29-1.33)	0.220	0.215	0.90 (0.44-1.85)	0.775	0.770	0.89 (0.37-2.13)	0.798	0.797
Dendritic cells	0.63 (0.00 - 6.94)	0.80 (0.39-1.66)	0.555	0.554	1.46 (0.68-3.16)	0.331	0.327	0.68 (0.33-1.42)	0.305	0.292	0.87 (0.37-2.05)	0.758	0.756

Table 2.12. Immune cell populations at baseline: Multivariate analysis

Immune Cell Baseline Populations		Overall Survival						Progression-Free Survival					
		Multivariate Analysis						Multivariate Analysis					
Immune Cells	Median (Range)	Atezolizumab (Arm A)			Atezolizumab + Cobimetinib (Arm B)			Atezolizumab (Arm A)			Atezolizumab + Cobimetinib (Arm B)		
		Hazard Ratio (95% CI)	HR p-value	Overall p-value	Hazard Ratio (95% CI)	HR p-value	Overall p-value	Hazard Ratio (95% CI)	HR p-value	Overall p-value	Hazard Ratio (95% CI)	HR p-value	Overall p-value
CD4+ T cells													
Total	74.00 (38.40 - 96.40)	1.14 (0.53-2.46)	0.734	0.734	0.69 (0.28-1.70)	0.416	0.416	1.01 (0.49-2.09)	0.981	0.981	1.67 (0.56-5.03)	0.359	0.359
PD-1+	3.20 (0.82 - 10.20)	1.03 (0.50-2.14)	0.929	0.929	0.72 (0.31-1.71)	0.461	0.461	1.42 (0.68-2.98)	0.356	0.356	1.26 (0.51-3.16)	0.616	0.616
TIM3+	0.94 (0.00 - 7.77)	1.42 (0.68-2.98)	0.351	0.351	1.05 (0.35-3.09)	0.937	0.937	1.38 (0.63-3.03)	0.420	0.420	2.06 (0.63-6.75)	0.231	0.231
BTLA+	58.21 (2.37 - 96.90)	1.39 (0.66-2.93)	0.391	0.391	1.31 (0.60-2.85)	0.502	0.502	0.97 (0.44-2.16)	0.950	0.950	0.74 (0.30-1.81)	0.503	0.503
LAG3+	1.09 (0.00 - 14.70)	1.44 (0.66-3.14)	0.357	0.357	1.78 (0.56-5.65)	0.325	0.325	1.84 (0.82-4.14)	0.138	0.138	1.72 (0.61-4.90)	0.308	0.308
VISTA+	0.94 (0.00 - 6.57)	1.66 (0.79-3.48)	0.183	0.183	1.45 (0.64-3.29)	0.370	0.370	1.99 (0.90-4.41)	*0.091*	*0.091*	0.97 (0.40-2.38)	0.956	0.956
CD8+ T cells													
Total	20.90 (3.06 - 56.60)	0.68 (0.31-1.48)	0.336	0.336	2.11 (0.79-5.64)	0.138	0.138	0.84 (0.41-1.75)	0.645	0.645	0.52 (0.17-1.63)	0.265	0.265
PD-1+	3.48 (0.23 - 19.50)	0.58 (0.29-1.18)	0.132	0.132	1.17 (0.49-2.79)	0.730	0.730	1.03 (0.49-2.15)	0.940	0.940	1.00 (0.36-2.80)	0.995	0.995
TIM3+	0.86 (0.00 - 7.14)	0.93 (0.45-1.93)	0.855	0.855	0.73 (0.31-1.68)	0.453	0.453	1.08 (0.49-2.40)	0.850	0.850	1.36 (0.56-3.34)	0.499	0.499
BTLA+	15.30 (0.00 - 66.30)	1.35 (0.55-3.29)	0.511	0.511	2.06 (0.89-4.79)	*0.092*	*0.092*	0.97 (0.39-2.39)	0.946	0.946	1.12 (0.44-2.87)	0.805	0.805
LAG3+	0.75 (0.00 - 3.13)	0.51 (0.19-1.35)	0.175	0.175	2.03 (0.73-5.60)	0.174	0.174	0.71 (0.21-2.47)	0.594	0.594	1.17 (0.41-3.34)	0.766	0.766
VISTA+	0.96 (0.00 - 19.30)	0.52 (0.22-1.20)	0.125	0.125	1.34 (0.54-3.35)	0.528	0.528	0.46 (0.19-1.13)	*0.090*	*0.090*	2.35 (0.84-6.59)	0.103	0.103
CD38+HLA-DR+	0.74 (0.00 - 17.60)	0.81 (0.35-1.87)	0.626	0.626	0.79 (0.30-2.10)	0.640	0.640	0.88 (0.37-2.11)	0.775	0.775	0.97 (0.37-2.54)	0.952	0.952
PD-1+TIM3-	3.62 (0.33 - 17.10)	0.57 (0.28-1.16)	0.119	0.119	1.19 (0.47-3.05)	0.712	0.712	1.08 (0.52-2.24)	0.843	0.843	0.90 (0.33-2.46)	0.831	0.831
Myeloid													
Classical monocytes	11.6 (0.00 - 55.40)	1.24 (0.59-2.63)	0.567	0.567	1.10 (0.46-2.65)	0.830	0.830	1.55 (0.71-3.36)	0.268	0.268	0.91 (0.35-2.33)	0.837	0.837
Intermediate monocytes	0.17 (0.00 - 4.90)	3.25 (1.28-8.21)	***0.013***	***0.013***	1.48 (0.58-3.75)	0.415	0.415	1.28 (0.58-2.83)	0.536	0.536	0.61 (0.21-1.80)	0.375	0.375
M-MDSC	1.12 (0.00 - 19.80)	1.93 (0.90-4.14)	*0.091*	*0.091*	1.03 (0.41-2.56)	0.951	0.951	1.35 (0.64-2.84)	0.427	0.427	0.86 (0.34-2.20)	0.759	0.759
PMN-MDSC	1.13 (0.00 - 6.94)	1.01 (0.44-2.33)	0.973	0.973	0.67 (0.29-1.59)	0.366	0.366	0.73 (0.31-1.70)	0.464	0.464	1.23 (0.46-3.30)	0.683	0.683
Dendritic cells	0.63 (0.00 - 6.94)	0.60 (0.25-1.44)	0.254	0.254	1.23 (0.48-3.19)	0.669	0.669	0.52 (0.22-1.20)	0.124	0.124	0.79 (0.28-2.24)	0.656	0.656

Chapter 3: MEK inhibition alters immunomodulatory factor production in biliary tract cancer cell lines, modulates immune cell phenotypes, and impairs T cell activation in biliary tract cancer patients.

3.1. Author Contributions and Acknowledgement of Reproduction

This chapter contains sections of unpublished data, a section that is reproduced with minor edits from Figure 5 of Lauren Dennison[1], Amanda Ruggieri[2], Aditya Mohan[1], James Leatherman[1], Kayla Cruz[1], Skylar Woolman[1], Nilofer Azad[1], Gregory B. Lesinski[2], Elizabeth M. Jaffee[1], and Mark Yarchoan[1], Context-Dependent Immunomodulatory Effects of MEK Inhibition are Enhanced with T-cell Agonist Therapy, *Cancer Immunol Res*, 2021; 9(10): 1187-1201. https://doi.org/10.1158/2326-6066.CIR-21-0147, and a section that contains data described in Mark Yarchoan[1], Leslie Cope[1], Amanda N. Ruggieri[2], Robert A. Anders[1], Anne M. Noonan[3], Laura W. Goff[4], Lipika Goyal[5], Jill Lacy[6], Daneng Li[7], Anuj K. Patel[8], Aiwu R. He[9], Ghassan K. Abou-Alfa[10,11], Kristen Spencer[12], Edward J. Kim[13], S. Lindsey Davis[14], Autumn J. McRee[15], Paul R. Kunk[16], Subir Goyal[2], Yuan Liu[2], Lauren Dennison[1], Stephanie Xavier[1], Aditya A. Mohan[1], Qingfeng Zhu[1], Andrea Wang-Gillam[17], Andrew Poklepovic[18], Helen X. Chen[19], Elad Sharon[19], Gregory B. Lesinski[2], and Nilofer S. Azad[1], Multicenter Randomized Phase II Trial of Atezolizumab With or Without Cobimetinib in Biliary Tract Cancers, *J Clin Invest*. 2021; 121(24):e152670. https://doi.org/10.1172/JCI152670.

Author contributions for Dennison, L. et al. are as follows: L. Dennison: Conceptualization, data curation, formal analysis, validation, investigation, visualization, methodology, writing–original draft, project administration, writing–review and editing. A. Ruggieri: Data curation, investigation. A. Mohan: Data curation, formal analysis, investigation. J.

Leatherman: Investigation. K. Cruz: Investigation. S. Woolman: Conceptualization, funding acquisition, investigation. N. Azad: Conceptualization, resources, funding acquisition, investigation, writing–review and editing. G.B. Lesinski: Conceptualization, resources, supervision, funding acquisition, writing–review and editing. E.M. Jaffee: Conceptualization, resources, supervision, funding acquisition, writing–original draft, writing–review and editing. M. Yarchoan: Conceptualization, resources, supervision, funding acquisition, investigation, writing–original draft, writing–review and editing.

Author contributions for Yarchoan, M. et al. are as follows: MY, NSA, and LC conceived and designed the study. MY, GBL, NSA and LC drafted the manuscript. LC, SG, and YL provided statistical analysis of primary and secondary outcomes. MY, NSA, and GBL obtained funding. MY, GBL, NSA, and LC supervised the study. MY, LC, ANR, RAA, AMN, LWG, LG, JL, DL, AKP, ARH, GKA, KS, EK, SLD, AJM, PRK, SG, YL, LD, SX, AAM, QZ, AWG, AP, HXC, ES, GBL, and NSA acquired, analyzed, or interpreted data. Additionally, all authors critically revised the manuscript for important intellectual content; provided administrative, technical, or material support; and reviewed, edited, and approved the manuscript. MY, NSA, and LC had access to all of the clinical data at all times, and the full data were shared with all of the study authors at the time the manuscript was submitted. The corresponding authors take responsibility for the integrity of the data and the accuracy of the data analysis.

Affiliations:

[1]Johns Hopkins University, Baltimore, Maryland, USA.

[2]Winship Cancer Institute of Emory University, Atlanta, Georgia, USA.

[3]The Ohio State University, Columbus, Ohio, USA.

[4]Vanderbilt-Ingram Cancer Center, Nashville, Tennessee, USA.

[5]Massachusetts General Hospital Cancer Center, Boston, Massachusetts, USA.

[6]Yale Cancer Center, New Haven, Connecticut, USA.

[7]City of Hope, Duarte, California, USA.

[8]Dana-Farber Cancer Institute, Boston, Massachusetts, USA.

[9]Georgetown University, Washington, DC, USA.

[10]Memorial Sloan Kettering Cancer Center, New York City, New York, USA.

[11]Weill Medical College at Cornell University, New York City, New York, USA.

[12]Rutgers Cancer Institute, New Brunswick, New Jersey, USA.

[13]UC Davis, Sacramento, California, USA.

[14]University of Colorado Hospital, Aurora, Colorado, USA.

[15]University of North Carolina, Chapel Hill, North Carolina, USA.

[16]University of Virginia, Charlottesville, Virginia, USA.

[17]Washington University in St. Louis, Siteman Cancer Center, St. Louis, Missouri, USA.

[18]Virginia Commonwealth University, Massey Cancer Center, Richmond, Virginia, USA.

[19]NCI Cancer Therapy Evaluation Program, Bethesda, Maryland, USA.

3.2 Introduction

Biliary tract cancers (BTC) are often diagnosed at late stage when they are refractory to many therapies and surgical resection is not possible. The frequency of tumor infiltrating lymphocytes

(TILs) is a prognostic indicator for improved outcomes in several cancers including melanoma and breast cancer[260, 261]. TILs are notoriously excluded from the BTC tumor microenvironment (TME), with one study revealing 45% of iCCA was devoid of infiltrating lymphocytes, and only 11% of all samples had significant TIL infiltration[262]. While PD-1/PD-L1-targeting immune checkpoint blockade (ICB) can promote tumor regression and the restoration of $CD8^+$ T cell effector functionality, it is not sufficient to induce T cell infiltration into tumors that lack TILs[263]. Therefore, combination strategies have been investigated to both improve cytotoxic T cell function and promote their infiltration into tumors, especially the combination of MEK inhibitors with ICB.

The Ras/Raf/MEK/ERK signaling pathway contributes significantly to the development and progression of BTCs, with activating KRAS mutations identified in up to 22% of patients with BTC[241]. Aside from the obvious roles this pathway has in supporting tumor cellular proliferation and survival, the inhibition of MEK signaling has been investigated in other cancer models for its ability to modulate $CD8^+$ T cell migration and tumor infiltration[187, 264, 265]. However, the mechanism by which this occurs has yet to be delineated. Using a panel of BTC cell lines with constitutive MEK activation, we hypothesized that MEK inhibition modulates the production of chemokines by tumor cells to promote T cell recruitment and infiltration.

The combination of MEK inhibition and PD-L1 blockade was investigated in patients with advanced BTC, as discussed in Chapter 2. While the primary endpoint of the trial was achieved, objective responses were disappointing, contradicting the hypothesis that MEKi could synergize with PD-L1 blockade for improved anti-tumor T cell activity. Therefore, comprehensive immune profiling was performed to evaluate the effects that this combination has on immune responses in advanced BTC and uncover strategies to improve this combination in this patient population.

3.3 Results

3.3.1 Cobimetinib inhibits ERK phosphorylation in BTC cell lines but does not interrupt cell viability

MEK inhibition (MEKi) can cause tumor regression and prolong survival in vivo[187]. Several biliary tract cancer cell lines harbor constitutively active MEK, visualized by the presence of phosphorylated ERK (pERK). To determine if the MEK inhibition had direct cytotoxic effects on cancer cells, cell viability was evaluated in a panel of BTC cell lines treated with the MEK inhibitor cobimetinib. Cells were cultured and treated with cobimetinib, at concentrations ranging from 0.05μM to 5μM, for 48 hours. Pathway inhibition was confirmed via Western blotting which showed complete loss of phosphorylated ERK by 1μM of treatment (Figure 3.1). However, even with complete abrogation of pERK, cells viability did not significantly decrease as determined by MTT assay (Figure 3.2). Despite the frequent dependence of BTCs on MAPK signaling for their development and progression, targeting this pathway in cancer cells alone is not sufficient to elicit a tumor-killing effect. Therefore, we hypothesized that the MEKi-mediated antitumor effects observed in other tumor models may instead be due to the role of MEK signaling in the tumor microenvironment.

3.3.2 MEK inhibition modulates the production of soluble factors by BTC cells

MEK inhibition has been linked to increased tumor infiltrating T cells correlating with reduction in tumor burden. Immune cell recruitment is mediated by chemokines, which are chemoattractant proteins that induce the motility of immune cells on a gradient. Chemokines can be produced by several sources in the tumor microenvironment, including stromal cells and by tumors themselves[266]. After demonstrating that MEK inhibition does not directly impose a tumor-killing effect on BTC cells, we hypothesized that MEKi may mediate the production of chemokines and

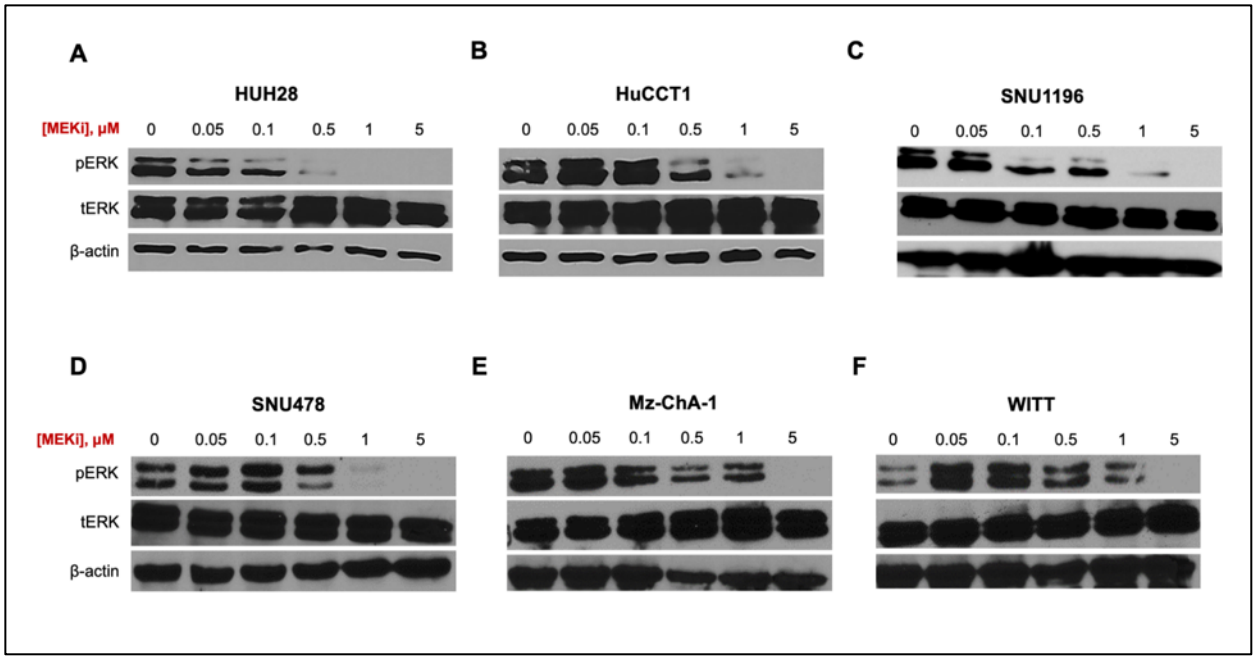

Figure 3.1. Cobimetinib sufficiently reduces p-ERK expression in BTC cell lines. Representative Western blot images showing inhibition of phosphorylated ERK by MEK inhibition for the BTC cell lines (A) HUH28, (B) HuCCT1, (C) SNU1196, (D) SNU478, (E) Mz-ChA-1, and (F) WITT. Cells were treated with increasing concentrations of cobimetinib for 48 hours prior to harvest.

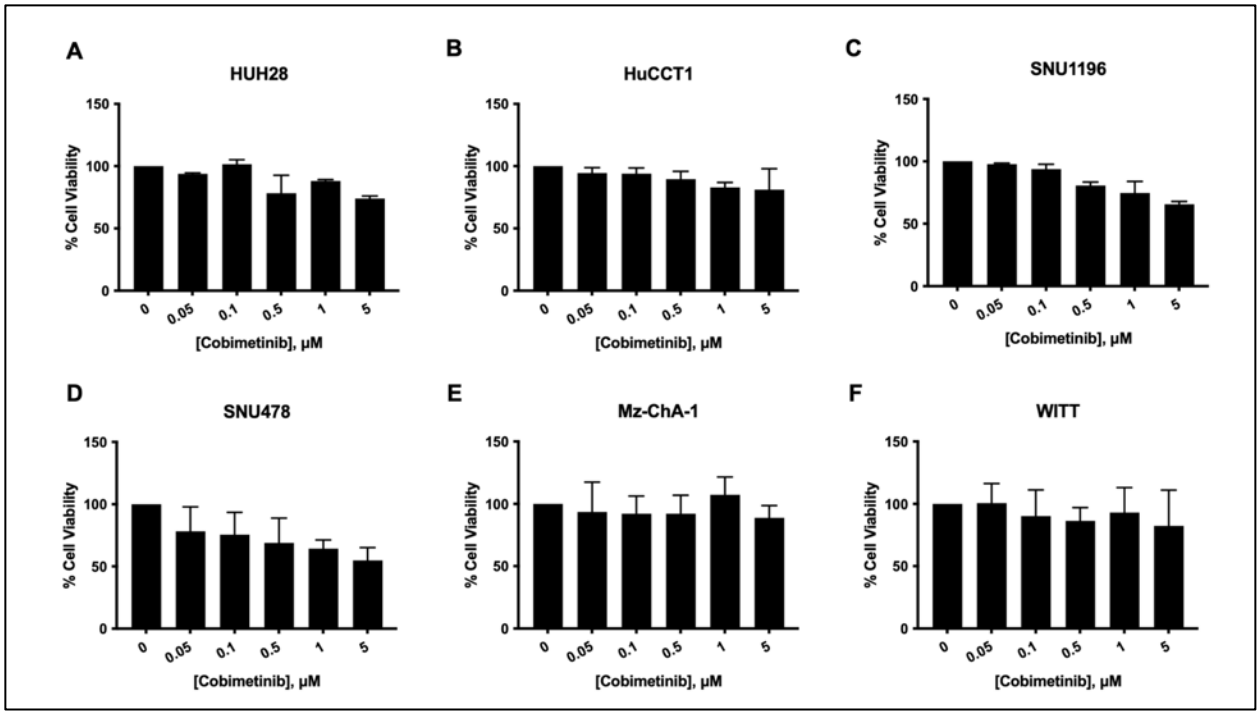

Figure 3.2. Cobimetinib does not significantly limit cell viability in BTC cell lines despite potent inhibition of ERK activation. MTT assays were used to evaluate cell viability following treatment with MEK inhibitor in the BTC cell lines (A) HUH28, (B) HuCCT1, (C) SNU1196, (D) SNU478, (E) Mz-ChA-1, and (F) WITT. Cells were treated with cobimetinib for 48 hours prior to MTT assay.

immunomodulatory factors in the TME. We harvested culture supernatants from BTC cells before and after treatment with 5μM cobimetinib and performed a bioplex analysis of soluble factors using the Luminex platform. We simultaneously measured 45 cytokines, chemokines, and growth factors directly produced by BTC cells and found that MEKi modulates the production of several immune factors in vitro (Figure 3.3). The most significantly altered soluble factors included the chemokine CXCL10/IP-10 and the pro-inflammatory cytokines GM-CSF and LIF. In particular, 5/6 cell lines evaluated had significant increases in CXCL10 production, 4/6 cell lines had significant decreases in GM-CSF production, and all 6 cell lines had highly significant decreases in LIF production. The degree of modulation of these soluble factors varied among the cell lines evaluated, with no apparent correlation to BTC anatomic subtype each cell line was derived from.

3.3.3. Comprehensive immune profiling of advanced BTC patients receiving atezolizumab with or without cobimetinib revealed relationships between immune checkpoint expression and clinical outcomes.

Correlative analysis of cryopreserved PBMCs from patients was conducted in an exploratory manner to assess T cell-focused biomarkers and relationship to clinical outcome measures and treatment. For this analysis, we focused on differences in biomarkers attributable to the combination treatment versus monotherapy by incorporating an interaction effect (Table 3.1). At baseline, patients in the combination arm with a higher than median percentage of $LAG3^+$ $CD8^+$ T cells (HR = 0.43, P = 0.035) had better OS than in the monotherapy arm, while more $TIM3^+$ $CD4^+$ T cells (OR = 4.8, P = 0.033) were indicative of more favorable response by RECIST in the combination arm versus the monotherapy arm. These biomarkers, however, were not significant predictors of better survival or clinical response at baseline when data from all patients, regardless of treatment arm, were compiled for analysis. In addition to assessing biomarkers at baseline, we

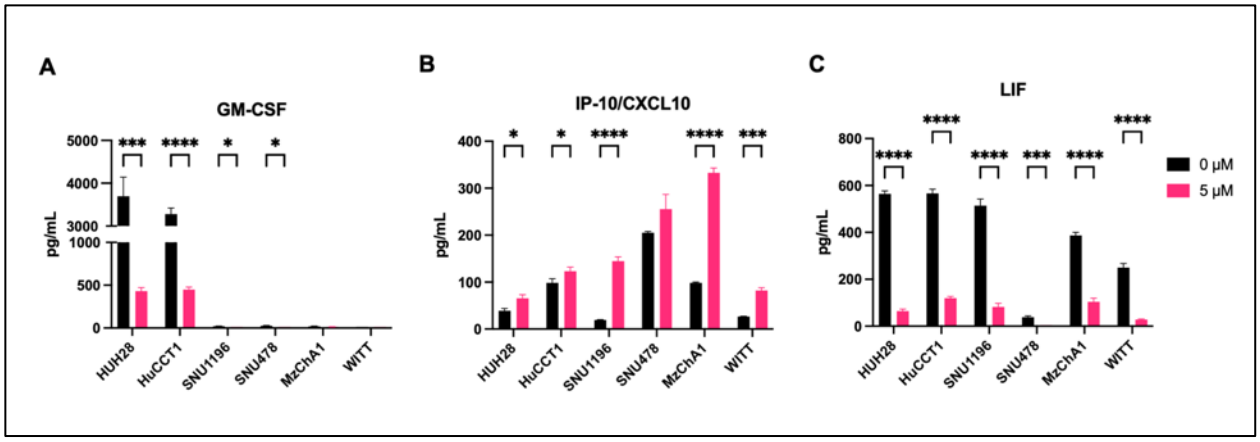

Figure 3.3. Cobimetinib significantly alters the production of GM-CSF, CXCL10, and LIF in BTC cell lines. Bioplex analysis of BTC cell culture derived supernatants revealed significant changes in concentration of (A) GM-CSF, (B) CXCL10/IP-10, and (C) LIF. Changes were analyzed via multiple t tests, and multiple corrections were adjusted for by the Holm-Šídák method. *p<0.05, ***p<0.001, ****p<0.0001.

also evaluated fold-change in cell percentages from baseline to cycle 2 day 1 (C2D1). This approach revealed that patients in the combination arm with a decrease in several T cell–focused biomarkers had better OS. These included decreases in $LAG3^+$ (HR = 0.36, P = 0.024) and $BTLA^+$ (HR = 0.31, P = 0.014) $CD4^+$ T cells. Complementing these data was the observation that patients in Arm B with a decrease in $VISTA^+$ $CD8^+$ T cells (HR = 0.23, P = 0.004) from baseline to C2D1 had significantly longer PFS.

3.3.4. Addition of cobimetinib impairs T cell activation in patients receiving concurrent PD-L1 inhibition

As a validation of preclinical findings demonstrating that systemic MEKi impairs effector T cell function, blood samples from advanced BTC patients receiving atezolizumab with or without cobimetinib were used to specifically isolate the effects of systemic MEKi in the context of anti–PD-L1 (Figure 3.4A). Using peripheral blood samples, we analyzed the proportion of $CD8^+$ T cells expressing CD38, a marker of human T-cell activation, at baseline and compared this with the proportion expressing CD38 at day 15, by which time all patients would have received 1 dose of atezolizumab and patients in arm B would have received 14 days of cobimetinib treatment. Given that PD-1 expression can also define T cells that are in a more heightened state of T-cell activation in addition to its role as a biomarker for T-cell exhaustion, we also analyzed the proportion of $CD8^+$ T cells that were $PD\text{-}1^+$ but did not express the exhaustion marker TIM3. We observed that the percentage of $CD8^+$ T cells expressing CD38 as well as the percentage of $CD8^+$ T cells that were $PD\text{-}1^+$ $TIM3^-$ increased in arm A between cycle 1 day 1 (C1D1) and cycle 1 day 15 (C1D15; mean fold change between the two time points was 1.58 and 1.631, respectively), whereas the percentage of $CD8^+$ T cells expressing CD38 and that were $PD\text{-}1^+TIM3^-$ remained constant between the two time points in arm B (mean fold change was 1.01 and 1.114 respectively;

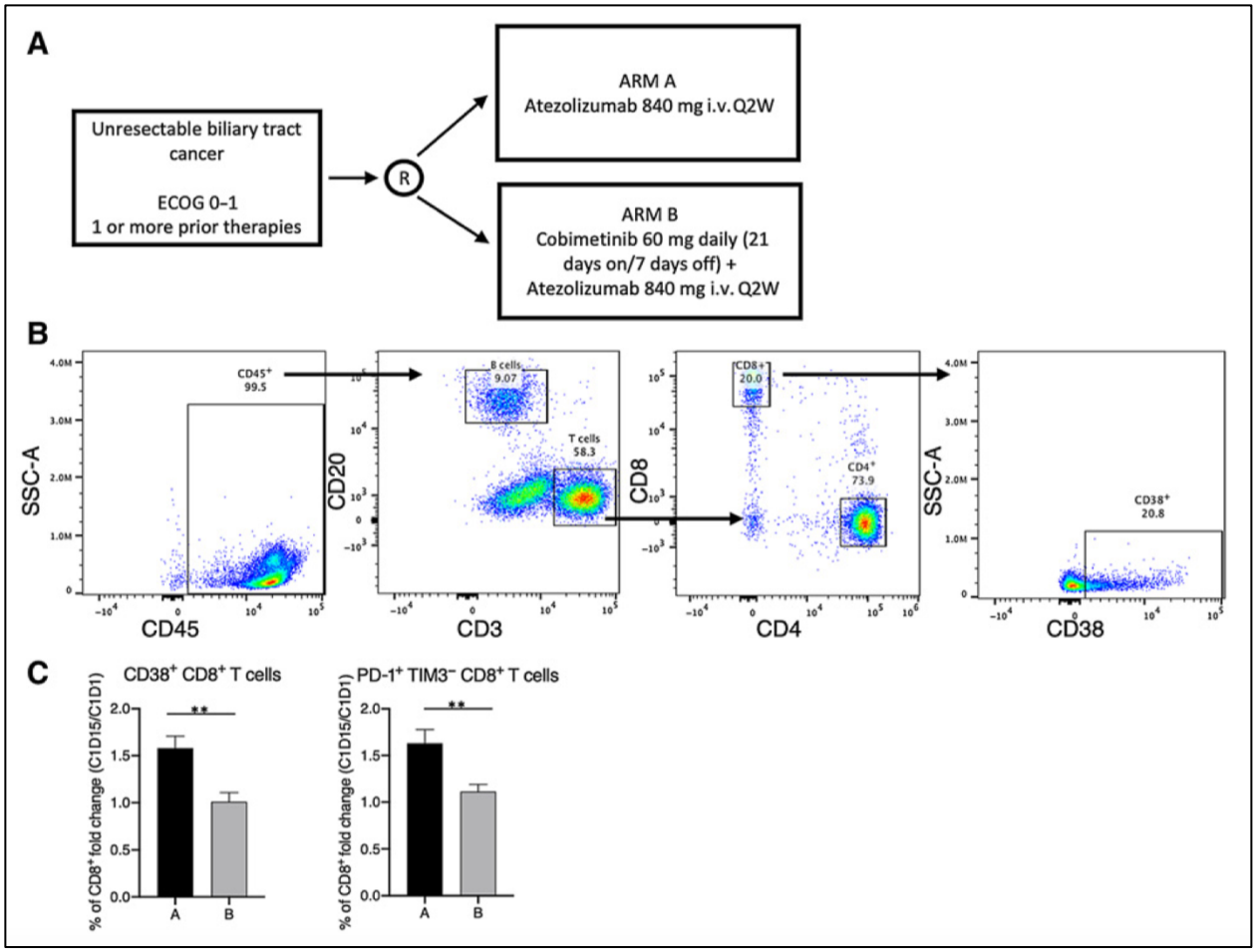

Figure 3.4. Addition of cobimetinib to atezoluzimab in a phase II clinical trial leads to a decrease in T-cell activation. (A) Treatment scheme for the multicenter randomized phase II trial of atezolizumab as a monotherapy or in combination with cobimentinib (NCT03201458). (B) Example of flow cytometry gating strategy used to analyze activated T cells from patient peripheral blood samples taken at baseline (C1D1 and at day 15 of treatment (C1D15). (C) Fold change of the proportion of activated $CD38^{+}$ $CD8^{+}$ T cells and $PD\text{-}1^{+}$ $TIM3^{-}$ $CD8^{+}$ T cells between peripheral blood patient samples taken at C1D15 and C1D1. Each bar represents mean +/- SEM (n = 26 for arm A and n = 21 for arm B). Two-tailed unpaired t tests were used to compare the two arms. ECOG, Eastern Cooperative Oncology Group performance status; q2w, every 2 weeks.

Figure 3.4B, 3.4C). The difference in fold change between arm A and arm B was statistically significant in both cases (P = 0.002 and 0.009). While circulating T cells typically may have a low frequency of tumor antigen–specific clones, this clinical trial material was in agreement with our preclinical observations that systemic MEKi globally impairs T-cell activation in the clinical setting.

3.4 Discussion

In these studies, we show that MEK inhibition modulates the production of soluble immune factors from BTC tumor cells without a significant reduction in cell viability. Accordingly, previously observed MEKi-mediated tumor regression may not be due to tumor cell intrinsic effects of MEKi on cell proliferation and survival. Rather, MEK inhibition of BTC tumor cells could provoke tumor microenvironmental alterations to reduce immunosuppression and T cell exclusion that is characteristic of advanced BTC. This corresponds to previous work from our lab which demonstrates that BTC cell culture supernatants contain high concentrations of pro-inflammatory cytokines, including GM-CSF, and promote the expansion of myeloid-derived suppressor cells (MDSC), which contribute significantly to immunosuppression in BTC by limiting the activity and proliferation of $CD8^+$ T cells[267]. Coupling this data with our finding that MEKi reduces GM-CSF production by the same BTC cell lines, we hypothesize that MEKi may limit MDSC expansion, which may in turn restore T cell activity to support improved antitumor responses (Figure 3.5). We propose future investigation into the role of MEK inhibition in the modulation of MDSC expansion and function in the context of the BTC tumor microenvironment.

To compliment the in vitro experiments that demonstrate the regulation of the production of soluble factors from BTC cells at a localized level, which does not necessarily reflect the systemic

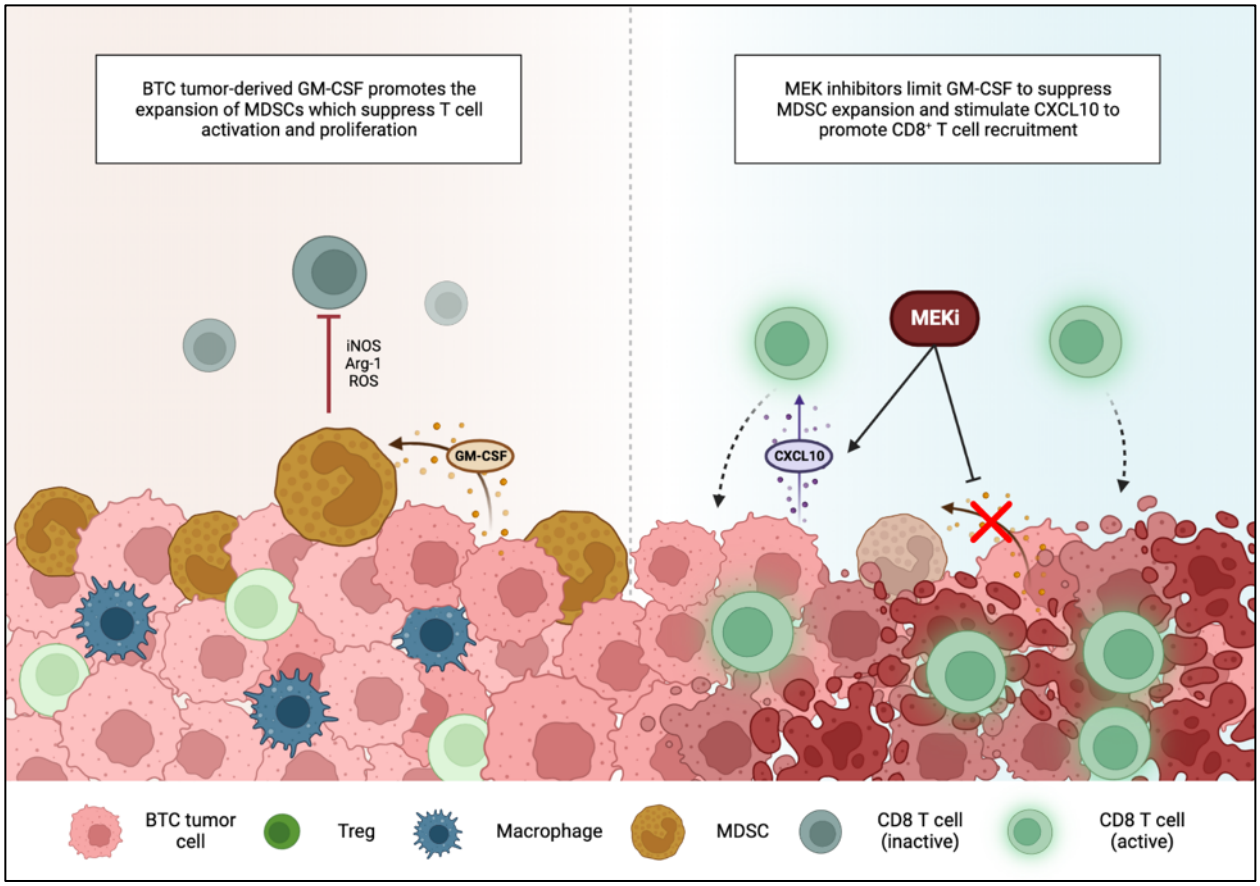

Figure 3.5. Model figure for proposed mechanism of MEKi-mediated T cell infiltration. Cell culture derived supernatants from BTC cell lines promote MDSC expansion from PBMCs in vitro, in a GM-CSF- and IL-6- dependent manner[267]. MDSCs limit $CD8^+$ T cell proliferation and activation via secretion of iNOS, arginase, and ROS. Treatment of BTC cell lines with the MEK inhibitor cobimetinib significantly reduces GM-CSF production and promotes production of the $CD8^+$ T cell-recruiting chemokine CXCL10. Since MEKi has been shown to promote $CD8^+$ T cell migration into tumors, we propose that this may occur by suppressing MDSC expansion to restore T cell activity while inducing CXCL10-mediated migration into BTC tumors.

effects of MEK inhibitor administration, our clinical trial analysis provides evidence that systemic MEK inhibition impairs effector T cell function in peripheral blood As established previously, patients enrolled in our clinical trial investigating cobimetinib and atezolizumab in advanced BTC, MEK inhibition limits T cell activation compared to PD-L1 blockade alone[224]. Furthermore, when similar bioplex analysis was performed on peripheral plasma samples from this trial as it was on BTC cells in vitro, the same trends were not observed for these soluble factors when evaluated systemically, though there were additional significant modulations in the production of different soluble factors in patient plasma (Chapter 2). These data do, however, support the necessity for future investigations into these soluble factors to understand their roles in MEKi-mediated immune responses in the tumor microenvironment, and how they can be utilized to improve therapeutic strategies for advanced biliary tract cancers.

3.5 Methods

3.5.1. Cell culture

Human SNU-478 and SNU-1196 cell lines were purchased from the Korean Cell Line Bank (Seoul, Korea) and authenticated prior to receipt. Human CCA cell lines HUH28, HuCCT1, and WITT (Sk-ChA-1) were a gift from Dr. Tushar Patel (Mayo Clinic, Jacksonville, FL), and Mz-ChA-1 was a gift from Dr. Shannon Glaser (Texas A&M Health Sciences Center, Bryan, TX). These cells were authenticated through ATCC cell line authentication service (Kit #135-XV). HUH28, HuCCT1, SNU478, and SNU1196 were cultured in RPMI-1640 media (Gibco) supplemented with 10% fetal bovine serum (FBS), 1% L-glutamine, and antibiotics. Mz-ChA-1 and WITT were cultured in Dulbecco's Modified Eagle Medium (Gibco, DMEM) supplemented with 10% FBS, 1% L-glutamine, and antibiotics.

3.5.2. Immunoblot analysis

Protein extraction and immunoblot analysis was performed as previously described, using antibodies for ERK1/2, phospho-ERK1/2, and β-actin (Cell Signaling Technologies, Danvers, MA, USA). Following incubation with horseradish peroxidase-conjugated secondary antibody, immune complexes were detected using SuperSignal® West Pico Chemiluminescent Substrate (Thermo Fisher Scientific, Waltham, MA, USA) and visualized on autoradiography film.

3.5.3. Cell viability assay

Cells were added to 96-well flat-bottom plates to adhere overnight, before initiating treatment with increasing concentrations of cobimetinib from 0.05μM to 5μM, and sterile deionized water was used as a medium control. After 48 hours, 10 μL MTT reagent (30-1010K, ATCC) was added to each well, and cells were incubated for 3 hours at 37°C with 5% CO2. Media was then removed, and 200μL of DMSO was added per well with careful mixing. Absorbance at a wavelength of 595 nm was measured using a Synergy H1 plate reader (BioTek). Cells were plated in triplicate for each experimental condition. Data was normalized to the medium control for percent cell viability.

3.5.4. Cytokine, chemokine, and growth factor analysis

Cells were plated in 12-well plates and treated with increasing concentrations of cobimetinib, from 0.05μM to 5μM, for 48 hours. Cell culture supernatants were analyzed using a panel of 45 cytokines, chemokines, and growth factors on a Luminex magnetic bead-based platform according to manufacturer protocol (ProcartaPlex Cytokine/Chemokine/Growth Factor Panel 1, EPX450-12171-901, ProcartaPlex Immunoassays, Invitrogen; Waltham, MA). Samples were analyzed in duplicate on a Luminex 100 instrument and quantified using analyte-specific standard curves. Three biological replicates were performed and all replicates were analyzed on the same plate.

3.5.5. Flow cytometry

Comprehensive phenotypic analysis of peripheral immune cells was conducted via 23-color flow cytometry. Antibodies are detailed in Table 2.2. Cryopreserved PBMCs were thawed at 37°C, washed, centrifuged, and resuspended in FACS buffer (PBS + 3% FBS + 0.05 mM EDTA). Cells were incubated with surface antibody for 30 min at 4°C, washed, permeabilized and fixed overnight using the FoxP3/Transcription Factor Staining Buffer set (00-5523-00, eBioscience). Cells were incubated with intracellular antibodies for one hour at room temperature, washed, and resuspended in FACS buffer for analysis. Flow cytometric analysis was conducted on a Cytek Aurora (Cytek Biosciences, Fremont, CA). Compensation controls were generated using UltraComp eBeads Compensation Beads (01-2222-41, Invitrogen; Waltham, MA). Data were analyzed using FlowJo software version 10.7.2 (FlowJo, LLC; Ashland, OR).

3.5.6. Patient sample processing

Peripheral blood was drawn prior to administration of cobimetinib and/or atezolizumab at baseline, cycle 1 day 15, and cycle 2 day 1. Blood was collected in 10-mL tubes containing EDTA as an anticoagulant and shipped overnight to a central site (Lesinski Laboratory, Winship Cancer Institute of Emory University, Atlanta, GA) for processing. Upon arrival to the central site, blood samples were centrifuged at room temperature at 805 x g for 10 minutes. Peripheral blood mononuclear cells (PBMCs) were collected by density gradient centrifugation using Ficoll-Paque. All PBMCs were stored in liquid nitrogen until time of analysis by flow cytometry.

3.5.7. Statistical Analysis

Descriptive statistics were used to summarize data for each individual biomarker at baseline and follow-up time points. The change at the follow-up time from baseline was calculated as the fold-

change between the 2 time points. All those biomarker measurements were further compared between 2 treatment arms using Student's t test. The association with clinical outcomes was explored using Cox proportional hazard model for time-to-event outcomes (e.g., OS or PFS) or logistic regression model for binary outcome (e.g., best response via RECIST). The biomarker value at baseline or its fold-change at a follow-up time point were further dichotomized by the median value noted above versus below-median for all available patients regardless of treatment group. The interaction effect between a dichotomized biomarker and treatment groups were tested in Cox and logistic regression model, in which we compared treatment arms (Arm B: cobimetinib + atezolizumab vs. Arm A: atezolizumab alone) inside each stratum by a biomarker. A significant interaction term indicates there is differential patient's response or outcome in treatments given their biomarker status. Such a biomarker is also referred to as a predictive biomarker. Multiple comparisons were corrected for using the Holm-Šídák method. Cell viability by MTT assay was evaluated using one-way ANOVA. Significance was determined as $p<0.05$.

3.6. Tables

Table 3.1. Biomarker correlative analyses in subgroups defined by biomarkers for OS, PFS, and best response

Clinical Endpoint	Biomarker	Hazard Ratio	P-value
Best response[A]	CD4+TIM3+ above the median at baseline	4.80 (1.14-20.27)	0.033
OS[B]	CD8+LAG3+ above median at baseline	0.43 (0.20-0.94)	0.035
	CD4+LAG3+ fold-change at C2D1 below the median	0.36 (0.14-0.87)	0.024
	CD4+BTLA+ fold-change at C2D1 below the median	0.31 (0.12-0.79)	0.014
	CD8+VISTA+ fold-change at C2D1 below the median		
PFS[B]	CD8+VISTA+ fold-change at C2D1 below the median	0.23 (0.08-0.63)	0.004

[A]Logistic regression with estimated odds ratio and 95% CI for comparison between Arm B and Arm A. [B]Cox proportional hazard model with estimated hazard ratio and 95% CI for comparison between Arm B and Arm A.

Chapter 4: Conclusions, Future Directions, and Closing Remarks

4.1 Introduction

The use of immune checkpoint blockade (ICB) in combination with inhibitors of MEK, a kinase with aberrant activation in many cases of biliary tract cancer (BTC), has been an important focus for advancing treatment strategies with patients with advanced BTC[205, 207, 243, 244, 268]. In other cancers, MEK inhibition promotes the infiltration of $CD8^+$ T cells into tumors to enhance T cell-mediated antitumor activity[187, 188, 269]. However, it was recently found that MEK inhibition can limit the activation of $CD8^+$ T cells that ICB would otherwise reinvigorate to initiate tumor killing effects in BTC[224]. In this dissertation, this emerging clinical strategy is investigated with a comprehensive analysis of a recent clinical trial and supportive preclinical studies to uncover new insights into improving therapeutic strategies for BTC.

First, patients with advanced BTC receiving a combination of the MEK inhibitor cobimetinib and the PD-L1 blocking antibody atezolizumab had significant decreases in peripheral levels of the growth factors PDGF-BB, PlGF-1, and BDNF, and decreasing PDGF-BB correlated with improved overall and progression-free survival (Figure 2.3). Additionally, patients receiving dual MEK/PD-L1 blockade had increased populations of $CD4^+TIM3^+$ T cells, which correlated with worse OS (Figure 2.4). Furthermore, increasing populations of $CD4^+$ and $CD8^+$ T cells expressing BTLA correlated with improved OS and PFS in patients receiving atezolizumab alone, and higher baseline populations of $CD8^+BTLA^+$ T cells were indicative of better overall survival across all patients regardless of treatment received (Figure 2.2). In preclinical studies, BTC cell lines treated with cobimetinib in vitro did not exhibit a decrease in cell viability despite a potent inhibition of MEK activity (Figure 3.1, Figure 3.2). Cobimetinib did, however, alter the concentrations of

soluble factors in cell culture supernatants derived from BTC cell lines. In particular, GM-CSF and LIF were significantly decreased in most or all cell lines, while the chemokine CXCL10 was increased in some cell lines (Figure 3.3). While these data do not provide mechanistic evidence for how MEKi elicits tumor killing activity, they support the hypothesis that MEKi influences the immune microenvironment in BTC tumors via soluble factor production and modulation of the tumor microenvironment.

4.2. MEK inhibition mediates the production of soluble factors in the tumor microenvironment

Following our finding that cobimetinib does not limit BTC cell viability, despite a potent inhibition of ERK phosphorylation (Figure 3.1, Figure 3.2), we hypothesized that the antitumor activity of MEK inhibitors observed in other tumor models may be the result of alterations in the tumor microenvironment, especially affecting the production of soluble immune factors. Accordingly, we found that the production of certain cytokines and growth factors, particularly GM-CSF, CXCL10, and LIF, by BTC cells was modulated by MEKi (Figure 3.3), which corroborates similar findings in other tumor models treated with MEK inhibitors. Along with the regulation of cell survival and proliferation, activated ERK is known to have several hundred direct phosphorylation targets, many of which are transcription factors that regulate the expression of various proteins[178-180]. ERK can also indirectly signal through NF-κB, which has many target genes that encode for cytokines, growth factors, and other mediators of cell proliferation, including CXCL10 and GM-CSF[270]. This regulatory mechanism has yet to be confirmed in the context of biliary tract cancer but may be plausible given the relationship between known ERK phosphorylation targets and cytokine production.

Granulocyte macrophage colony-stimulating factor (GM-CSF) is a pro-inflammatory cytokine and growth factor that regulates the expansion and function of myeloid cells and has important roles in inflammatory reactions and immunosuppression in cancer[271, 272]. MDSC expansion is also mediated by other cytokines like IL-6 and M-CSF, but GM-CSF is a major driver of immunosuppressive activity of MDSCs and the accumulation of MDSCs in areas of inflammation that lead to tumorigenesis[78, 273, 274]. MEK/ERK signaling controls autocrine production of GM-CSF downstream of its receptor, CSFR2, supporting the observation of MEKi leading to reduced production of GM-CSF from BTC cell lines[275, 276]. Additionally in the context of BTC, Ware et al. showed cell culture supernatants containing high concentrations of GM-CSF and IL-6 induced significant expansion of functionally suppressive MDSCs[267]. This further supports the concept that BTC can promote an immunosuppressive TME through the secretion of immunomodulatory soluble factors.

CXCL10, or interferon-γ inducible protein 10 (IP-10), serves as a major chemoattractant protein for activated T cells, monocytes, and NK cells, and is one of three ligands for CXCR3 (along with CXCL9 and CXCL11)[277, 278]. Signaling between CXCR3 and CXCL10 is obligatory for intratumoral $CD8^+$ T cell trafficking compared to CCR5 and CCR2 interactions, and the expression and function of both CXCR3 and CXCL10 are mediated by MAPK signaling[279, 280]. MEKi-mediated increase in CXCL10 production observed in BTC cell lines was also observed in head and neck squamous cell carcinoma (HNSCC) cells, where it also correlated with increased T cell infiltration and improved antitumor activity[189]. Additionally, the MEK inhibitor trametinib induced CXCL10 production when combined with IFN-γ and TNF-α, and synergized further with the EGFR inhibitor cetuximab[281]. Treatment of human KRAS-mutant lung cancer cells with the MEK inhibitor trametinib induced CXCL10 production when combined with IFN-γ and TNF-α[282].

Excitingly, a recent study in NSCLC revealed that MEK inhibitors, including cobimetinib and trametinib, promote CXCL10-mediated $CD8^+$ T cell recruitment via TLR9 activation, additionally synergizing with chemotherapy to induce immunogenic cell death (ICD)[283]. An important caveat to note is that CXCR3 signaling can also have pro-tumorigenic effects, depending on the isoform of the receptor that is expressed[284, 285]. In particular, CXCR3-A is indicated in chemotaxis and cell proliferation, while CXCR3-B can inhibit migration and induce apoptosis. As a result, CXCR3-A that is expressed by tumor cells can actually induce metastatic migration and angiogenesis[286, 287]. Therefore, careful examination of the role of CXCL10 in promoting $CD8^+$ T cell migration and tumor infiltration is still required, especially in the context of tumor models like BTC where CXCR3 isoform expression is not yet known.

Leukemia inhibitory factor (LIF) exhibited the most striking reduction in production by BTC cell lines following cobimetinib treatment. LIF signaling with its receptor, LIFR, has several roles in the tumor microenvironment and carcinogenesis[288]. The overexpression of LIF is noted in many cancers, including CRC, breast cancer, lung cancer, and melanoma, and serves as a growth factor to promote proliferation and metastatic abilities of tumor cells[289-291]. Notably, LIF was found to promote chemoresistance in CCA, though this was observed in a PI3K/AKT-dependent, MEK/ERK-independent manner[292]. In medullary thyroid cancer, LIF regulates tumor cell proliferation via JAK/STAT3 signaling, but activation of the Ras/Raf/MEK/ERK pathway also induced the production of LIF, indicating a paracrine-autocrine loop in these cells[293]. Furthermore, the LIF promoter region contains several binding sites for the ETS transcription factors, which are a well-known target of activation by ERK[294]. There is also evidence that suggests high baseline serum levels of LIF serve as a predictive biomarker for poor prognosis following ICB therapy, and LIF levels are inversely correlated to the presence of tertiary lymphoid structures in tumors, which

are dense populations of B cells and TFH cells[295]. Thus, when combined with our finding that MEKi significantly limits LIF production in BTC cells, LIF may serve as an additional potential therapeutic target for improving the response to ICB.

Overall, our findings in BTC cell lines, and observations from others outlined above, suggest that MEK inhibitors can mediate the production of cytokines and other soluble factors by tumor cells. This regulation likely occurs at the transcriptional level, since many phosphorylation targets of activated ERK are transcription factors with putative binding sites in the promoter regions of genes encoding for these factors. Soluble factors like GM-CSF, CXCL10, and LIF have important roles in regulating the immune response, some of which correlate with MEK inhibition. Therefore, we speculate that MEK inhibition promotes antitumor immune responses by altering the production of cytokines, chemokines, and growth factors via transcription factor activation of genes encoding for these soluble factors. Future investigation is necessary to delineate this mechanism in order to understand the relationship between MEK inhibition and antitumor activity in the TME.

4.3. Peripheral factors altered by MEK inhibition in advanced BTC patients

In our clinical trial evaluating dual MEK and PD-L1 inhibition in advanced BTC patients, the levels of three growth factors in patient plasma were significantly reduced following the combination of cobimetinib and atezolizumab compared to single agent atezolizumab (Figure 2.3). Intriguingly, all three growth factors (PDGF-BB, PlGF-1, and BDNF) have previously identified roles in biliary tract cancer[247, 248, 296]. First, platelet derived growth factor (PDGF)-BB is produced by myofibroblasts in high amounts and interacts with BTC tumors in a paracrine fashion, contributing to pro-survival signaling[248]. Genetic and pharmacologic inhibition of PDGFRβ, the cognate receptor for PDGF-BB, directly promotes apoptosis and reduces tumor growth in BTC

and has been promoted as a potential therapeutic strategy for BTC[130]. In advanced BTC patients, we observed that patients receiving dual MEK and PD-L1 blockade who also had a reduction in PDGF-BB plasma levels also had improved overall survival and progression-free survival (Figure 2.4, Table 2.5). Next, placental growth factor (PlGF-1), a member of the vascular endothelial growth factor (VEGF) family, is also present in high amounts in BTC patients, with higher expression found in patients with more advanced disease[247]. Similar to PDGF-BB, plasma levels of PlGF-1 were reduced following dual MEK/PD-L1 blockade, but this decrease did not correlate with overall survival or progression-free survival in advanced BTC patients. However, inhibition of PlGF in a murine CCA model decreased tumor burden, limited macrophage recruitment, and decreased vascularization surrounding CCA tumors[249]. PlGF-1 binds to VEGFR1, neuropilin-1 (Nrp1), and neuropilin-2 (Nrp2) to regulate angiogenesis and metastasis in several cancers, and these receptors are well known to execute their functions via MAPK signaling[247, 297, 298]. PlGF also contributes to liver inflammation and macrophage recruitment in mice, which may create an immunosuppressive microenvironment that could support the development and progression of hepatobiliary cancers[299]. Finally, brain-derived neurotrophic factor (BDNF) is mainly involved in maintenance of the nervous system, but also has demonstrated functions in non-neuronal cell proliferation, differentiation, and survival, and these functions are mediated by MEK/ERK and PI3K/AKT signaling pathways[296, 300, 301]. In BTC, high BDNF expression is associated with reduced overall survival and facilitates the invasion of intrahepatic CCA cells via intraneural invasion[296]. Furthermore, advanced BTC patients with high baseline plasma levels of BDNF were more likely to have improved progression-free survival after receiving dual MEK/PD-L1 blockade (Table 2.7, Table 2.8).

The decrease in expression of these growth factors following MEK inhibition in plasma from this cohort of advanced BTC patients could be anticipated, as each of these factors and growth factors in general have well-established connections to Ras/Raf/MEK/ERK signaling. First, most growth factor receptors are receptor tyrosine kinases (RTKs), which initiate the Ras-MAPK pathway as one of the main signal transduction axes for RTK function[302]. Second, the promoter regions of many growth factor genes contain binding sites for transcription factors that are directly phosphorylated and activated by MEK/ERK signaling[303]. As a result, the MEK/ERK pathway mediates autocrine production of many growth factors, and inhibition of this pathway would be expected to contribute to decreased production of these proteins. A caveat to be addressed, however, is that in many of the studies mentioned above, growth factor expression was evaluated directly in tumor tissues using immunohistochemical approaches, whereas for our cohort of advanced BTC patients, these growth factors were measured in peripheral blood plasma samples. Therefore, mechanistic connections cannot be as easily defined for these growth factors in our cohort of BTC patients who received cobimetinib, since these factors execute most of their function at a tumor-localized level. However, the finding that the levels of these factors measured in patient plasma samples were still strikingly altered following MEK inhibition reinforces the significance of the role of MEK signaling in the systemic regulation of growth factors.

4.4. Roles for other immune checkpoint molecules in advanced BTC and immunotherapeutic development

Upon combining PD-L1 blockade with MEK inhibition in advanced biliary tract cancer patients, we also identified alterations in immune checkpoint-expressing T cell populations in peripheral blood, some of which correlated with clinical outcomes. Most notably, a significant increase in

$CD4^+$ T cells that were positive for T cell immunoglobulin and mucin domain 3 (TIM3) following dual MEK/PD-L1 blockade correlated with worse progression-free survival. This finding was consistent with previous studies that show MEKi increases TIM3 expression on lymphocytes in melanoma, and high TIM3 expression on T cells correlates with poor clinical response in gastric cancer, colorectal cancer, and hepatocellular carcinoma[255, 256, 304, 305]. High TIM3 expression is characteristic of highly immunosuppressive Tregs in the TME, and expression on $CD8^+$ T cells limits memory formation. [306, 307]. TIM3 can also mediate resistance to PD-l/PD-L1 blockade, as upregulation of TIM3 on therapeutic antibody-bound T cells was demonstrated in NSCLC and melanoma. This mechanism may be of particular relevance to our clinical study which utilized a PD-L1 blocking antibody for all patients, though the increase in $TIM3^+$ T cells was much more pronounced in patients additionally receiving MEKi (Figure 2.5). Fortunately, previous studies have demonstrated that TIM3 blockade with MEK inhibitors or with anti-PD-1/PD-L1 can have potent antitumor efficacy, suggesting addition of anti-TIM3 therapy to dual MEKi/PD-L1 blockade may enhance antitumor immune responses[255, 308].

Another immune checkpoint molecule that exhibited interesting trends in our patient sample analysis is B and T lymphocyte attenuator (BTLA), a co-stimulatory molecule related to CD28 expressed on T cells, B cells, NK cells, and antigen-presenting cells (APC). BTLA is unique in that it exerts both positive and negative regulatory effects on the immune response[309]. In one study of metastatic melanoma, $CD8^+BTLA^+$ T cells persisted for longer time in contact with their target and could kill multiple target cells, as they did not succumb to activation-induced cell death (AICD)[309]. However, BLTA limits the proliferation of antigen-specific $CD8^+$ T cells, even after prolonged antigen stimulation, but also can promote proliferation in the presence of IL-2 in a different context[310, 311]. In this cohort of advanced BTC patients, increased expression of BTLA

on both $CD4^+$ and $CD8^+$ T cells correlated with better OS and PFS in patients receiving anti-PD-L1 alone, and higher baseline populations of $CD8^+BTLA^+$ cells were indicative of better OS in patients regardless of treatment received (Figure 2.3). This positive correlation between BTLA expression on T cells and improved prognosis has also been observed in melanoma and CRC[257, 311]. There is still much to be understood about the contradictory roles of BTLA in tumor immune responses when considering its utility in antitumor immunotherapy. While inhibiting BLTA can restore antigen-specific $CD8^+$ T cell effector functions, the clear association with high BTLA expression and improved patient prognosis leads to hesitation in supporting BTLA inhibition as a necessary addition to current immunotherapeutic strategies.

4.5. Restoring MEK-mediated inhibition of T cell activation for improved clinical outcomes in advanced BTC

Some of the initial rationale for the combination of MEK inhibition and PD-L1 blockade stemmed from two hypotheses: first, that MEK inhibition could promote $CD8^+$ T cell infiltration in otherwise TIL-exclusionary tumors, and second, that anti-PD-L1 could reignite the effector activity of these T cells for enhanced antitumor immunity. Unfortunately, analysis of patient peripheral blood samples instead revealed that while atezolizumab alone increased populations of $CD8^+$ T cells with an activated phenotype, dual blockade of MEK and PD-L1 caused no change in these cells[224]. This unfavorable result was further confirmed in a murine model of CRC, where MEK-knockout tumors increased antigen presentation and T cells isolated from these tumors had an activated phenotype, but systemic administration of cobimetinib in vivo impaired T cell effector function and limited tumor infiltration[224]. An important question emerged from this finding: could T cell function be maintained in a different manner while still in the presence of MEKi and anti-

PD-L1, which provided benefit to other aspects of the antitumor immune response? The answer appears to lie in the use of costimulatory agonist antibodies, some of which can mediate T cell activation independent of MEK/ERK signaling. Indeed, the use of immune agonists against 4-1BB and OX-40 were shown to restore T cell effector function and proliferation, while MEKi could still be used to prime tumor immunogenicity and facilitate tumor infiltration[224, 242]. Furthermore, triple combination therapy of cobimetinib, anti-PD-1, and anti-4-1BB substantially improved survival in murine CRC and led to significantly higher populations of intratumoral $CD8^+$ T cells that were more proliferative and produced higher amounts of granzyme B to produce a more potent antitumor immune response (Figure 4.1)[224].

With preclinical evidence supporting costimulatory agonist antibodies could reverse MEKi-mediated immune suppression, a more important question emerged: could this be effective in advanced BTC patients to improve antitumor immunity? To address this, a new clinical trial was recently initiated to test the triple combination of cobimetinib, atezolizumab, and the CD27 agonist varlilumab in advanced, metastatic BTC patients, with the goal of improving upon the previous moderately successful dual blockade of MEK and PD-L1. CD27 is another costimulatory molecule expressed T cells, most NK cells, and on primed and activated B cells[312]. Unlike 4-1BB, whose expression is inducible upon T cell receptor stimulation, CD27 is expressed more broadly in nearly all stages of T cell development, which could be more beneficial for the treatment of immunologically exclusive tumors that have limited antigen-T cell stimulation. Varlilumab is a clinically available agonist with an acceptable safety profile that has demonstrated notable efficacy in some tumor models even as a single agent[313]. Based on the preclinical evidence, we are optimistic that the use of agonist antibodies could have significant benefit for patients with advanced BTC and other immunosuppressive tumors.

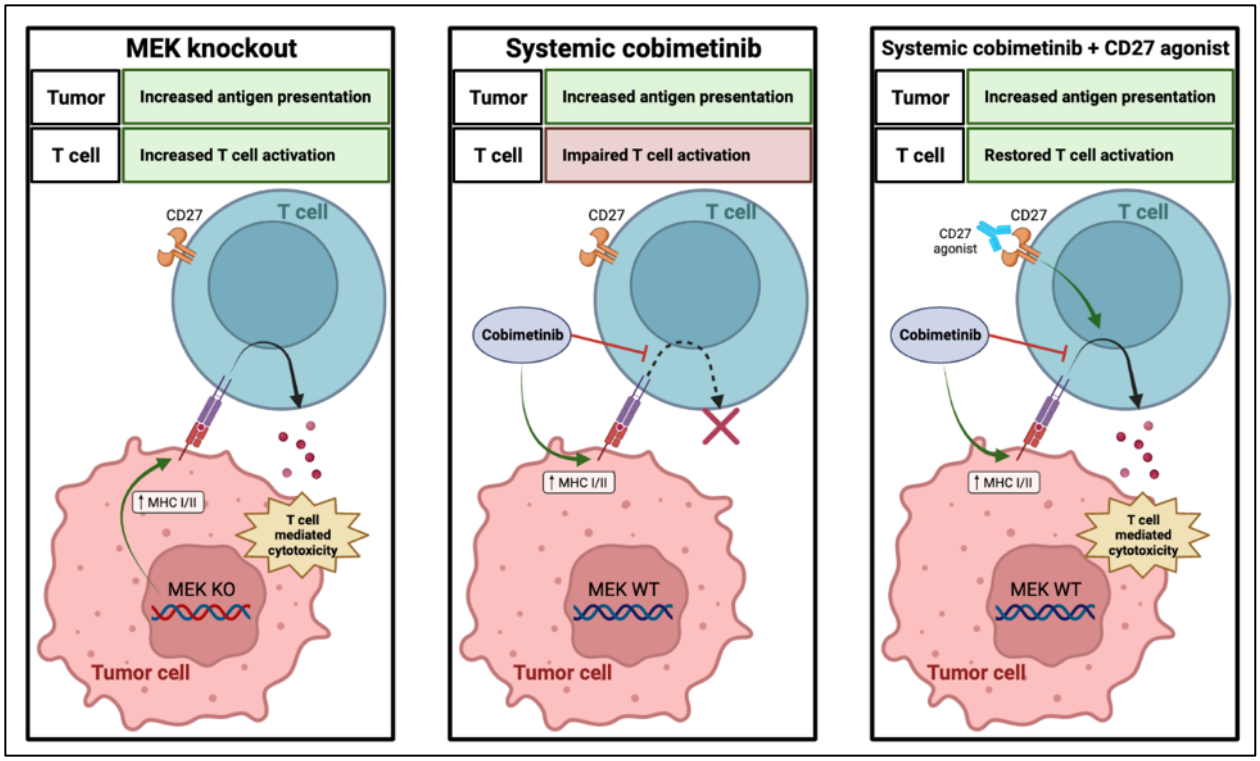

Figure 4.1. Immunomodulatory effects of genetic versus systemic MEK inhibition in BTC and rescue with costimulatory agonist antibodies. In murine CRC cells in vitro, genetic ablation of MEK increases antigen presentation to T cells, which produce heightened IFNγ and GZMB to elicit tumor cell cytotoxicity. However, administration of cobimetinib in vivo and in patients with BTC exhibited impaired T cell activation and suppression of cytotoxic activity. Addition of an agonist antibody for costimulatory receptors like 4-1BB or CD27 can rescue T cell activation and restore tumor directed cytotoxicity. Adapted from Dennison, L. et al, 2021.

4.6. Modulation of the tumor microenvironment as a means to regulate antitumor T cell activity

Although inhibitors of Raf and MEK have been clinically developed, with some achieving FDA approval for the treatment of melanoma and non-small cell lung cancer (NSCLC), the number of cancer patients with MAPK-driven tumors far outweighs the number of clinical successes from targeting this pathway[314, 315]. In the development of effective treatment strategies that utilize MEK inhibition, it is important to consider that MAPK signaling does not only regulate the proliferation and survival of tumor cells. Rather, the MAPK pathway also has established roles in the regulation of immune cells[133, 187, 316]. For example, ERK2 has a central role in the regulation of $CD8^+$ T cell survival following TCR activation via modulation of Bcl-2 family proteins[317]. MEKi also limits T cell proliferation, IFNγ production, and T cell priming, and additionally blocks TAM differentiation and MDSC expansion[132, 187, 193, 242, 318-321]. In order for the reinvigoration of T cells mediated by ICB to be effective against tumors, T cells must come into direct contact with the tumor cells that express its cognate antigen. Consequently, $CD8^+$ TIL density often correlates with better responses to ICB therapy[263]. Unfortunately, a tumor microenvironment with a dense stromal component that excludes tumor antigen-specific $CD8^+$ T cells is characteristic of many tumors, including BTC[168]. Many have hypothesized, our own group included, that MEKi may promotes effector T cell infiltration into tumors and may subsequently synergize with ICB to restore effector function and sensitize immune cell-exclusive tumors to ICB therapy[133, 188, 322]. In response, several clinical trials have been initiated to investigate these combinations, but the results have been mixed and generally unfavorable[218, 221, 323]. Despite the recurrent observation of MEK-mediated T cell infiltration, the mechanism by which MEK mediates $CD8^+$ T cell migration and infiltration has yet

to be delineated. Based on our prior preclinical observations in BTC cell lines, the production of soluble factors to that mediate responses in the tumor microenvironment may be responsible for the promotingmediation of T cell infiltration.

Over time, myeloid derived suppressor cells (MDSC) have been consistently observed to substantially regulate antitumor immune responses. They are frequently upregulated in tumors that do not respond well to immunotherapies, and they largely suppress T cell proliferation and effector functions by producing arginase (Arg1), inducible nitric oxide synthase (iNOS), and reactive oxygen species (ROS), which are well established inhibitors of T cell function[78, 79, 81, 273, 324, 325]. MDSCs also highly express PD-L1 as an additional mode of immune suppression in the TME[79, 84]. MDSCs are expanded by a number of factors including SCF, M-CSF, IL-6, VEGF, and of particular relevance to this project, GM-CSF[78]. In pancreatic cancer, tumor-derived GM-CSF induces the expansion of functionally suppressive MDSCs[82]. Biliary tract cancer cell culture supernatants that contain high concentrations of GM-CSF can significantly expand MDSCs from normal peripheral blood mononuclear cells[267]. Further, a murine model of BTC demonstrated that $CD8^+$ T cells in the TME were restricted to the tumor margins, interacting closely with suppressive myeloid cells and suggests that these immunosuppressive cells may directly mediate tumor infiltrating T lymphocytes[326]. Although GM-CSF-mediated expansion of MDSCs is accomplished through Jak/STAT signaling, MDSC expansion is also connected to MEK/ERK signaling. In both murine lung cancer and breast cancer models, MEK inhibition substantially reduces MDSC expansion in tumors while increasing intratumoral $CD8^+$ T cell populations[220, 321]. In murine triple negative breast cancer (TNBC), MEK activation supports myeloid recruitment to tumors by regulating the expression of CXCL1/2, and MEKi markedly reduced the presence of myeloid cells positive for Gr-1, a marker for MDSCs, in tumors[327]. This, coupled with our finding that MEK

inhibition significantly reduces GM-CSF production in certain BTC cell lines, has led to the development of the hypothesis that MEKi-mediated T cell infiltration into tumors may actually be the result of a depletion of MDSCs in the BTC tumor microenvironment. While it has not been confirmed experimentally, the evidence above from our group and others supports further investigation into understanding the mechanism that controls T cell infiltration in the presence of MEK inhibitors and ICB.

4.7. Future studies and concluding remarks

Immunotherapy has persisted as an important strategy that can be used to overcome the burden of cancer, despite the rates of success continuing to be disappointingly low for many patients. Our understanding of the antitumor immune response has grown tremendously in the last few decades, but we are still quite far from harnessing the full power of the immune system in the tumor microenvironment. In biliary tract cancers, combination immunotherapy has emerged as been especially promising, with the addition of durvalumab to the first line chemotherapy regimen of gemcitabine and cisplatin emerging as the new standard of care for patients with advanced BTC[197]. Our recent clinical investigation in advanced BTC of anti-PD-L1 therapy combined with an inhibitor of MEK, whose constitutive activation is a significant driver of tumorigenesis in BTC, resulted in a significant, albeit short, extension of progression-free survival[221]. More importantly, our work uncovered several immune features that may provide the key to understanding how MEK inhibition and PD-L1 blockade can be effective for some patients with BTC.

Despite the limited success of combining MEK inhibition and ICB as a therapeutic strategy, our work demonstrates that this combination, especially MEK inhibition, is still a valuable tool for the treatment of advanced solid tumors like BTC. There appears to be an important balance to strike

for effective control of these tumors. On one hand, MEK inhibition alters soluble factor production that may impact immunosuppressive cell activity in the tumor microenvironment and recruit T cells to infiltrate the tumor. Simultaneously, however, MEKi also impacts $CD8^+$ T cell effector function, even in the presence of an immune checkpoint blocking antibody (Figure 3.4). From here, important questions emerge – is MEKi-mediated T cell suppression the most significant limiting factor to the efficacy of dual MEK/PD-L1 blockade? Does this outweigh the apparent benefits that MEKi has in MAPK-driven tumors? How can we enhance these benefits, rather than cover up the limitations that MEKi imparts on T cells, to improve this combination in the clinic?

Much remains to be understood regarding our understanding of the mechanisms that connect MEK signaling to the immunomodulatory responses observed in various tumor models. First, the mechanism by which MEK inhibition promotes increased $CD8^+$ T cell infiltration into tumors has yet to be fully delineated, though it has been observed in several tumor models and correlates with improved antitumor activity. Much of the direct impact that MEKi has on T cells results in a reduction in effector function, even with increased T cell infiltration. While we did observe an increase in CXCL10 production in BTC cell lines following MEKi, which is a chemokine capable of recruiting T cells, a broader view of the BTC tumor microenvironment suggests that MEKi is more likely to promote T cell infiltration indirectly through modulation of immunosuppressive myeloid cells. In particular, the striking decrease in GM-CSF production in some cell lines may be linked to a reduction of TAM and MDSC expansion in the TME, which in turn can improve T cell proliferation and function (Figure 3.5). By limiting the presence of these immunosuppressive cells, effector $CD8^+$ T cells may be able to better infiltrate into BTC tumors. A recent study utilizing GM-CSF blockade in a murine model of iCCA demonstrated that tumor-derived GM-

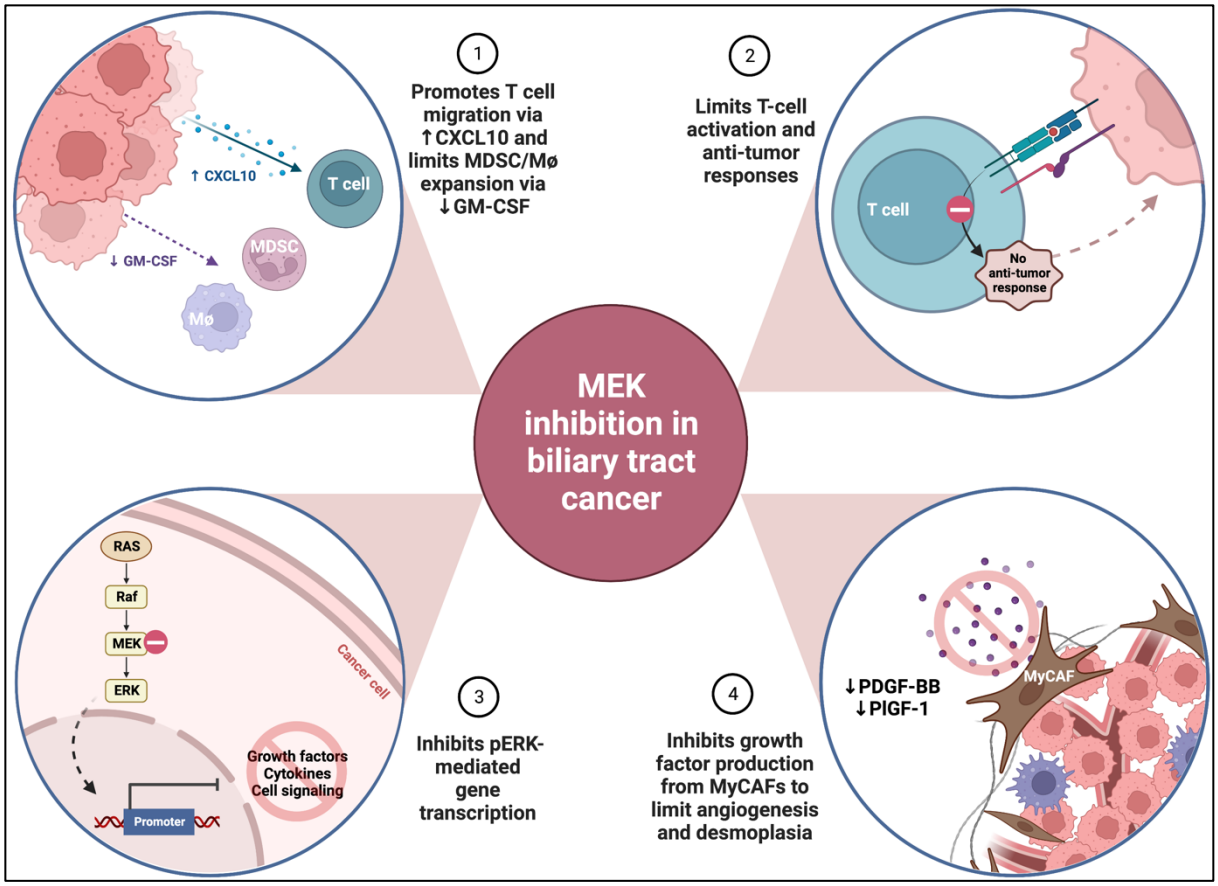

Figure 4.2. Graphical abstract of proposed roles of MEK inhibition in biliary tract cancer. (1) MEKi induces CXCL10 production and limits GM-CSF production from BTC cell lines, which can recruit T cells and suppress MDSC and macrophage expansion, respectively. (2) Systemic MEKi inhibits T cell activation to limit anti-tumor responses. (3) MEKi inhibits downstream ERK phosphorylation which disrupts activation of promoters for genes controlling growth factor and cytokine production. (4). MEKi limits production of PDGF-BB and PlGF-1, which are produced by myofibroblasts and contribute to desmoplastic transformation of BTC tumors.

CSF is required for the expansion and polarization of TAMs in the TME, and GM-CSF neutralization facilitates enhanced $CD8^+$ T cell effector functions and infiltration into tumors[328].

Future investigations should determine if MEKi-mediated suppression of GM-CSF production from BTC tumor cells is sufficient to decrease immunosuppressive cells and enhance $CD8^+$ T cell infiltration and antitumor activity as observed with GM-CSF blockade. In particular, is MEKi-mediated suppression of GM-CSF limited to tumor cells, or can systemic MEKi also manipulate the production of GM-CSF from other cells in the TME? Additionally, we must investigate how MEKi impacts other immune cells in the TME, including MDSCs, macrophages, and NK cells, especially since we have already observed that it can negatively affect T cell activity. Ultimately, delineating the complex roles of MEKi across cell types and understanding why and how it affects some differently than others will guide the development of improved therapeutic strategies that can still utilize the positive aspects of MEKi and PD-L1 blockade in advanced BTC. Ultimately, fully delineating the mechanisms controlling T cell infiltration into immunologically suppressed tumors can guide better strategies for improving immunotherapeutic approaches for patients with advanced malignancies.

Another avenue to explore involves PDGF-BB and PlGF-1, which are both depleted following MEKi in advanced BTC patients. As previously mentioned, inhibition of these growth factors linked to decreased tumor burden in models of BTC[247, 248]. Both are produced largely by myelofibroblasts and contribute to increased vascularization and desmoplastic transformation of BTC tumors. However, the decrease in these two growth factors following MEKi was observed in peripheral blood and does not necessarily reflect their activity in the TME. Therefore, future studies should include investigations into the role of MEK inhibition in the production of these factors in the context of BTC tumors. PDGF-BB and PlGF-1 blockade have both been safely used

in mouse models of CCA with promising antitumor activity, and given the demonstrated role of MEK/ERK signaling in the control of these two factors, it is likely that MEK inhibition could further promote tumor control via modulation of the production of these factors in the TME.

In biliary tract cancer, we are on the cusp of identifying treatment strategies that can be successful for a broad population of patients. While dual MEK and PD-L1 blockade in advanced BTC demonstrated modest improvement in progression-free survival, modulation of several immune features was observed that are deserving of further investigation, based on previously demonstrated connections to BTC and MAPK signaling. This work advances our understanding of the MEK inhibition-mediated immune response in biliary tract cancer, both in the tumor microenvironment and systemically. Improvements to this therapeutic strategy have already been initiated in response with the addition of a CD27 agonist to restore T cell activation that is limited by MEKi, with the hope that this approach will provide marked benefit for an important patient population that is currently without viable treatment options. Additionally, exploring the role of MEK signaling in soluble factor production and activity in the TME will further our understanding of intricate tumor dynamics in biliary tract cancer.

Chapter 5: References

1. Sung H, Ferlay J, Siegel RL, Laversanne M, Soerjomataram I, Jemal A*, et al.*, *Global Cancer Statistics 2020: GLOBOCAN Estimates of Incidence and Mortality Worldwide for 36 Cancers in 185 Countries.* CA: A Cancer Journal for Clinicians, 2021. **71**(3): p. 209-249.
2. Bray F, Laversanne M, Weiderpass E, and Soerjomataram I, *The ever-increasing importance of cancer as a leading cause of premature death worldwide.* Cancer, 2021. **127**(16): p. 3029-3030.
3. Copier J, Dalgleish AG, Britten CM, Finke LH, Gaudernack G, Gnjatic S*, et al.*, *Improving the efficacy of cancer immunotherapy.* European Journal of Cancer, 2009. **45**(8): p. 1424-1431.
4. Medzhitov R and Janeway C, *Innate Immunity.* New England Journal of Medicine, 2000. **343**(5): p. 338-344.
5. Medzhitov R and Janeway CA, *Innate immunity: impact on the adaptive immune response.* Current Opinion in Immunology, 1997. **9**(1): p. 4-9.
6. Hozumi N and Tonegawa S, *Evidence for somatic rearrangement of immunoglobulin genes coding for variable and constant regions.* Proc Natl Acad Sci U S A, 1976. **73**(10): p. 3628-32.
7. Chaplin DD, *Overview of the immune response.* Journal of Allergy and Clinical Immunology, 2010. **125**(2, Supplement 2): p. S3-S23.
8. Chi X, Li Y, and Qiu X, *V(D)J recombination, somatic hypermutation and class switch recombination of immunoglobulins: mechanism and regulation.* Immunology, 2020. **160**(3): p. 233-247.
9. Janeway CA, *The immune system evolved to discriminate infectious nonself from noninfectious self.* Immunology Today, 1992. **13**(1): p. 11-16.
10. Koch U and Radtke F, *Mechanisms of T Cell Development and Transformation.* Annual Review of Cell and Developmental Biology, 2011. **27**(1): p. 539-562.
11. Roth DB, *V(D)J Recombination: Mechanism, Errors, and Fidelity.* Microbiol Spectr, 2014. **2**(6).
12. Nishana M and Raghavan SC, *Role of recombination activating genes in the generation of antigen receptor diversity and beyond.* Immunology, 2012. **137**(4): p. 271-281.
13. Bonilla FA and Oettgen HC, *Adaptive immunity.* Journal of Allergy and Clinical Immunology, 2010. **125**(2): p. S33-S40.
14. E Robey a and Fowlkes BJ, *Selective Events in T Cell Development.* Annual Review of Immunology, 1994. **12**(1): p. 675-705.
15. Derbinski J, Schulte A, Kyewski B, and Klein L, *Promiscuous gene expression in medullary thymic epithelial cells mirrors the peripheral self.* Nature Immunology, 2001. **2**(11): p. 1032-1039.
16. Kyewski B and Derbinski J, *Self-representation in the thymus: an extended view.* Nature Reviews Immunology, 2004. **4**(9): p. 688-698.
17. Schroeder HW, Jr. and Cavacini L, *Structure and function of immunoglobulins.* J Allergy Clin Immunol, 2010. **125**(2 Suppl 2): p. S41-52.
18. Golubovskaya V and Wu L, *Different Subsets of T Cells, Memory, Effector Functions, and CAR-T Immunotherapy.* Cancers (Basel), 2016. **8**(3).

19. Raphael I, Nalawade S, Eagar TN, and Forsthuber TG, *T cell subsets and their signature cytokines in autoimmune and inflammatory diseases.* Cytokine, 2015. **74**(1): p. 5-17.
20. Wakim LM and Bevan MJ, *From the thymus to longevity in the periphery.* Curr Opin Immunol, 2010. **22**(3): p. 274-8.
21. Dutton R, Bradley L, and Swain S, *T cell memory.* Annual review of immunology, 1998. **16**: p. 201.
22. Germain RN, *MHC-dependent antigen processing and peptide presentation: Providing ligands for T lymphocyte activation.* Cell, 1994. **76**(2): p. 287-299.
23. Janeway C, Travers P, Walport M, and Shlomchik MJ, *Antigen Recognition by B-cell and T-cell Receptors*, in *Immunobiology: The Immune System in Health and Disease*. 2001, Garland Science: New York.
24. Janeway C, Travers P, Walport M, and Shlomchik MJ, *Antigen Presentation to T Lymphocytes*, in *Immunobiology: The Immune System in Health and Disease*. 2001, Garland Science: New York.
25. Pieters J, *MHC class II-restricted antigen processing and presentation*, in *Advances in Immunology*. 2000, Academic Press. p. 159-208.
26. Reith W, LeibundGut-Landmann S, and Waldburger J-M, *Regulation of MHC class II gene expression by the class II transactivator.* Nature Reviews Immunology, 2005. **5**(10): p. 793-806.
27. Hewitt CR and Feldmann M, *Human T cell clones present antigen.* The Journal of Immunology, 1989. **143**(2): p. 762.
28. LaSalle JM, Ota K, and Hafler DA, *Presentation of autoantigen by human T cells.* The Journal of Immunology, 1991. **147**(3): p. 774.
29. Holling TM, Schooten E, Langerak AW, and van den Elsen PJ, *Regulation of MHC class II expression in human T-cell malignancies.* Blood, 2004. **103**(4): p. 1438-1444.
30. Joffre OP, Segura E, Savina A, and Amigorena S, *Cross-presentation by dendritic cells.* Nature Reviews Immunology, 2012. **12**(8): p. 557-569.
31. Cresswell P, Ackerman AL, Giodini A, Peaper DR, and Wearsch PA, *Mechanisms of MHC class I-restricted antigen processing and cross-presentation.* Immunological Reviews, 2005. **207**(1): p. 145-157.
32. Rock KL and Shen L, *Cross-presentation: underlying mechanisms and role in immune surveillance.* Immunological Reviews, 2005. **207**(1): p. 166-183.
33. Lin M-L, Zhan Y, Villadangos JA, and Lew AM, *The cell biology of cross-presentation and the role of dendritic cell subsets.* Immunology & Cell Biology, 2008. **86**(4): p. 353-362.
34. García Morán GA, Parra-Medina R, Cardona AG, Quintero-Ronderos P, and Garavito Rodríguez É, *Cytokines, Chemokines, and Growth Factors*, in *Autoimmunity: From Bench to Bedside*, J. Anaya, Y. Shoenfeld, and A. Rojas-Villarraga, Editors. 2013, El Rosario University Press: Bogota, Colombia.
35. Kelso A, *Cytokines: Principles and prospects.* Immunology & Cell Biology, 1998. **76**(4): p. 300-317.
36. Dinarello CA, *Historical insights into cytokines.* European Journal of Immunology, 2007. **37**(S1): p. S34-S45.
37. Zhang JM and An J, *Cytokines, inflammation, and pain.* Int Anesthesiol Clin, 2007. **45**(2): p. 27-37.

38. Vajdic CM and van Leeuwen MT, *Cancer incidence and risk factors after solid organ transplantation.* Int J Cancer, 2009. **125**(8): p. 1747-54.
39. Mayor PC, Eng KH, Singel KL, Abrams SI, Odunsi K, Moysich KB*, et al.*, *Cancer in primary immunodeficiency diseases: Cancer incidence in the United States Immune Deficiency Network Registry.* Journal of Allergy and Clinical Immunology, 2018. **141**(3): p. 1028-1035.
40. Martin D and Gutkind JS, *Human tumor-associated viruses and new insights into the molecular mechanisms of cancer.* Oncogene, 2008. **27**(2): p. S31-S42.
41. McLaughlin-Drubin ME and Munger K, *Viruses associated with human cancer.* Biochimica et Biophysica Acta (BBA) - Molecular Basis of Disease, 2008. **1782**(3): p. 127-150.
42. von Knebel Doeberitz M, Oltersdorf T, Schwarz E, and Gissmann L, *Correlation of modified human papilloma virus early gene expression with altered growth properties in C4-1 cervical carcinoma cells.* Cancer Res, 1988. **48**(13): p. 3780-6.
43. Flore O, Rafii S, Ely S, O'Leary JJ, Hyjek EM, and Cesarman E, *Transformation of primary human endothelial cells by Kaposi's sarcoma-associated herpesvirus.* Nature, 1998. **394**(6693): p. 588-92.
44. Coussens LM and Werb Z, *Inflammation and cancer.* Nature, 2002. **420**(6917): p. 860-7.
45. Singh N, Baby D, Rajguru JP, Patil PB, Thakkannavar SS, and Pujari VB, *Inflammation and cancer.* Ann Afr Med, 2019. **18**(3): p. 121-126.
46. Liao JB, *Viruses and human cancer.* Yale J Biol Med, 2006. **79**(3-4): p. 115-22.
47. Virchow R, *Cellular Pathology as Based Upon Physiological and Pathological Histology.* 1863.
48. Serhan CN, Ward PA, and Gilroy DW, *Fundamentals of inflammation*. 2010: Cambridge University Press.
49. Medzhitov R, *Origin and physiological roles of inflammation.* Nature, 2008. **454**(7203): p. 428-435.
50. Jackson JR, Seed MP, Kircher CH, Willoughby DA, and Winkler JD, *The codependence of angiogenesis and chronic inflammation.* The FASEB Journal, 1997. **11**(6): p. 457-465.
51. Hanahan D and Weinberg Robert A, *Hallmarks of Cancer: The Next Generation.* Cell, 2011. **144**(5): p. 646-674.
52. Nagorsen D, Scheibenbogen C, Marincola FM, Letsch A, and Keilholz U, *Natural T Cell Immunity against Cancer.* Clinical Cancer Research, 2003. **9**(12): p. 4296-4303.
53. Nowarski R, Gagliani N, Huber S, and Flavell RA, *Innate Immune Cells in Inflammation and Cancer.* Cancer Immunology Research, 2013. **1**(2): p. 77-84.
54. Liu Y and Zeng G, *Cancer and innate immune system interactions: translational potentials for cancer immunotherapy.* J Immunother, 2012. **35**(4): p. 299-308.
55. Gordon S and Martinez FO, *Alternative Activation of Macrophages: Mechanism and Functions.* Immunity, 2010. **32**(5): p. 593-604.
56. Ghiringhelli Fo, Puig PE, Roux S, Parcellier A, Schmitt E, Solary E*, et al.*, *Tumor cells convert immature myeloid dendritic cells into TGF-β–secreting cells inducing CD4+CD25+ regulatory T cell proliferation.* Journal of Experimental Medicine, 2005. **202**(7): p. 919-929.
57. Martínez-Sabadell A, Arenas EJ, and Arribas J, *IFNγ Signaling in Natural and Therapy-Induced Antitumor Responses.* Clinical Cancer Research, 2022. **28**(7): p. 1243-1249.

58. Sica A and Mantovani A, *Macrophage plasticity and polarization: in vivo veritas.* The Journal of Clinical Investigation, 2012. **122**(3): p. 787-795.
59. Vigneron N, *Human Tumor Antigens and Cancer Immunotherapy.* Biomed Res Int, 2015. **2015**: p. 948501.
60. Burnet M, *Immunological surveillance*. 1970: Elsevier.
61. Beatty GL and Gladney WL, *Immune escape mechanisms as a guide for cancer immunotherapy.* Clin Cancer Res, 2015. **21**(4): p. 687-92.
62. Dunn GP, Old LJ, and Schreiber RD, *The Immunobiology of Cancer Immunosurveillance and Immunoediting.* Immunity, 2004. **21**(2): p. 137-148.
63. Dunn GP, Bruce AT, Ikeda H, Old LJ, and Schreiber RD, *Cancer immunoediting: from immunosurveillance to tumor escape.* Nature Immunology, 2002. **3**(11): p. 991-998.
64. Dunn GP, Old LJ, and Schreiber RD, *The three Es of cancer immunoediting.* Annu Rev Immunol, 2004. **22**: p. 329-60.
65. Kaplan DH, Shankaran V, Dighe AS, Stockert E, Aguet M, Old LJ*, et al.*, *Demonstration of an interferon gamma-dependent tumor surveillance system in immunocompetent mice.* Proc Natl Acad Sci U S A, 1998. **95**(13): p. 7556-61.
66. Wheelock EF, Weinhold KJ, and Levich J, *The tumor dormant state.* Adv Cancer Res, 1981. **34**: p. 107-40.
67. Loeb LA, Loeb KR, and Anderson JP, *Multiple mutations and cancer.* Proc Natl Acad Sci U S A, 2003. **100**(3): p. 776-81.
68. Pollard JW, *Tumour-educated macrophages promote tumour progression and metastasis.* Nature Reviews Cancer, 2004. **4**(1): p. 71-78.
69. Miyara M and Sakaguchi S, *Natural regulatory T cells: mechanisms of suppression.* Trends in Molecular Medicine, 2007. **13**(3): p. 108-116.
70. Sakaguchi S, *Naturally Arising CD4+ Regulatory T Cells for Immunologic Self-Tolerance and Negative Control of Immune Responses.* Annual Review of Immunology, 2004. **22**(1): p. 531-562.
71. Togashi Y, Shitara K, and Nishikawa H, *Regulatory T cells in cancer immunosuppression — implications for anticancer therapy.* Nature Reviews Clinical Oncology, 2019. **16**(6): p. 356-371.
72. Lim HW, Hillsamer P, Banham AH, and Kim CH, *Cutting edge: direct suppression of B cells by CD4+ CD25+ regulatory T cells.* J Immunol, 2005. **175**(7): p. 4180-3.
73. Ghiringhelli F, Ménard C, Terme M, Flament C, Taieb J, Chaput N*, et al.*, *CD4+CD25+ regulatory T cells inhibit natural killer cell functions in a transforming growth factor-beta-dependent manner.* J Exp Med, 2005. **202**(8): p. 1075-85.
74. Misra N, Bayry J, Lacroix-Desmazes S, Kazatchkine MD, and Kaveri SV, *Cutting edge: human CD4+CD25+ T cells restrain the maturation and antigen-presenting function of dendritic cells.* J Immunol, 2004. **172**(8): p. 4676-80.
75. Beyer M and Schultze JL, *Regulatory T cells in cancer.* Blood, 2006. **108**(3): p. 804-811.
76. Woo EY, Chu CS, Goletz TJ, Schlienger K, Yeh H, Coukos G*, et al.*, *Regulatory CD4+CD25+ T Cells in Tumors from Patients with Early-Stage Non-Small Cell Lung Cancer and Late-Stage Ovarian Cancer1.* Cancer Research, 2001. **61**(12): p. 4766-4772.
77. Liyanage UK, Moore TT, Joo H-G, Tanaka Y, Herrmann V, Doherty G*, et al.*, *Prevalence of Regulatory T Cells Is Increased in Peripheral Blood and Tumor Microenvironment of Patients with Pancreas or Breast Adenocarcinoma.* The Journal of Immunology, 2002. **169**(5): p. 2756-2761.

78. Gabrilovich DI and Nagaraj S, *Myeloid-derived suppressor cells as regulators of the immune system.* Nature reviews. Immunology, 2009. **9**(3): p. 162-174.
79. Umansky V, Blattner C, Gebhardt C, and Utikal J, *The Role of Myeloid-Derived Suppressor Cells (MDSC) in Cancer Progression.* Vaccines (Basel), 2016. **4**(4).
80. Morad G, Helmink BA, Sharma P, and Wargo JA, *Hallmarks of response, resistance, and toxicity to immune checkpoint blockade.* Cell, 2021. **184**(21): p. 5309-5337.
81. Lesokhin AM, Hohl TM, Kitano S, Cortez C, Hirschhorn-Cymerman D, Avogadri F*, et al.*, *Monocytic CCR2(+) myeloid-derived suppressor cells promote immune escape by limiting activated CD8 T-cell infiltration into the tumor microenvironment.* Cancer Res, 2012. **72**(4): p. 876-86.
82. Bayne LJ, Beatty GL, Jhala N, Clark CE, Rhim AD, Stanger BZ*, et al.*, *Tumor-derived granulocyte-macrophage colony-stimulating factor regulates myeloid inflammation and T cell immunity in pancreatic cancer.* Cancer Cell, 2012. **21**(6): p. 822-35.
83. Vinay DS, Ryan EP, Pawelec G, Talib WH, Stagg J, Elkord E*, et al.*, *Immune evasion in cancer: Mechanistic basis and therapeutic strategies.* Seminars in Cancer Biology, 2015. **35**: p. S185-S198.
84. Gajewski TF, Woo SR, Zha Y, Spaapen R, Zheng Y, Corrales L*, et al.*, *Cancer immunotherapy strategies based on overcoming barriers within the tumor microenvironment.* Curr Opin Immunol, 2013. **25**(2): p. 268-76.
85. De Sousa Linhares A, Leitner J, Grabmeier-Pfistershammer K, and Steinberger P, *Not All Immune Checkpoints Are Created Equal.* Frontiers in Immunology, 2018. **9**: p. 1909.
86. Xing Y and Hogquist KA, *T-cell tolerance: central and peripheral.* Cold Spring Harbor perspectives in biology, 2012. **4**(6): p. a006957.
87. Toor SM, Sasidharan Nair V, Decock J, and Elkord E, *Immune checkpoints in the tumor microenvironment.* Seminars in Cancer Biology, 2020. **65**: p. 1-12.
88. Kochenderfer JN, Yu Z, Frasheri D, Restifo NP, and Rosenberg SA, *Adoptive transfer of syngeneic T cells transduced with a chimeric antigen receptor that recognizes murine CD19 can eradicate lymphoma and normal B cells.* Blood, 2010. **116**(19): p. 3875-86.
89. Zhao Y, Moon E, Carpenito C, Paulos CM, Liu X, Brennan AL*, et al.*, *Multiple injections of electroporated autologous T cells expressing a chimeric antigen receptor mediate regression of human disseminated tumor.* Cancer Res, 2010. **70**(22): p. 9053-61.
90. Hodi FS, O'Day SJ, McDermott DF, Weber RW, Sosman JA, Haanen JB*, et al.*, *Improved survival with ipilimumab in patients with metastatic melanoma.* N Engl J Med, 2010. **363**(8): p. 711-23.
91. Robert C, Long GV, Brady B, Dutriaux C, Maio M, Mortier L*, et al.*, *Nivolumab in previously untreated melanoma without BRAF mutation.* N Engl J Med, 2015. **372**(4): p. 320-30.
92. Hamid O, Robert C, Daud A, Hodi FS, Hwu WJ, Kefford R*, et al.*, *Safety and tumor responses with lambrolizumab (anti-PD-1) in melanoma.* N Engl J Med, 2013. **369**(2): p. 134-44.
93. Ito A, Kondo S, Tada K, and Kitano S, *Clinical Development of Immune Checkpoint Inhibitors.* Biomed Res Int, 2015. **2015**: p. 605478.
94. Couzin-Frankel J, *Cancer Immunotherapy.* Science, 2013. **342**(6165): p. 1432-1433.
95. Leach DR, Krummel MF, and Allison JP, *Enhancement of Antitumor Immunity by CTLA-4 Blockade.* Science, 1996. **271**(5256): p. 1734-1736.

96. Nishimura H, Nose M, Hiai H, Minato N, and Honjo T, *Development of lupus-like autoimmune diseases by disruption of the PD-1 gene encoding an ITIM motif-carrying immunoreceptor.* Immunity, 1999. **11**(2): p. 141-51.
97. Wolchok JD, Kluger H, Callahan MK, Postow MA, Rizvi NA, Lesokhin AM*, et al.*, *Nivolumab plus Ipilimumab in Advanced Melanoma.* New England Journal of Medicine, 2013. **369**(2): p. 122-133.
98. Topalian SL, Hodi FS, Brahmer JR, Gettinger SN, Smith DC, McDermott DF*, et al.*, *Safety, Activity, and Immune Correlates of Anti–PD-1 Antibody in Cancer.* New England Journal of Medicine, 2012. **366**(26): p. 2443-2454.
99. Pardoll DM, *The blockade of immune checkpoints in cancer immunotherapy.* Nat Rev Cancer, 2012. **12**(4): p. 252-64.
100. Vignali DAA, Collison LW, and Workman CJ, *How regulatory T cells work.* Nature Reviews Immunology, 2008. **8**(7): p. 523-532.
101. Walker LS, *Treg and CTLA-4: two intertwining pathways to immune tolerance.* J Autoimmun, 2013. **45**(100): p. 49-57.
102. Oyewole-Said D, Konduri V, Vazquez-Perez J, Weldon SA, Levitt JM, and Decker WK, *Beyond T-Cells: Functional Characterization of CTLA-4 Expression in Immune and Non-Immune Cell Types.* Frontiers in Immunology, 2020. **11**.
103. Ha D, Tanaka A, Kibayashi T, Tanemura A, Sugiyama D, Wing JB*, et al.*, *Differential control of human Treg and effector T cells in tumor immunity by Fc-engineered anti–CTLA-4 antibody.* Proceedings of the National Academy of Sciences, 2019. **116**(2): p. 609-618.
104. Wing K, Onishi Y, Prieto-Martin P, Yamaguchi T, Miyara M, Fehervari Z*, et al.*, *CTLA-4 control over Foxp3+ regulatory T cell function.* Science, 2008. **322**(5899): p. 271-5.
105. Qureshi OS, Zheng Y, Nakamura K, Attridge K, Manzotti C, Schmidt EM*, et al.*, *Trans-Endocytosis of CD80 and CD86: A Molecular Basis for the Cell-Extrinsic Function of CTLA-4.* Science, 2011. **332**(6029): p. 600-603.
106. Ribas A, Camacho LH, Lopez-Berestein G, Pavlov D, Bulanhagui CA, Millham R*, et al.*, *Antitumor activity in melanoma and anti-self responses in a phase I trial with the anti-cytotoxic T lymphocyte-associated antigen 4 monoclonal antibody CP-675,206.* J Clin Oncol, 2005. **23**(35): p. 8968-77.
107. Chikuma S, Terawaki S, Hayashi T, Nabeshima R, Yoshida T, Shibayama S*, et al.*, *PD-1-Mediated Suppression of IL-2 Production Induces CD8⁺ T Cell Anergy In Vivo.* The Journal of Immunology, 2009. **182**(11): p. 6682.
108. Kim H-D, Song G-W, Park S, Jung MK, Kim MH, Kang HJ*, et al.*, *Association Between Expression Level of PD1 by Tumor-Infiltrating CD8+ T Cells and Features of Hepatocellular Carcinoma.* Gastroenterology, 2018. **155**(6): p. 1936-1950.e17.
109. Kitano A, Ono M, Yoshida M, Noguchi E, Shimomura A, Shimoi T*, et al.*, *Tumour-infiltrating lymphocytes are correlated with higher expression levels of PD-1 and PD-L1 in early breast cancer.* ESMO Open, 2017. **2**(2): p. e000150.
110. Ahmadzadeh M, Johnson LA, Heemskerk B, Wunderlich JR, Dudley ME, White DE*, et al.*, *Tumor antigen–specific CD8 T cells infiltrating the tumor express high levels of PD-1 and are functionally impaired.* Blood, 2009. **114**(8): p. 1537.
111. Hudson K, Cross N, Jordan-Mahy N, and Leyland R, *The Extrinsic and Intrinsic Roles of PD-L1 and Its Receptor PD-1: Implications for Immunotherapy Treatment.* Frontiers in Immunology, 2020. **11**.

112. Wei SC, Duffy CR, and Allison JP, *Fundamental Mechanisms of Immune Checkpoint Blockade Therapy.* Cancer Discovery, 2018. **8**(9): p. 1069-1086.
113. Yi M, Niu M, Xu L, Luo S, and Wu K, *Regulation of PD-L1 expression in the tumor microenvironment.* Journal of Hematology & Oncology, 2021. **14**(1): p. 10.
114. Yearley JH, Gibson C, Yu N, Moon C, Murphy E, Juco J*, et al.*, *PD-L2 Expression in Human Tumors: Relevance to Anti-PD-1 Therapy in Cancer.* Clinical Cancer Research, 2017. **23**(12): p. 3158-3167.
115. Mkrtichyan M, Najjar YG, Raulfs EC, Liu L, Langerman S, Guittard G*, et al.*, *B7-DC-Ig Enhances Vaccine Effect by a Novel Mechanism Dependent on PD-1 Expression Level on T Cell Subsets.* The Journal of Immunology, 2012. **189**(5): p. 2338-2347.
116. Niu M, Yi M, Li N, Luo S, and Wu K, *Predictive biomarkers of anti-PD-1/PD-L1 therapy in NSCLC.* Experimental Hematology & Oncology, 2021. **10**(1): p. 18.
117. Klemen ND, Wang M, Feingold PL, Cooper K, Pavri SN, Han D*, et al.*, *Patterns of failure after immunotherapy with checkpoint inhibitors predict durable progression-free survival after local therapy for metastatic melanoma.* J Immunother Cancer, 2019. **7**(1): p. 196.
118. Wang Q and Wu X, *Primary and acquired resistance to PD-1/PD-L1 blockade in cancer treatment.* International Immunopharmacology, 2017. **46**: p. 210-219.
119. Kelderman S, Schumacher TNM, and Haanen JBAG, *Acquired and intrinsic resistance in cancer immunotherapy.* Molecular Oncology, 2014. **8**(6): p. 1132-1139.
120. Sun J-Y, Zhang D, Wu S, Xu M, Zhou X, Lu X-J*, et al.*, *Resistance to PD-1/PD-L1 blockade cancer immunotherapy: mechanisms, predictive factors, and future perspectives.* Biomarker Research, 2020. **8**(1): p. 35.
121. Sharma P, Hu-Lieskovan S, Wargo JA, and Ribas A, *Primary, Adaptive, and Acquired Resistance to Cancer Immunotherapy.* Cell, 2017. **168**(4): p. 707-723.
122. Duan Z and Luo Y, *Targeting macrophages in cancer immunotherapy.* Signal Transduction and Targeted Therapy, 2021. **6**(1): p. 127.
123. Saleh R and Elkord E, *Treg-mediated acquired resistance to immune checkpoint inhibitors.* Cancer Letters, 2019. **457**: p. 168-179.
124. Wang W, Erbe AK, Hank JA, Morris ZS, and Sondel PM, *NK Cell-Mediated Antibody-Dependent Cellular Cytotoxicity in Cancer Immunotherapy.* Front Immunol, 2015. **6**: p. 368.
125. Yu P, Lee Y, Liu W, Krausz T, Chong A, Schreiber H*, et al.*, *Intratumor depletion of CD4+ cells unmasks tumor immunogenicity leading to the rejection of late-stage tumors.* Journal of Experimental Medicine, 2005. **201**(5): p. 779-791.
126. Shimizu J, Yamazaki S, and Sakaguchi S, *Induction of tumor immunity by removing CD25+CD4+ T cells: a common basis between tumor immunity and autoimmunity.* J Immunol, 1999. **163**(10): p. 5211-8.
127. Ribas A, Hamid O, Daud A, Hodi FS, Wolchok JD, Kefford R*, et al.*, *Association of Pembrolizumab With Tumor Response and Survival Among Patients With Advanced Melanoma.* JAMA, 2016. **315**(15): p. 1600-1609.
128. Zhou B, Gao Y, Zhang P, and Chu Q, *Acquired Resistance to Immune Checkpoint Blockades: The Underlying Mechanisms and Potential Strategies.* Frontiers in Immunology, 2021. **12**.

129. Pitt Jonathan M, Vétizou M, Daillère R, Roberti María P, Yamazaki T, Routy B*, et al.*, *Resistance Mechanisms to Immune-Checkpoint Blockade in Cancer: Tumor-Intrinsic and -Extrinsic Factors.* Immunity, 2016. **44**(6): p. 1255-1269.
130. Fingas CD, Mertens JC, Razumilava N, Bronk SF, Sirica AE, and Gores GJ, *Targeting PDGFR-β in Cholangiocarcinoma.* Liver international : official journal of the International Association for the Study of the Liver, 2012. **32**(3): p. 400-409.
131. Brahmer JR, Tykodi SS, Chow LQ, Hwu WJ, Topalian SL, Hwu P*, et al.*, *Safety and activity of anti-PD-L1 antibody in patients with advanced cancer.* N Engl J Med, 2012. **366**(26): p. 2455-65.
132. Boni A, Cogdill AP, Dang P, Udayakumar D, Njauw C-NJ, Sloss CM*, et al.*, *Selective BRAFV600E Inhibition Enhances T-Cell Recognition of Melanoma without Affecting Lymphocyte Function.* Cancer Research, 2010. **70**(13): p. 5213-5219.
133. Liu L, Mayes PA, Eastman S, Shi H, Yadavilli S, Zhang T*, et al.*, *The BRAF and MEK Inhibitors Dabrafenib and Trametinib: Effects on Immune Function and in Combination with Immunomodulatory Antibodies Targeting PD-1, PD-L1, and CTLA-4.* Clinical Cancer Research, 2015. **21**(7): p. 1639.
134. Hu-Lieskovan S, Mok S, Homet Moreno B, Tsoi J, Robert L, Goedert L*, et al.*, *Improved antitumor activity of immunotherapy with BRAF and MEK inhibitors in BRAF(V600E) melanoma.* Sci Transl Med, 2015. **7**(279): p. 279ra41.
135. Kang S, El-Rayes BF, and Akce M, *Evolving Role of Immunotherapy in Advanced Biliary Tract Cancers.* Cancers, 2022. **14**(7): p. 1748.
136. Rizvi S, Khan SA, Hallemeier CL, Kelley RK, and Gores GJ, *Cholangiocarcinoma - evolving concepts and therapeutic strategies.* Nature reviews. Clinical oncology, 2018. **15**(2): p. 95-111.
137. Rizzo A and Brandi G, *Pitfalls, challenges, and updates in adjuvant systemic treatment for resected biliary tract cancer.* Expert Review of Gastroenterology & Hepatology, 2021. **15**(5): p. 547-554.
138. Zhang Y, Ma Z, Li C, Wang C, Jiang W, Chang J*, et al.*, *The genomic landscape of cholangiocarcinoma reveals the disruption of post-transcriptional modifiers.* Nature Communications, 2022. **13**(1): p. 3061.
139. Bridgewater JA, Goodman KA, Kalyan A, and Mulcahy MF, *Biliary Tract Cancer: Epidemiology, Radiotherapy, and Molecular Profiling.* American Society of Clinical Oncology Educational Book, 2016(36): p. e194-e203.
140. Churi CR, Shroff R, Wang Y, Rashid A, Kang HC, Weatherly J*, et al.*, *Mutation profiling in cholangiocarcinoma: prognostic and therapeutic implications.* PloS one, 2014. **9**(12): p. e115383-e115383.
141. Cigliano A, Chen X, and Calvisi DF, *Current challenges to underpinning the genetic basis for cholangiocarcinoma.* Expert Review of Gastroenterology & Hepatology, 2021. **15**(5): p. 511-526.
142. Jiao Y, Pawlik TM, Anders RA, Selaru FM, Streppel MM, Lucas DJ*, et al.*, *Exome sequencing identifies frequent inactivating mutations in BAP1, ARID1A and PBRM1 in intrahepatic cholangiocarcinomas.* Nat Genet, 2013. **45**(12): p. 1470-1473.
143. Lowery MA, Ptashkin R, Jordan E, Berger MF, Zehir A, Capanu M*, et al.*, *Comprehensive Molecular Profiling of Intrahepatic and Extrahepatic Cholangiocarcinomas: Potential Targets for Intervention.* Clin Cancer Res, 2018. **24**(17): p. 4154-4161.

144. Zou S, Li J, Zhou H, Frech C, Jiang X, Chu JSC*, et al.*, *Mutational landscape of intrahepatic cholangiocarcinoma.* Nature Communications, 2014. **5**(1): p. 5696.
145. Tannapfel A, Sommerer F, Benicke M, Katalinic A, Uhlmann D, Witzigmann H*, et al.*, *Mutations of the BRAF gene in cholangiocarcinoma but not in hepatocellular carcinoma.* Gut, 2003. **52**(5): p. 706.
146. Yang W and Sun Y, *Promising Molecular Targets for the Targeted Therapy of Biliary Tract Cancers: An Overview.* Onco Targets Ther, 2021. **14**: p. 1341-1366.
147. Javle M, Bekaii-Saab T, Jain A, Wang Y, Kelley RK, Wang K*, et al.*, *Biliary cancer: Utility of next-generation sequencing for clinical management.* Cancer, 2016. **122**(24): p. 3838-3847.
148. Mahipal A, Tella SH, Kommalapati A, Anaya D, and Kim R, *FGFR2 genomic aberrations: Achilles heel in the management of advanced cholangiocarcinoma.* Cancer Treatment Reviews, 2019. **78**: p. 1-7.
149. Cardinale V, Carpino G, Reid L, Gaudio E, and Alvaro D, *Multiple cells of origin in cholangiocarcinoma underlie biological, epidemiological and clinical heterogeneity.* World J Gastrointest Oncol, 2012. **4**(5): p. 94-102.
150. Brandi G, Farioli A, Astolfi A, Biasco G, and Tavolari S, *Genetic heterogeneity in cholangiocarcinoma: a major challenge for targeted therapies.* Oncotarget, 2015. **6**(17): p. 14744-53.
151. Kendall T, Verheij J, Gaudio E, Evert M, Guido M, Goeppert B*, et al.*, *Anatomical, histomorphological and molecular classification of cholangiocarcinoma.* Liver International, 2019. **39**(S1): p. 7-18.
152. Hayashi A, Misumi K, Shibahara J, Arita J, Sakamoto Y, Hasegawa K*, et al.*, *Distinct Clinicopathologic and Genetic Features of 2 Histologic Subtypes of Intrahepatic Cholangiocarcinoma.* Am J Surg Pathol, 2016. **40**(8): p. 1021-30.
153. Liau J-Y, Tsai J-H, Yuan R-H, Chang C-N, Lee H-J, and Jeng Y-M, *Morphological subclassification of intrahepatic cholangiocarcinoma: etiological, clinicopathological, and molecular features.* Modern Pathology, 2014. **27**(8): p. 1163-1173.
154. Banales JM, Cardinale V, Carpino G, Marzioni M, Andersen JB, Invernizzi P*, et al.*, *Cholangiocarcinoma: current knowledge and future perspectives consensus statement from the European Network for the Study of Cholangiocarcinoma (ENS-CCA).* Nature Reviews Gastroenterology & Hepatology, 2016. **13**(5): p. 261-280.
155. Rizvi S, Khan SA, Hallemeier CL, Kelley RK, and Gores GJ, *Cholangiocarcinoma — evolving concepts and therapeutic strategies.* Nature Reviews Clinical Oncology, 2018. **15**(2): p. 95-111.
156. Sriamporn S, Pisani P, Pipitgool V, Suwanrungruang K, Kamsa-ard S, and Parkin DM, *Prevalence of Opisthorchis viverrini infection and incidence of cholangiocarcinoma in Khon Kaen, Northeast Thailand.* Trop Med Int Health, 2004. **9**(5): p. 588-94.
157. Braconi C and Patel T, *Cholangiocarcinoma: new insights into disease pathogenesis and biology.* Infectious disease clinics of North America, 2010. **24**(4): p. 871-vii.
158. Andrews RH, Sithithaworn P, and Petney TN, *Opisthorchis viverrini: an underestimated parasite in world health.* Trends in parasitology, 2008. **24**(11): p. 497-501.
159. Sithithaworn P, Yongvanit P, Duenngai K, Kiatsopit N, and Pairojkul C, *Roles of liver fluke infection as risk factor for cholangiocarcinoma.* Journal of Hepato-Biliary-Pancreatic Sciences, 2014. **21**(5): p. 301-308.

160. Navas M-C, Glaser S, Dhruv H, Celinski S, Alpini G, and Meng F, *Hepatitis C Virus Infection and Cholangiocarcinoma: An Insight into Epidemiologic Evidences and Hypothetical Mechanisms of Oncogenesis.* The American Journal of Pathology, 2019. **189**(6): p. 1122-1132.
161. Cardinale V, Semeraro R, Torrice A, Gatto M, Napoli C, Bragazzi MC*, et al.*, *Intra-hepatic and extra-hepatic cholangiocarcinoma: New insight into epidemiology and risk factors.* World J Gastrointest Oncol, 2010. **2**(11): p. 407-16.
162. Li H, Hu B, Zhou ZQ, Guan J, Zhang ZY, and Zhou GW, *Hepatitis C virus infection and the risk of intrahepatic cholangiocarcinoma and extrahepatic cholangiocarcinoma: evidence from a systematic review and meta-analysis of 16 case-control studies.* World J Surg Oncol, 2015. **13**: p. 161.
163. Roskams T, *Liver stem cells and their implication in hepatocellular and cholangiocarcinoma.* Oncogene, 2006. **25**(27): p. 3818-3822.
164. Kalluri R and Neilson EG, *Epithelial-mesenchymal transition and its implications for fibrosis.* J Clin Invest, 2003. **112**(12): p. 1776-84.
165. Bose Sandip K, Meyer K, Di Bisceglie Adrian M, Ray Ratna B, and Ray R, *Hepatitis C Virus Induces Epithelial-Mesenchymal Transition in Primary Human Hepatocytes.* Journal of Virology, 2012. **86**(24): p. 13621-13628.
166. Ciner AT, Jones K, Muschel RJ, and Brodt P, *The unique immune microenvironment of liver metastases: Challenges and opportunities.* Semin Cancer Biol, 2021. **71**: p. 143-156.
167. Kubes P and Jenne C, *Immune Responses in the Liver.* Annu Rev Immunol, 2018. **36**: p. 247-277.
168. Fabris L, Sato K, Alpini G, and Strazzabosco M, *The Tumor Microenvironment in Cholangiocarcinoma Progression.* Hepatology, 2021. **73 Suppl 1**(Suppl 1): p. 75-85.
169. Kasper HU, Drebber U, Stippel DL, Dienes HP, and Gillessen A, *Liver tumor infiltrating lymphocytes: comparison of hepatocellular and cholangiolar carcinoma.* World J Gastroenterol, 2009. **15**(40): p. 5053-7.
170. Loeuillard E, Conboy CB, Gores GJ, and Rizvi S, *Immunobiology of cholangiocarcinoma.* JHEP Rep, 2019. **1**(4): p. 297-311.
171. Malenica I, Donadon M, and Lleo A, *Molecular and Immunological Characterization of Biliary Tract Cancers: A Paradigm Shift Towards a Personalized Medicine.* Cancers (Basel), 2020. **12**(8).
172. Hasita H, Komohara Y, Okabe H, Masuda T, Ohnishi K, Lei XF*, et al.*, *Significance of alternatively activated macrophages in patients with intrahepatic cholangiocarcinoma.* Cancer Sci, 2010. **101**(8): p. 1913-9.
173. Martín-Sierra C, Martins R, Laranjeira P, Abrantes AM, Oliveira RC, Tralhão JG*, et al.*, *Functional Impairment of Circulating FcεRI(+) Monocytes and Myeloid Dendritic Cells in Hepatocellular Carcinoma and Cholangiocarcinoma Patients.* Cytometry B Clin Cytom, 2019. **96**(6): p. 490-495.
174. Morrison DK, *MAP kinase pathways.* Cold Spring Harb Perspect Biol, 2012. **4**(11).
175. Dhillon AS, Hagan S, Rath O, and Kolch W, *MAP kinase signalling pathways in cancer.* Oncogene, 2007. **26**(22): p. 3279-3290.
176. Roberts PJ and Der CJ, *Targeting the Raf-MEK-ERK mitogen-activated protein kinase cascade for the treatment of cancer.* Oncogene, 2007. **26**: p. 3291.

177. Caunt CJ, Sale MJ, Smith PD, and Cook SJ, *MEK1 and MEK2 inhibitors and cancer therapy: the long and winding road.* Nature Reviews Cancer, 2015. **15**(10): p. 577-592.
178. Eblen ST, *Extracellular-Regulated Kinases: Signaling From Ras to ERK Substrates to Control Biological Outcomes.* Adv Cancer Res, 2018. **138**: p. 99-142.
179. Ünal EB, Uhlitz F, and Blüthgen N, *A compendium of ERK targets.* FEBS Letters, 2017. **591**(17): p. 2607-2615.
180. Yang L, Zheng L, Chng WJ, and Ding JL, *Comprehensive Analysis of ERK1/2 Substrates for Potential Combination Immunotherapies.* Trends in Pharmacological Sciences, 2019. **40**(11): p. 897-910.
181. Katz M, Amit I, and Yarden Y, *Regulation of MAPKs by growth factors and receptor tyrosine kinases.* Biochim Biophys Acta, 2007. **1773**(8): p. 1161-76.
182. Temraz S, Mukherji D, and Shamseddine A, *Dual Inhibition of MEK and PI3K Pathway in KRAS and BRAF Mutated Colorectal Cancers.* International Journal of Molecular Sciences, 2015. **16**(9): p. 22976-22988.
183. Britten CD, *PI3K and MEK inhibitor combinations: examining the evidence in selected tumor types.* Cancer Chemotherapy and Pharmacology, 2013. **71**(6): p. 1395-1409.
184. Zhang W and Liu HT, *MAPK signal pathways in the regulation of cell proliferation in mammalian cells.* Cell Research, 2002. **12**(1): p. 9-18.
185. Yoon J-H, Werneburg NW, Higuchi H, Canbay AE, Kaufmann SH, Akgul C*, et al.*, *Bile Acids Inhibit Mcl-1 Protein Turnover via an Epidermal Growth Factor Receptor/Raf-1-dependent Mechanism1.* Cancer Research, 2002. **62**(22): p. 6500-6505.
186. Wang A, Rud J, Olson CM, Anguita J, and Osborne BA, *Phosphorylation of Nur77 by the MEK-ERK-RSK Cascade Induces Mitochondrial Translocation and Apoptosis in T Cells.* The Journal of Immunology, 2009. **183**(5): p. 3268.
187. Ebert PJR, Cheung J, Yang Y, McNamara E, Hong R, Moskalenko M*, et al.*, *MAP Kinase Inhibition Promotes T Cell and Anti-tumor Activity in Combination with PD-L1 Checkpoint Blockade.* Immunity, 2016. **44**(3): p. 609-621.
188. Loi S, Dushyanthen S, Beavis PA, Salgado R, Denkert C, Savas P*, et al.*, *RAS/MAPK Activation Is Associated with Reduced Tumor-Infiltrating Lymphocytes in Triple-Negative Breast Cancer: Therapeutic Cooperation Between MEK and PD-1/PD-L1 Immune Checkpoint Inhibitors.* Clinical Cancer Research, 2016. **22**(6): p. 1499-1509.
189. Kang SH, Keam B, Ahn YO, Park HR, Kim M, Kim TM*, et al.*, *Inhibition of MEK with trametinib enhances the efficacy of anti-PD-L1 inhibitor by regulating anti-tumor immunity in head and neck squamous cell carcinoma.* Oncoimmunology, 2019. **8**(1): p. e1515057.
190. Franklin DA, James JL, Axelrod ML, and Balko JM, *MEK inhibition activates STAT signaling to increase breast cancer immunogenicity via MHC-I expression.* Cancer Drug Resist, 2020. **3**(3): p. 603-612.
191. Sumimoto H, Imabayashi F, Iwata T, and Kawakami Y, *The BRAF–MAPK signaling pathway is essential for cancer-immune evasion in human melanoma cells.* 2006. **203**(7): p. 1651-1656.
192. Brea EJ, Oh CY, Manchado E, Budhu S, Gejman RS, Mo G*, et al.*, *Kinase Regulation of Human MHC Class I Molecule Expression on Cancer Cells.* Cancer Immunology Research, 2016. **4**(11): p. 936-947.

193. Bedognetti D, Roelands J, Decock J, Wang E, and Hendrickx W, *The MAPK hypothesis: immune-regulatory effects of MAPK-pathway genetic dysregulations and implications for breast cancer immunotherapy.* Emerg Top Life Sci, 2017. **1**(5): p. 429-445.
194. Valle J, Wasan H, Palmer DH, Cunningham D, Anthoney A, Maraveyas A*, et al.*, *Cisplatin plus Gemcitabine versus Gemcitabine for Biliary Tract Cancer.* New England Journal of Medicine, 2010. **362**(14): p. 1273-1281.
195. Roth MT and Goff LW, *Gemcitabine, Cisplatin, and nab-Paclitaxel for Patients With Advanced Biliary Tract Cancer: Closing the GAP.* JAMA Oncology, 2019. **5**(6): p. 831-832.
196. *FDA approves durvalumab for locally advanced or metastatic biliary tract cancer*. 2022, FDA: Food and Drug Administration.
197. Oh D-Y, He AR, Qin S, Chen L-T, Okusaka T, Vogel A*, et al.*, *A phase 3 randomized, double-blind, placebo-controlled study of durvalumab in combination with gemcitabine plus cisplatin (GemCis) in patients (pts) with advanced biliary tract cancer (BTC): TOPAZ-1.* Journal of Clinical Oncology, 2022. **40**(4_suppl): p. 378-378.
198. Shroff RT, Javle MM, Xiao L, Kaseb AO, Varadhachary GR, Wolff RA*, et al.*, *Gemcitabine, Cisplatin, and nab-Paclitaxel for the Treatment of Advanced Biliary Tract Cancers: A Phase 2 Clinical Trial.* JAMA Oncology, 2019. **5**(6): p. 824-830.
199. Phelip J-M, Edeline J, Blanc J-F, Barbier E, Michel P, Bourgeois V*, et al.*, *Modified FOLFIRINOX versus CisGem first-line chemotherapy for locally advanced non resectable or metastatic biliary tract cancer (AMEBICA)-PRODIGE 38: Study protocol for a randomized controlled multicenter phase II/III study.* Digestive and Liver Disease, 2019. **51**(2): p. 318-320.
200. Rizzo A, Ricci AD, Cusmai A, Acquafredda S, De Palma G, Brandi G*, et al.*, *Systemic Treatment for Metastatic Biliary Tract Cancer: State of the Art and a Glimpse to the Future.* Current Oncology, 2022. **29**(2): p. 551-564.
201. Ricci AD, Rizzo A, Bonucci C, Tober N, Palloni A, Mollica V*, et al.*, *PARP Inhibitors in Biliary Tract Cancer: A New Kid on the Block?* Medicines (Basel), 2020. **7**(9).
202. Lamarca A, Barriuso J, McNamara MG, and Valle JW, *Molecular targeted therapies: Ready for "prime time" in biliary tract cancer.* Journal of Hepatology, 2020. **73**(1): p. 170-185.
203. Manne A, Woods E, Tsung A, and Mittra A, *Biliary Tract Cancers: Treatment Updates and Future Directions in the Era of Precision Medicine and Immuno-Oncology.* Frontiers in Oncology, 2021. **11**.
204. Persano M, Puzzoni M, Ziranu P, Pusceddu V, Lai E, Pretta A*, et al.*, *Molecular-driven treatment for biliary tract cancer: the promising turning point.* Expert Review of Anticancer Therapy, 2021: p. 1-12.
205. Chen C, Nelson LJ, Ávila MA, and Cubero FJ, *Mitogen-Activated Protein Kinases (MAPKs) and Cholangiocarcinoma: The Missing Link.* Cells, 2019. **8**(10): p. 1172.
206. Chapnick DA, Warner L, Bernet J, Rao T, and Liu X, *Partners in crime: the TGFβ and MAPK pathways in cancer progression.* Cell Biosci, 2011. **1**: p. 42.
207. Finn RS, Javle MM, Tan BR, Weekes CD, Bendell JC, Patnaik A*, et al.*, *A phase I study of MEK inhibitor MEK162 (ARRY-438162) in patients with biliary tract cancer.* Journal of Clinical Oncology, 2012. **30**(4_suppl): p. 220-220.
208. Bekaii-Saab T, Phelps MA, Li X, Saji M, Goff L, Kauh JSW*, et al.*, *Multi-institutional phase II study of selumetinib in patients with metastatic biliary cancers.* Journal of

clinical oncology : official journal of the American Society of Clinical Oncology, 2011. **29**(17): p. 2357-2363.
209. Finn RS, Ahn DH, Javle MM, Tan BR, Weekes CD, Bendell JC*, et al.*, *Phase 1b investigation of the MEK inhibitor binimetinib in patients with advanced or metastatic biliary tract cancer.* Investigational New Drugs, 2018. **36**(6): p. 1037-1043.
210. Subbiah V, Lassen U, Élez E, Italiano A, Curigliano G, Javle M*, et al.*, *Dabrafenib plus trametinib in patients with BRAFV600E-mutated biliary tract cancer (ROAR): a phase 2, open-label, single-arm, multicentre basket trial.* The Lancet Oncology, 2020. **21**(9): p. 1234-1243.
211. Talbert EE, Yang J, Mace TA, Farren MR, Farris AB, Young GS*, et al.*, *Dual Inhibition of MEK and PI3K/Akt Rescues Cancer Cachexia through both Tumor-Extrinsic and -Intrinsic Activities.* Molecular Cancer Therapeutics, 2017. **16**(2): p. 344-356.
212. Piha-Paul SA, Oh D-Y, Ueno M, Malka D, Chung HC, Nagrial A*, et al.*, *Efficacy and safety of pembrolizumab for the treatment of advanced biliary cancer: Results from the KEYNOTE-158 and KEYNOTE-028 studies.* International Journal of Cancer, 2020. **147**(8): p. 2190-2198.
213. Kim RD, Chung V, Alese OB, El-Rayes BF, Li D, Al-Toubah TE*, et al.*, *A Phase 2 Multi-institutional Study of Nivolumab for Patients With Advanced Refractory Biliary Tract Cancer.* JAMA Oncology, 2020. **6**(6): p. 888-894.
214. Kriegsmann M, Roessler S, Kriegsmann K, Renner M, Longuespée R, Albrecht T*, et al.*, *Programmed cell death ligand 1 (PD-L1, CD274) in cholangiocarcinoma – correlation with clinicopathological data and comparison of antibodies.* BMC Cancer, 2019. **19**(1): p. 72.
215. Cowzer D and Harding JJ, *Advanced Bile Duct Cancers: A Focused Review on Current and Emerging Systemic Treatments.* Cancers, 2022. **14**(7): p. 1800.
216. Homma Y, Taniguchi K, Nakazawa M, Matsuyama R, Mori R, Takeda K*, et al.*, *Changes in the immune cell population and cell proliferation in peripheral blood after gemcitabine-based chemotherapy for pancreatic cancer.* Clin Transl Oncol, 2014. **16**(3): p. 330-5.
217. Ribas A, Lawrence D, Atkinson V, Agarwal S, Miller WH, Carlino MS*, et al.*, *Combined BRAF and MEK inhibition with PD-1 blockade immunotherapy in BRAF-mutant melanoma.* Nature Medicine, 2019. **25**(6): p. 936-940.
218. Eng C, Kim TW, Bendell J, Argilés G, Tebbutt NC, Di Bartolomeo M*, et al.*, *Atezolizumab with or without cobimetinib versus regorafenib in previously treated metastatic colorectal cancer (IMblaze370): a multicentre, open-label, phase 3, randomised, controlled trial.* The Lancet Oncology, 2019. **20**(6): p. 849-861.
219. Hellmann MD, Kim TW, Lee CB, Goh BC, Miller WH, Jr., Oh DY*, et al.*, *Phase Ib study of atezolizumab combined with cobimetinib in patients with solid tumors.* Annals of Oncology, 2019. **30**(7): p. 1134-1142.
220. Lee JW, Zhang Y, Eoh KJ, Sharma R, Sanmamed MF, Wu J*, et al.*, *The Combination of MEK Inhibitor With Immunomodulatory Antibodies Targeting Programmed Death 1 and Programmed Death Ligand 1 Results in Prolonged Survival in Kras/p53-Driven Lung Cancer.* J Thorac Oncol, 2019. **14**(6): p. 1046-1060.
221. Yarchoan M, Cope L, Ruggieri AN, Anders RA, Noonan AM, Goff LW*, et al.*, *Multicenter randomized phase II trial of atezolizumab with or without cobimetinib in biliary tract cancers.* The Journal of Clinical Investigation, 2021. **131**(24).

222. Wabitsch S, Tandon M, Ruf B, Zhang Q, McCallen JD, McVey JC*, et al.*, *Anti–PD-1 in Combination With Trametinib Suppresses Tumor Growth and Improves Survival of Intrahepatic Cholangiocarcinoma in Mice.* Cellular and Molecular Gastroenterology and Hepatology, 2021. **12**(3): p. 1166-1178.
223. Ribas A, Algazi A, Ascierto PA, Butler MO, Chandra S, Gordon M*, et al.*, *PD-L1 blockade in combination with inhibition of MAPK oncogenic signaling in patients with advanced melanoma.* Nature Communications, 2020. **11**(1): p. 6262.
224. Dennison L, Ruggieri A, Mohan A, Leatherman J, Cruz K, Woolman S*, et al.*, *Context-Dependent Immunomodulatory Effects of MEK Inhibition Are Enhanced with T-cell Agonist Therapy.* Cancer Immunology Research, 2021. **9**(10): p. 1187-1201.
225. Kim RD, McDonough S, El-Khoueiry AB, Bekaii-Saab TS, Stein SM, Sahai V*, et al.*, *Randomised phase II trial (SWOG S1310) of single agent MEK inhibitor trametinib Versus 5-fluorouracil or capecitabine in refractory advanced biliary cancer.* Eur J Cancer, 2020. **130**: p. 219-227.
226. Ikeda M, Ioka T, Fukutomi A, Morizane C, Kasuga A, Takahashi H*, et al.*, *Efficacy and safety of trametinib in Japanese patients with advanced biliary tract cancers refractory to gemcitabine.* Cancer Sci, 2018. **109**(1): p. 215-224.
227. Doherty MK, Tam VC, McNamara MG, Jang R, Hedley D, Chen E*, et al.*, *Randomised, Phase II study of selumetinib, an oral inhibitor of MEK, in combination with cisplatin and gemcitabine chemotherapy for patients with advanced biliary tract cancer.* Br J Cancer, 2022.
228. Lowery MA, Bradley M, Chou JF, Capanu M, Gerst S, Harding JJ*, et al.*, *Binimetinib plus Gemcitabine and Cisplatin Phase I/II Trial in Patients with Advanced Biliary Cancers.* Clinical Cancer Research, 2019. **25**(3): p. 937-945.
229. Marabelle A, Le DT, Ascierto PA, Giacomo AMD, Jesus-Acosta AD, Delord J-P*, et al.*, *Efficacy of Pembrolizumab in Patients With Noncolorectal High Microsatellite Instability/Mismatch Repair–Deficient Cancer: Results From the Phase II KEYNOTE-158 Study.* Journal of Clinical Oncology, 2020. **38**(1): p. 1-10.
230. Doki Y, Ueno M, Hsu CH, Oh DY, Park K, Yamamoto N*, et al.*, *Tolerability and efficacy of durvalumab, either as monotherapy or in combination with tremelimumab, in patients from Asia with advanced biliary tract, esophageal, or head-and-neck cancer.* Cancer Med, 2022. **11**(13): p. 2550-2560.
231. Klein O, Kee D, Nagrial A, Markman B, Underhill C, Michael M*, et al.*, *Evaluation of Combination Nivolumab and Ipilimumab Immunotherapy in Patients With Advanced Biliary Tract Cancers: Subgroup Analysis of a Phase 2 Nonrandomized Clinical Trial.* JAMA Oncol, 2020. **6**(9): p. 1405-1409.
232. Feng K, Liu Y, Zhao Y, Yang Q, Dong L, Liu J*, et al.*, *Efficacy and biomarker analysis of nivolumab plus gemcitabine and cisplatin in patients with unresectable or metastatic biliary tract cancers: results from a phase II study.* J Immunother Cancer, 2020. **8**(1).
233. Chen X, Wu X, Wu H, Gu Y, Shao Y, Shao Q*, et al.*, *Camrelizumab plus gemcitabine and oxaliplatin (GEMOX) in patients with advanced biliary tract cancer: a single-arm, open-label, phase II trial.* Journal for ImmunoTherapy of Cancer, 2020. **8**(2): p. e001240.
234. Li W, Yu Y, Xu X, Guo X, Wang Y, Li Q*, et al.*, *Toripalimab with chemotherapy as first-line treatment for advanced biliary tract tumors: Update analytic results of an open-label phase II clinical study (JS001-ZS-BC001).* Journal of Clinical Oncology, 2021. **39**(15_suppl): p. e16170-e16170.

235. Arkenau HT, Martin-Liberal J, Calvo E, Penel N, Krebs MG, Herbst RS*, et al.*, *Ramucirumab Plus Pembrolizumab in Patients with Previously Treated Advanced or Metastatic Biliary Tract Cancer: Nonrandomized, Open-Label, Phase I Trial (JVDF).* Oncologist, 2018. **23**(12): p. 1407-e136.
236. Villanueva L, Lwin Z, Chung HC, Gomez-Roca C, Longo F, Yanez E*, et al.*, *Lenvatinib plus pembrolizumab for patients with previously treated biliary tract cancers in the multicohort phase II LEAP-005 study.* Journal of Clinical Oncology, 2021. **39**(3_suppl): p. 321-321.
237. Chen X, Qin S, Gu S, Ren Z, Chen Z, Xiong J*, et al.*, *Camrelizumab plus oxaliplatin-based chemotherapy as first-line therapy for advanced biliary tract cancer: A multicenter, phase 2 trial.* International Journal of Cancer, 2021. **149**(11): p. 1944-1954.
238. Goyal L, Kongpetch S, Crolley VE, and Bridgewater J, *Targeting FGFR inhibition in cholangiocarcinoma.* Cancer Treatment Reviews, 2021. **95**: p. 102170.
239. Crispo F, Pietrafesa M, Condelli V, Maddalena F, Bruno G, Piscazzi A*, et al.*, *IDH1 Targeting as a New Potential Option for Intrahepatic Cholangiocarcinoma Treatment-Current State and Future Perspectives.* Molecules (Basel, Switzerland), 2020. **25**(16): p. 3754.
240. Oneda E, Abu Hilal M, and Zaniboni A, *Biliary Tract Cancer: Current Medical Treatment Strategies.* Cancers, 2020. **12**(5): p. 1237.
241. Valle JW, Lamarca A, Goyal L, Barriuso J, and Zhu AX, *New Horizons for Precision Medicine in Biliary Tract Cancers.* Cancer Discovery, 2017. **7**(9): p. 943.
242. Dushyanthen S, Teo ZL, Caramia F, Savas P, Mintoff CP, Virassamy B*, et al.*, *Agonist immunotherapy restores T cell function following MEK inhibition improving efficacy in breast cancer.* Nature Communications, 2017. **8**(1): p. 606.
243. Vogel A, Bathon M, and Saborowski A, *Immunotherapies in clinical development for biliary tract cancer.* Expert Opinion on Investigational Drugs, 2021. **30**(4): p. 351-363.
244. Yao W-Y and Gong W, *Immunotherapy in cholangiocarcinoma: From concept to clinical trials.* Surgery in Practice and Science, 2021. **5**: p. 100028.
245. Ji S, Chen H, Yang K, Zhang G, Mao B, Hu Y*, et al.*, *Peripheral cytokine levels as predictive biomarkers of benefit from immune checkpoint inhibitors in cancer therapy.* Biomedicine & Pharmacotherapy, 2020. **129**: p. 110457.
246. Brivio S, Cadamuro M, Strazzabosco M, and Fabris L, *Tumor reactive stroma in cholangiocarcinoma: The fuel behind cancer aggressiveness.* World journal of hepatology, 2017. **9**(9): p. 455-468.
247. Aoki S, Inoue K, Klein S, Halvorsen S, Chen J, Matsui A*, et al.*, *Placental growth factor promotes tumour desmoplasia and treatment resistance in intrahepatic cholangiocarcinoma.* Gut, 2021: p. gutjnl-2020-322493.
248. Fingas CD, Bronk SF, Werneburg NW, Mott JL, Guicciardi ME, Cazanave SC*, et al.*, *Myofibroblast-derived PDGF-BB promotes Hedgehog survival signaling in cholangiocarcinoma cells.* Hepatology, 2011. **54**(6): p. 2076-88.
249. Heindryckx F, Bogaerts E, Coulon SH, Devlies H, Geerts AM, Libbrecht L*, et al.*, *Inhibition of the placental growth factor decreases burden of cholangiocarcinoma and hepatocellular carcinoma in a transgenic mouse model.* European Journal of Gastroenterology & Hepatology, 2012. **24**(9).

250. Li T, Guo T, Liu H, Jiang H, and Wang Y, *Platelet-derived growth factor-BB mediates pancreatic cancer malignancy via regulation of the Hippo/Yes-associated protein signaling pathway.* Oncol Rep, 2021. **45**(1): p. 83-94.
251. Niba ETE, Nagaya H, Kanno T, Tsuchiya A, Gotoh A, Tabata C*, et al.*, *Crosstalk between PI3 Kinase/PDK1/Akt/Rac1 and Ras/Raf/MEK/ERK Pathways Downstream PDGF Receptor.* Cellular Physiology and Biochemistry, 2013. **31**(6): p. 905-913.
252. Steller EJA, Raats DA, Koster J, Rutten B, Govaert KM, Emmink BL*, et al.*, *PDGFRB promotes liver metastasis formation of mesenchymal-like colorectal tumor cells.* Neoplasia (New York, N.Y.), 2013. **15**(2): p. 204-217.
253. Lederle W, Stark H-J, Skobe M, Fusenig NE, and Mueller MM, *Platelet-derived growth factor-BB controls epithelial tumor phenotype by differential growth factor regulation in stromal cells.* The American journal of pathology, 2006. **169**(5): p. 1767-1783.
254. Ying HZ, Chen Q, Zhang WY, Zhang HH, Ma Y, Zhang SZ*, et al.*, *PDGF signaling pathway in hepatic fibrosis pathogenesis and therapeutics (Review).* Mol Med Rep, 2017. **16**(6): p. 7879-7889.
255. Liu Y, Cai P, Wang N, Zhang Q, Chen F, Shi L*, et al.*, *Combined blockade of Tim-3 and MEK inhibitor enhances the efficacy against melanoma.* Biochemical and Biophysical Research Communications, 2017. **484**(2): p. 378-384.
256. Saleh R, Toor SM, and Elkord E, *Targeting TIM-3 in solid tumors: innovations in the preclinical and translational realm and therapeutic potential.* Expert Opinion on Therapeutic Targets, 2020. **24**(12): p. 1251-1262.
257. Song J and Wu L, *Friend or Foe: Prognostic and Immunotherapy Roles of BTLA in Colorectal Cancer.* Frontiers in Molecular Biosciences, 2020. **7**: p. 148.
258. Voss JS, Holtegaard LM, Kerr SE, Fritcher EGB, Roberts LR, Gores GJ*, et al.*, *Molecular profiling of cholangiocarcinoma shows potential for targeted therapy treatment decisions.* Human Pathology, 2013. **44**(7): p. 1216-1222.
259. Kamphorst Alice O, Pillai Rathi N, Yang S, Nasti Tahseen H, Akondy Rama S, Wieland A*, et al.*, *Proliferation of PD-1+ CD8 T cells in peripheral blood after PD-1–targeted therapy in lung cancer patients.* Proceedings of the National Academy of Sciences, 2017. **114**(19): p. 4993-4998.
260. Denkert C, von Minckwitz G, Darb-Esfahani S, Lederer B, Heppner BI, Weber KE*, et al.*, *Tumour-infiltrating lymphocytes and prognosis in different subtypes of breast cancer: a pooled analysis of 3771 patients treated with neoadjuvant therapy.* Lancet Oncol, 2018. **19**(1): p. 40-50.
261. Tumeh PC, Harview CL, Yearley JH, Shintaku IP, Taylor EJ, Robert L*, et al.*, *PD-1 blockade induces responses by inhibiting adaptive immune resistance.* Nature, 2014. **515**(7528): p. 568-71.
262. Job S, Rapoud D, Dos Santos A, Gonzalez P, Desterke C, Pascal G*, et al.*, *Identification of Four Immune Subtypes Characterized by Distinct Composition and Functions of Tumor Microenvironment in Intrahepatic Cholangiocarcinoma.* Hepatology, 2020. **72**(3): p. 965-981.
263. Linette GP and Carreno BM, *Tumor-Infiltrating Lymphocytes in the Checkpoint Inhibitor Era.* Current Hematologic Malignancy Reports, 2019. **14**(4): p. 286-291.
264. Deken MA, Gadiot J, Jordanova ES, Lacroix R, van Gool M, Kroon P*, et al.*, *Targeting the MAPK and PI3K pathways in combination with PD1 blockade in melanoma.* OncoImmunology, 2016. **5**(12): p. e1238557.

265. Yarchoan M, Mohan AA, Dennison L, Vithayathil T, Ruggieri A, Lesinski GB*, et al.*, *MEK inhibition suppresses B regulatory cells and augments anti-tumor immunity.* PLOS ONE, 2019. **14**(10): p. e0224600.
266. Mollica Poeta V, Massara M, Capucetti A, and Bonecchi R, *Chemokines and Chemokine Receptors: New Targets for Cancer Immunotherapy.* Frontiers in Immunology, 2019. **10**.
267. Ware MB, Zaidi MY, Yang J, Turgeon MK, Krasinskas A, Mace TA*, et al.*, *Suppressive myeloid cells are expanded by biliary tract cancer-derived cytokines in vitro and associate with aggressive disease.* British journal of cancer, 2020. **123**(9): p. 1377-1386.
268. Rizzo A, Ricci AD, and Brandi G, *Recent advances of immunotherapy for biliary tract cancer.* Expert Review of Gastroenterology & Hepatology, 2021. **15**(5): p. 527-536.
269. Wilmott JS, Long GV, Howle JR, Haydu LE, Sharma RN, Thompson JF*, et al.*, *Selective BRAF Inhibitors Induce Marked T-cell Infiltration into Human Metastatic Melanoma.* Clinical Cancer Research, 2012. **18**(5): p. 1386-1394.
270. Pahl HL, *Activators and target genes of Rel/NF-κB transcription factors.* Oncogene, 1999. **18**(49): p. 6853-6866.
271. Fleetwood AJ, Cook AD, and Hamilton JA, *Functions of granulocyte-macrophage colony-stimulating factor.* Crit Rev Immunol, 2005. **25**(5): p. 405-28.
272. Egea L, Hirata Y, and Kagnoff MF, *GM-CSF: a role in immune and inflammatory reactions in the intestine.* Expert Rev Gastroenterol Hepatol, 2010. **4**(6): p. 723-31.
273. Ma N, Liu Q, Hou L, Wang Y, and Liu Z, *MDSCs are involved in the protumorigenic potentials of GM-CSF in colitis-associated cancer.* International Journal of Immunopathology and Pharmacology, 2017. **30**(2): p. 152-162.
274. Dolcetti L, Peranzoni E, Ugel S, Marigo I, Fernandez Gomez A, Mesa C*, et al.*, *Hierarchy of immunosuppressive strength among myeloid-derived suppressor cell subsets is determined by GM-CSF.* European Journal of Immunology, 2010. **40**(1): p. 22-35.
275. Uemura Y, Kobayashi M, Nakata H, Kubota T, Bandobashi K, Saito T*, et al.*, *Effects of GM-CSF and M-CSF on tumor progression of lung cancer: Roles of MEK1/ERK and AKT/PKB pathways.* Int J Mol Med, 2006. **18**(2): p. 365-373.
276. Kawaguchi M, Kokubu F, Odaka M, Watanabe S, Suzuki S, Ieki K*, et al.*, *Induction of granulocyte-macrophage colony-stimulating factor by a new cytokine, ML-1 (IL-17F), via Raf I-MEK-ERK pathway.* Journal of Allergy and Clinical Immunology, 2004. **114**(2): p. 444-450.
277. Neville LF, Mathiak G, and Bagasra O, *The immunobiology of interferon-gamma inducible protein 10 kD (IP-10): A novel, pleiotropic member of the C-X-C chemokine superfamily.* Cytokine & Growth Factor Reviews, 1997. **8**(3): p. 207-219.
278. Loetscher M, Loetscher P, Brass N, Meese E, and Moser B, *Lymphocyte-specific chemokine receptor CXCR3: regulation, chemokine binding and gene localization.* European Journal of Immunology, 1998. **28**(11): p. 3696-3705.
279. Mikucki ME, Fisher DT, Matsuzaki J, Skitzki JJ, Gaulin NB, Muhitch JB*, et al.*, *Non-redundant requirement for CXCR3 signalling during tumoricidal T-cell trafficking across tumour vascular checkpoints.* Nature Communications, 2015. **6**(1): p. 7458.
280. Datta D, Flaxenburg JA, Laxmanan S, Geehan C, Grimm M, Waaga-Gasser AM*, et al.*, *Ras-induced Modulation of CXCL10 and Its Receptor Splice Variant CXCR3-B in MDA-MB-435 and MCF-7 Cells: Relevance for the Development of Human Breast Cancer.* Cancer Research, 2006. **66**(19): p. 9509-9518.

281. Ma W, Concha-Benavente F, Santegoets SJAM, Welters MJP, Ehsan I, Ferris RL*, et al.*, *EGFR signaling suppresses type 1 cytokine-induced T-cell attracting chemokine secretion in head and neck cancer.* PLOS ONE, 2018. **13**(9): p. e0203402.
282. Xie M, Zheng H, Madan-Lala R, Dai W, Gimbrone NT, Chen Z*, et al.*, *MEK Inhibition Modulates Cytokine Response to Mediate Therapeutic Efficacy in Lung Cancer.* Cancer Research, 2019. **79**(22): p. 5812-5825.
283. Limagne E, Nuttin L, Thibaudin M, Jacquin E, Aucagne R, Bon M*, et al.*, *MEK inhibition overcomes chemoimmunotherapy resistance by inducing CXCL10 in cancer cells.* Cancer Cell, 2022.
284. Liu M, Guo S, and Stiles JK, *The emerging role of CXCL10 in cancer (Review).* Oncol Lett, 2011. **2**(4): p. 583-589.
285. Billottet C, Quemener C, and Bikfalvi A, *CXCR3, a double-edged sword in tumor progression and angiogenesis.* Biochimica et Biophysica Acta (BBA) - Reviews on Cancer, 2013. **1836**(2): p. 287-295.
286. Maru SV, Holloway KA, Flynn G, Lancashire CL, Loughlin AJ, Male DK*, et al.*, *Chemokine production and chemokine receptor expression by human glioma cells: Role of CXCL10 in tumour cell proliferation.* Journal of Neuroimmunology, 2008. **199**(1): p. 35-45.
287. Zipin-Roitman A, Meshel T, Sagi-Assif O, Shalmon B, Avivi C, Pfeffer RM*, et al.*, *CXCL10 Promotes Invasion-Related Properties in Human Colorectal Carcinoma Cells.* Cancer Research, 2007. **67**(7): p. 3396-3405.
288. Viswanadhapalli S, Dileep KV, Zhang KYJ, Nair HB, and Vadlamudi RK, *Targeting LIF/LIFR signaling in cancer.* Genes & Diseases, 2022. **9**(4): p. 973-980.
289. Yue X, Wu L, and Hu W, *The regulation of leukemia inhibitory factor.* Cancer Cell Microenviron, 2015. **2**(3).
290. Li X, Yang Q, Yu H, Wu L, Zhao Y, Zhang C*, et al.*, *LIF promotes tumorigenesis and metastasis of breast cancer through the AKT-mTOR pathway.* Oncotarget, 2014. **5**(3): p. 788-801.
291. Fitzgerald JS, Tsareva SA, Poehlmann TG, Berod L, Meissner A, Corvinus FM*, et al.*, *Leukemia inhibitory factor triggers activation of signal transducer and activator of transcription 3, proliferation, invasiveness, and altered protease expression in choriocarcinoma cells.* Int J Biochem Cell Biol, 2005. **37**(11): p. 2284-96.
292. Morton SD, Cadamuro M, Brivio S, Vismara M, Stecca T, Massani M*, et al.*, *Leukemia inhibitory factor protects cholangiocarcinoma cells from drug-induced apoptosis via a PI3K/AKT-dependent Mcl-1 activation.* Oncotarget, 2015. **6**(28): p. 26052-64.
293. Park J-I, Strock CJ, Ball DW, and Nelkin BD, *The Ras/Raf/MEK/Extracellular Signal-Regulated Kinase Pathway Induces Autocrine-Paracrine Growth Inhibition via the Leukemia Inhibitory Factor/JAK/STAT Pathway.* Molecular and Cellular Biology, 2003. **23**(2): p. 543-554.
294. Bamberger AM, Jenatschke S, Schulte HM, Ellebrecht I, Beil FU, and Bamberger CM, *Regulation of the human leukemia inhibitory factor gene by ETS transcription factors.* Neuroimmunomodulation, 2004. **11**(1): p. 10-9.
295. Loriot Y, Marabelle A, Guégan JP, Danlos FX, Besse B, Chaput N*, et al.*, *Plasma proteomics identifies leukemia inhibitory factor (LIF) as a novel predictive biomarker of immune-checkpoint blockade resistance.* Annals of Oncology, 2021. **32**(11): p. 1381-1390.

296. Li C, Lan N, and Chen YX, *High expression of brain-derived neurotrophic factor in intrahepatic cholangiocarcinoma is associated with intraneural invasion and unfavorable prognosis.* Int J Clin Exp Pathol, 2017. **10**(10): p. 10399-10405.
297. Ceci C, Atzori MG, Lacal PM, and Graziani G, *Role of VEGFs/VEGFR-1 Signaling and its Inhibition in Modulating Tumor Invasion: Experimental Evidence in Different Metastatic Cancer Models.* International journal of molecular sciences, 2020. **21**(4): p. 1388.
298. Matkar PN, Jong ED, Ariyagunarajah R, Prud'homme GJ, Singh KK, and Leong-Poi H, *Jack of many trades: Multifaceted role of neuropilins in pancreatic cancer.* Cancer Medicine, 2018. **7**(10): p. 5036-5046.
299. Li X, Jin Q, Yao Q, Zhou Y, Zou Y, Li Z*, et al.*, *Placental Growth Factor Contributes to Liver Inflammation, Angiogenesis, Fibrosis in Mice by Promoting Hepatic Macrophage Recruitment and Activation.* Frontiers in Immunology, 2017. **8**.
300. Tanaka K, Okugawa Y, Toiyama Y, Inoue Y, Saigusa S, Kawamura M*, et al.*, *Brain-derived neurotrophic factor (BDNF)-induced tropomyosin-related kinase B (Trk B) signaling is a potential therapeutic target for peritoneal carcinomatosis arising from colorectal cancer.* PLoS One, 2014. **9**(5): p. e96410.
301. Holgado-Madruga M, Moscatello DK, Emlet DR, Dieterich R, and Wong AJ, *Grb2-associated binder-1 mediates phosphatidylinositol 3-kinase activation and the promotion of cell survival by nerve growth factor.* Proc Natl Acad Sci U S A, 1997. **94**(23): p. 12419-24.
302. Lemmon MA and Schlessinger J, *Cell signaling by receptor tyrosine kinases.* Cell, 2010. **141**(7): p. 1117-34.
303. Chang F, Steelman LS, Lee JT, Shelton JG, Navolanic PM, Blalock WL*, et al.*, *Signal transduction mediated by the Ras/Raf/MEK/ERK pathway from cytokine receptors to transcription factors: potential targeting for therapeutic intervention.* Leukemia, 2003. **17**(7): p. 1263-93.
304. Wang Y, Zhao E, Zhang Z, Zhao G, and Cao H, *Association between Tim-3 and Gal-9 expression and gastric cancer prognosis.* Oncol Rep, 2018. **40**(4): p. 2115-2126.
305. Li H, Wu K, Tao K, Chen L, Zheng Q, Lu X*, et al.*, *Tim-3/galectin-9 signaling pathway mediates T-cell dysfunction and predicts poor prognosis in patients with hepatitis B virus-associated hepatocellular carcinoma.* Hepatology, 2012. **56**(4): p. 1342-51.
306. Avery L, Filderman J, Szymczak-Workman AL, and Kane LP, *Tim-3 co-stimulation promotes short-lived effector T cells, restricts memory precursors, and is dispensable for T cell exhaustion.* Proc Natl Acad Sci U S A, 2018. **115**(10): p. 2455-2460.
307. Banerjee H, Nieves-Rosado H, Kulkarni A, Murter B, McGrath KV, Chandran UR*, et al.*, *Expression of Tim-3 drives phenotypic and functional changes in Treg cells in secondary lymphoid organs and the tumor microenvironment.* Cell Reports, 2021. **36**(11): p. 109699.
308. Koyama S, Akbay EA, Li YY, Herter-Sprie GS, Buczkowski KA, Richards WG*, et al.*, *Adaptive resistance to therapeutic PD-1 blockade is associated with upregulation of alternative immune checkpoints.* Nature Communications, 2016. **7**(1): p. 10501.
309. Ritthipichai K, Haymaker CL, Martinez M, Aschenbrenner A, Yi X, Zhang M*, et al.*, *Multifaceted Role of BTLA in the Control of CD8(+) T-cell Fate after Antigen Encounter.* Clinical cancer research : an official journal of the American Association for Cancer Research, 2017. **23**(20): p. 6151-6164.

310. Fourcade J, Sun Z, Pagliano O, Guillaume P, Luescher IF, Sander C*, et al.*, *CD8⁺ T Cells Specific for Tumor Antigens Can Be Rendered Dysfunctional by the Tumor Microenvironment through Upregulation of the Inhibitory Receptors BTLA and PD-1.* Cancer Research, 2012. **72**(4): p. 887.
311. Haymaker CL, Wu RC, Ritthipichai K, Bernatchez C, Forget M-A, Chen JQ*, et al.*, *BTLA marks a less-differentiated tumor-infiltrating lymphocyte subset in melanoma with enhanced survival properties.* OncoImmunology, 2015. **4**(8): p. e1014246.
312. Borst J, Hendriks J, and Xiao Y, *CD27 and CD70 in T cell and B cell activation.* Current Opinion in Immunology, 2005. **17**(3): p. 275-281.
313. Starzer AM and Berghoff AS, *New emerging targets in cancer immunotherapy: CD27 (TNFRSF7).* ESMO Open, 2020. **4**(Suppl 3): p. e000629.
314. Han J, Liu Y, Yang S, Wu X, Li H, and Wang Q, *MEK inhibitors for the treatment of non-small cell lung cancer.* Journal of Hematology & Oncology, 2021. **14**(1): p. 1.
315. Long GV, Stroyakovskiy D, Gogas H, Levchenko E, de Braud F, Larkin J*, et al.*, *Dabrafenib and trametinib versus dabrafenib and placebo for Val600 BRAF-mutant melanoma: a multicentre, double-blind, phase 3 randomised controlled trial.* The Lancet, 2015. **386**(9992): p. 444-451.
316. Houde N, Beuret L, Bonaud A, Fortier-Beaulieu S-P, Truchon-Landry K, Aoidi R*, et al.*, *Fine-tuning of MEK signaling is pivotal for limiting B and T cell activation.* Cell Reports, 2022. **38**(2).
317. D'Souza WN, Chang C-F, Fischer AM, Li M, and Hedrick SM, *The Erk2 MAPK Regulates CD8 T Cell Proliferation and Survival.* The Journal of Immunology, 2008. **181**(11): p. 7617-7629.
318. Vella LJ, Pasam A, Dimopoulos N, Andrews M, Knights A, Puaux A-L*, et al.*, *MEK Inhibition, Alone or in Combination with BRAF Inhibition, Affects Multiple Functions of Isolated Normal Human Lymphocytes and Dendritic Cells.* Cancer Immunology Research, 2014. **2**(4): p. 351-360.
319. Poon E, Mullins S, Watkins A, Williams GS, Koopmann J-O, Di Genova G*, et al.*, *The MEK inhibitor selumetinib complements CTLA-4 blockade by reprogramming the tumor immune microenvironment.* Journal for ImmunoTherapy of Cancer, 2017. **5**(1): p. 63.
320. Allegrezza MJ, Rutkowski MR, Stephen TL, Svoronos N, Tesone AJ, Perales-Puchalt A*, et al.*, *IL15 Agonists Overcome the Immunosuppressive Effects of MEK Inhibitors.* Cancer Research, 2016. **76**(9): p. 2561-2572.
321. Allegrezza MJ, Rutkowski MR, Stephen TL, Svoronos N, Perales-Puchalt A, Nguyen JM*, et al.*, *Trametinib Drives T-cell–Dependent Control of KRAS-Mutated Tumors by Inhibiting Pathological Myelopoiesis.* Cancer Research, 2016. **76**(21): p. 6253-6265.
322. Yang B, Li X, Fu Y, Guo E, Ye Y, Li F*, et al.*, *MEK Inhibition Remodels the Immune Landscape of Mutant KRAS Tumors to Overcome Resistance to PARP and Immune Checkpoint Inhibitors.* Cancer Research, 2021. **81**(10): p. 2714-2729.
323. Dennison L, Mohan AA, and Yarchoan M, *Tumor and Systemic Immunomodulatory Effects of MEK Inhibition.* Current Oncology Reports, 2021. **23**(2): p. 23.
324. Ostrand-Rosenberg S and Sinha P, *Myeloid-Derived Suppressor Cells: Linking Inflammation and Cancer.* The Journal of Immunology, 2009. **182**(8): p. 4499.
325. Kumar V, Patel S, Tcyganov E, and Gabrilovich DI, *The Nature of Myeloid-Derived Suppressor Cells in the Tumor Microenvironment.* Trends in Immunology, 2016. **37**(3): p. 208-220.

326. Loeuillard E, Yang J, Buckarma E, Wang J, Liu Y, Conboy C*, et al.*, *Targeting tumor-associated macrophages and granulocytic myeloid-derived suppressor cells augments PD-1 blockade in cholangiocarcinoma.* J Clin Invest, 2020. **130**(10): p. 5380-5396.
327. Franklin DA, Sharick JT, Ericsson-Gonzalez PI, Sanchez V, Dean PT, Opalenik SR*, et al.*, *MEK activation modulates glycolysis and supports suppressive myeloid cells in TNBC.* JCI Insight, 2020. **5**(15).
328. Ruffolo LI, Jackson KM, Kuhlers PC, Dale BS, Figueroa Guilliani NM, Ullman NA*, et al.*, *GM-CSF drives myelopoiesis, recruitment and polarisation of tumour-associated macrophages in cholangiocarcinoma and systemic blockade facilitates antitumour immunity.* Gut, 2022. **71**(7): p. 1386.